Carbon dioxide and methane emissions from the Te Arawa lakes of Rotorua, New Zealand

A thesis

submitted in fulfilment of the requirements

for the degree of a

Doctor of Philosophy in the School of Sciences

at

The University of Waikato

by

ARIANTO BUDI SANTOSO

THE UNIVERSITY OF
WAIKATO
Te Whare Wānanga o Waikato

2016

Abstract

One of the biggest issues confronting humankind today is global warming due to the rapidly increasing greenhouse gas (GHG) emissions, namely CO_2, CH_4 and N_2O. The Intergovernmental Panel for Climate Change (IPCC) has prepared an emission reduction strategy. So far, inland waters, including lakes and reservoirs, have not been included in the global carbon cycle. However, the contribution of inland waters to global CO_2 and CH_4 emissions has been identified to be important. Inland waters are also known to be a major sink for GHG emissions by attenuating carbon that would otherwise be transported from the terrestrial landscape to the ocean. Lakes are also very sensitive to climate change as well as to human impacts generally, and these effects will need to be considered in understanding the future role of lakes in the global carbon cycle.

This study aimed to improve understanding of CO_2 and CH_4 emissions from lakes, and to quantify these emissions under changing climate and nutrient loading regimes in a regionally discrete group of lakes of volcanic origin in North Island of New Zealand. It included a comprehensive field study of one lake, application of process-based numerical modelling to the lake, and collation and critical analysis of existing datasets for the group of lakes. The primary study site was Okaro, a monomictic eutrophic lake where a major restoration program has been in place for more than one decade. The study also extended to 10 other lakes in order to give insights into effects of different nutrient and mixing regimes on carbon sources and sinks

Based on observations over a one-period (September 2013 – October 2014), Lake Okaro accumulated CO_2 and CH_4 in the hypolimnion during summer stratification. These gases were entrained into surface waters as lake started to turnover just prior to complete mixing in winter. As recorded in many other eutrophic lakes, the net CO_2 flux was mostly from the atmosphere to the lake. However, CO_2, together with CH_4, escaped from the lake as a pulsed emission in winter. Using a simple annual mass

balance model it was calculated that, ~31% of CH_4 sourced from the sediment escaped to the atmosphere through diffusive flux. The remainder was likely to be oxidized in the water column. The model also showed that on an annual basis the net CO_2 emission is out of the lake. These findings suggest that eutrophic lakes may actually be net emitters of greenhouse gases and that pulsed emissions may be an important contributor to the direction of the flux. This study did not account for CH_4 ebullition, however, and therefore the magnitude of GHG emissions from this lake is likely to be lower than predicted.

The effects on CO_2 and CH_4 emissions from Lake Okaro of a warming climate and changes in nutrient loads was simulated using a coupled hydrodynamic-ecological model (GLM-AED^2). Future possible changes were simulated by altering model forcing data, increasing air temperature by 2.5 °C. Internal and external nutrient (nitrogen and phosphorus) loads were also either halved or increased by one half. Model simulations showed that annual CO_2 uptake by the lake was enhanced under a warmer climate, but emissions of CH_4 increased during lake overturn as a result of greater diffusive fluxes. Total GHG emissions, as CO_2 equivalent (kg CO_2-eq m^{-2} y^{-1}), from the lake were predicted with model simulations to increase by 27% under a warming climate, relative to present conditions. This increase would be reduced to 19% if nutrient loading was halved.

A first-order diagenesis model was used to estimate the carbon deposition in the 11 Te Arawa lakes. The most productive lakes, using chlorophyll *a* as a proxy, had higher rates of carbon deposition in the bottom sediments than the less productive lakes. However, burial efficiency (buried carbon: deposited carbon) was lower in productive lakes meaning that most of the deposited carbon in these lakes is remineralized back into the water column. This remineralization process can be associated with CO_2 and CH_4 emissions from the lake.

The results of this study highlight that eutrophic lakes may contribute emit higher levels of GHGs to the atmosphere than has previously been estimated, primarily as a result of pulsed emissions associated with the

onset of seasonal mixing, at least in monomictic lakes. Eutrophication and climate warming are likely to enhance GHG emissions from lakes. The findings from this study have important implications for global GHG fluxes and indicate that fluxes into or from lakes need to be included in inventories. Reducing nutrient loads to lakes could offset some of the predicted increases in emissions of GHGs that are likely to occur with climate warming.

Acknowledgements

Alhamdulillah, Praise be to God, for His showers of blessing throughout years of my study.

I would like to express my deep and sincere gratitude to my chief supervisor Professor David Hamilton for his guidance, support and motivation throughout my study. I am particularly grateful for his detailed constructive reviews. Not to forget to all my other supervisory member, grateful thanks go to Prof. Louis Schipper, Associate Prof. Chris Hendy, and Dr Moritz Lehmann from The University of Waikato, New Zealand, Dr Deniz Özkundakci from Waikato Regional Council, and Dr Ilia Ostrovsky from Israel Oceanographic and Limnological Research for their inspirational advices.

Special thanks to Joseph Butterworth and Bay of Plenty Regional Council (BOPRC) for field work assistance and other technical support, and Paul Scholes of BOPRC for data provision. I gratefully acknowledge Janine Ryburn (The University of Waikato) for her helpful support in laboratory analysis. Special thanks also go to Dr Adam Hartland (The University of Waikato) for his knowledge sharing.

I am very grateful to the Global Lake Ecological Observatory Network (GLEON) for supporting my attendance at GLEON All Hands Meetings in Ireland and Canada, and providing full funding through GLEON Fellowship Program in the United States for in depth graduate student workshops in network science. I also thank Department of Biological Sciences for providing financial support towards my attendance at the Joint Assembly AGU-CGU-GAC-MAC (Geophysical Sciences) Meeting in Montreal, Canada.

To all my office-mates, Theo Kpodonu, Simon Stewart, Kohji Muraoka, Wang Me, Chris McBride, Mat Allan, Richard Lamont thank you for your

valuable time to share discussions and ideas. To Grant Tempero and Chris Dada, thank you for your last minute proof reading.

This PhD study was supported by the NZ-ASEAN Scholarship. Research funding for this study was also supported through the Lake Biodiversity Restoration program funded by the Ministry of Business, Innovation & Employment (UOWX0505) and the Bay of Plenty Chair in Lake Restoration at the University of Waikato.

Finally, my deepest gratitude belongs to my family, my wife Sofia and our two little angels Giras and Bagas, for their never ending love, support, encouragement and patience. It has been a fantastic adventure for us in New Zealand. To my parents, thank you for your prayer.

Preface

This thesis comprises five chapters, of which Chapters 2 – 4 are individual research contributions. Each research chapter is written in manuscript form, prepared for publication in peer-reviewed scientific journals. The work presented in this thesis, including study design, field and laboratory work, data analysis and writing, is based on my ideas and was conducted by me while under the supervision of Prof. David Hamilton, Prof. Louis Schipper, Associate Prof. Chris Hendy, and Dr Moritz Lehmann from The University of Waikato, New Zealand, Dr Deniz Özkundakci from Waikato Regional Council, and Prof. Ilia Ostrovsky from Israel Oceanographic and Limnological Research. Additionally, this thesis presents as an appendix the results from an international collaboration research project that I was involved in planning, analysing and writing as a co-author.

Co-authors of the chapters listed below have contributed with discussion, supporting data and revisions of the manuscripts. Dr. Matt Hipsey (University of Western Australia) provided support with compilation the hydrodynamic-ecological model code GLM-AED^2 which was used in Chapter 3. Long-term water quality data for Chapter 4 was obtained from Bay of Plenty Regional Council.

Chapter 2 has been prepared for submission to the scientific journal *Biogeochemistry* under the title "CO_2 and CH_4 emissions from a small, eutrophic, monomictic lake: a mass balance approach" by Arianto B. Santoso, David P. Hamilton, Chris H. Hendy, Louis A. Schipper and Ilia S. Ostrovsky.

Chapter 3 has been prepared for submission to the scientific journal *Global Change Biology* under the title "CO_2 and CH_4 emissions from a eutrophic monomictic lake under changing climate and nutrient regimes: a hydrodynamic-ecological model simulation" by Arianto B. Santoso, David P. Hamilton, Moritz K. Lehmann, Deniz Özkundakci and Matt R. Hipsey.

Chapter 4 has been prepared for submission to the scientific journal *Hydrobiologia* under the tittle “Carbon dioxide emissions and sediment organic carbon burial across a trophic state gradient of eleven New Zealand lakes” by Arianto B. Santoso, David P. Hamilton, Chris H. Hendy and Louis A. Schipper.

Appendix I has been accepted in for publication in Inland Waters under the title: Consequences of gas flux model choice on the interpretation of metabolic balance across 15 lakes, by Hilary A. Dugan, Richard I. Woolway, Arianto B. Santoso, Jessica R. Corman, Aline Jaimes, Emily R. Nodine, Vijay P. Patil, Jake A. Zwart, Jennie A. Bentrup, Amy L. Hetherington, Samantha K. Oliver, Jordan S. Read, Kristen M. Winters, Paul C. Hanson, Emily K. Read, Luke A. Winslow, Kathleen C. Weathers.

Table of contents

Lists of figures

Lists of tables

Chapter 1 Introduction

1.1. Motivation

1.1.1. Global carbon accounting from freshwater ecosystems

Climate change due to greenhouse gas (GHG) emissions is one of the biggest issues confronting humankind today (IPCC, 2007). The increase in GHGs, namely carbon dioxide (CO_2); methane (CH_4); and nitrous oxide (N_2O) that accompanied the industrial revolution in the 18th century is largely responsible for the current rate of increase of global temperatures (Foster *et al.*, 2007). Efforts have therefore been initiated to reduce GHG emissions to slow down global warming. Estimates of global GHG emissions have been made for three different compartments on earth: the land biosphere, the atmosphere and the ocean (IPCC, 2007). This approach has identified knowledge gaps, partly as a result of budgetary imbalances of GHGs (IPCC, 2007; Levin *et al.*, 2010; Le Quéré *et al.*, 2015). Process-based insights and understanding of GHG cycles (e.g. Battin *et al.*, 2009; Reigner *et al.*, 2013) is therefore required to improve estimates and identify targeted GHG reductions.

Inland water ecosystems have been identified to contribute an important component in the global carbon balance (Figure 1.1). Although covering <3% of the earth's surface (Downing *et al.*, 2006) inland waters (including ponds, lakes, wetlands, reservoirs, stream and rivers) are important in the transfer of terrestrial carbon to the ocean (Aufdenkampe *et al.*, 2011; Reigner *et al.*, 2013). Inland waters also act as "active pipes" in modifying carbon through various internal processes (metabolism, sedimentation and weathering) during the transfer (Cole *et al.*, 2007; Tranvik *et al.*, 2009). Recent synthesis suggests that inland waters emit 0.8 – 2.1 Pg C y^{-1} to the atmosphere as CO_2 (Cole *et al.*, 2007; Tranvik *et al.*, 2009; Raymond *et al.*, 2013; Reigner *et al.*, 2013). This emission level is of the same magnitude as the global atmospheric carbon sink in the open ocean (1.85 – 2.6 Pg C y^{-1}) and the global residual terrestrial CO_2 sink (2.05 – 2.9 Pg C y^{-1}) (Reigner *et al.*, 2013; Le Quéré *et al.*, 2015). Inland waters have

been estimated to receive 1.9 – 2.9 Pg C y^{-1} from terrestrial environments and transport 0.9 – 1.0 Pg C y^{-1} to the global ocean (Cole *et al.*, 2007; Tranvik *et al.*, 2009; Reigner *et al.*, 2013). About 0.23 – 0.6 Pg y^{-1} of this lateral transport of carbon is estimated to remain as a sink in lake sediments (Battin *et al.*, 2009; Cole *et al.*, 2007; Tranvik *et al.*, 2009; Reigner *et al.*, 2013). In addition, CH_4 is also identified to be released in a large amount during the lateral transport. Bastviken et al. (2011) estimated that 0.65 Pg C y^{-1} is released to the atmosphere as CH_4 from inland waters. Given that global warming potential (GWP) of CH_4 over a 100-year horizon is 34 times larger than that of CO_2 (Myhre *et al.* 2013), inland waters are clearly highly important in the global greenhouse gas emission accounting scheme.

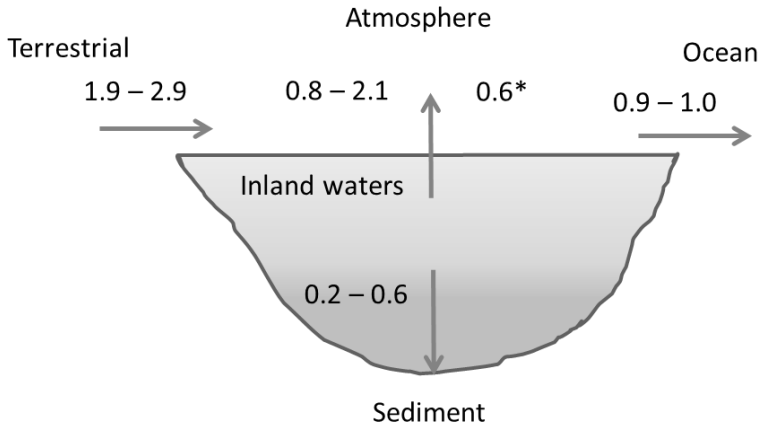

Figure 1.1 Schematic diagram of the role of inland waters in regulating global carbon balance. Units are in Pg C y^{-1}. Atmospheric carbon emissions are identified as CO_2 and CH_4 (*). See text for details.

While it has become clear over the last two decades that inland waters are an essential component of the global carbon cycle and global warming (e.g. Cole *et al.*, 1994), they have not been part of the assessment of global carbon budgets (IPCC 2007; Le Quéré *et al.*, 2015). This exclusion is attributed to the lack of a framework for estimating carbon emissions from inland waters, thus presenting uncertainties in the accuracy of measurements underpinning global CO_2 databases (Raymond *et al.*, 2013). Limitations in the methodology used for global estimates include underestimates of CH_4 ebullition, which can be highly, spatially heterogeneous, lack of night-time CO_2 flux measurements, as well as the complexity and immense diversity of inland water systems that make it difficult to upscale specific types of inland waters to derive global-scale estimates (Tranvik *et al.*, 2009; Panneer Selvam *et al.*, 2014). In addition, changes in inland waters as a result of human activities and climate change complicate efforts aimed at estimating the contribution of inland waters to the global carbon balance (Tranvik *et al.*, 2009). Given these limitations, there is an urgent need for further comprehensive studies on carbon flux from inland water systems, with a view to making reliable contributions to global budget calculations.

1.1.2. CO_2 and CH_4 emissions from lakes and responses to climate and water quality change

The seminal paper of Cole *et al.* (1994) showed that vast majority of world's lakes can be regarded as atmospheric CO_2 sources. Based on their study, surface water partial CO_2 pressure (pCO_2) was at equilibrium with atmospheric pCO_2 in less than 10% of lakes worldwide. More than 80% of the lakes in the study were supersaturated, with about three times the atmospheric CO_2 equilibrium concentration. Freshwater ecosystems (including lake water and sediments) have also been identified to be one of the hot spots for CH_4 emissions to the atmosphere (Kirschke *et al.*, 2013).

Organic matter mineralization in sediment plays an important role in the production of CO_2 and CH_4 in lakes (Kuivila and Murray, 1984). When

organic matter exists largely in labile form, there is a greater tendency for it to be decomposed (into CO_2 and CH_4) rather than being merely buried in the sediment (Sobek *et al.,* 2009). This implies that lake sediment which receives more labile organic carbon, i.e. mostly from phytoplankton production (autochthonous input), is likely to produce greater CO_2 and CH_4 to the water column than sediment that accumulates more recalcitrant allochthonous organic carbon (i.e. land-plant derived). Adams (2005) noted that diffusion rates of CO_2 and CH_4 across the sediment-water interface of eutrophic lakes and reservoirs (3.8 – 4.2 and 3.9 – 5.2 mmol m^{-2} d^{-1}, respectively) is about one order of magnitude higher than in the oligotrophic lakes and reservoirs (0.34 and 0.19 mmol m^{-2} d^{-1}, respectively).

Although CO_2 and CH_4 are mainly produced in lake sediments, biogeochemical processes in the water column may transform these gases and, may therefore be an important control on their release to the atmosphere. It has been identified that the CO_2 concentration in lakes is driven by an interplay of physical, chemical and biological processes which includes external carbon inputs (Maberly *et al.*, 2013), lake water circulation due to hydrodynamics (Striegl and Michmerhuizen, 1998), biological community metabolism (Cole *et al.*, 2000), and carbonate equilibria (Stets *et al.*, 2009). Methane dynamics in the water column, on the other hand, are mainly controlled by the interaction of hydrodynamics and CH_4 oxidation (mostly regulated by levels of dissolved oxygen) (Fernandez *et al.*, 2014). Therefore, in stratified eutrophic lakes with characteristically high concentrations of nutrients to generate phytoplankton production, supersaturation of dissolved oxygen is common in the surface waters during the day and anoxic conditions can be persistent in the lake bottom waters (e.g., Özkundakci *et al.*, 2011), CO_2 and CH_4 are usually present at low concentrations in the surface water but accumulate in the bottom waters (Striegl and Michmerhuizen, 1998; Riera *et al.*, 1999; López Bellido *et al.* 2011). At the onset of water column mixing, the accumulated CO_2 and CH_4 can be circulated into the surface and released rapidly to the atmosphere (Fernández *et al.* 2014;

Weyhenmeyer *et al.* 2015). A substantial amount of the CH_4 may be transformed into CO_2 through oxidation, at rates dependent on the availability of oxygen, which in turn is regulated by rates of vertical transport. The extent that oxidation reduces CH_4 emissions from lake is still debatable (Schubert *et al.* 2012; Fernández *et al.* 2014). This complicates estimates of GHG emission potential from lakes, particularly from those that are eutrophic, with anoxic bottom waters.

Carbon dioxide and methane dynamics in lakes are affected by human activities at scales from local (e.g., increases in nutrient inputs: Maberly *et al.*, 2013; Gonzalez-Valencia *et al.*, 2013) to global (e.g., warming climate: Marotta *et al.*, 2014; Rasilo *et al.*, 2015). Increased nutrient concentrations may lead to greater autotrophic fixation of CO_2 (Hanson *et al.*, 2004). Warmer climate, on the other hand, may alter the hydrodynamics of lakes and extend periods of stratification (Bueche and Vetter, 2015), thus promoting greater accumulation of CO_2 and CH_4 in bottom waters. Eutrophication has been predicted to be intensified by climate change as a result of a synergistic response to increasing temperature and elevated nutrient levels (Trolle *et al.*, 2011; Hamilton *et al.*, 2013) and it may therefore be expected to increase concentrations of CO_2 and CH_4 in the bottom waters of lakes. However, the balance of increased GHG generation in bottom waters and increasing demand for CO_2 from autochthonous production are poorly understood.

1.2. Objectives

The overarching objective of this thesis was to better understand the emissions of CO_2 and CH_4 from lakes, and to predict the occurrence of these emissions under changing climate and nutrient regimes. Additionally, this thesis examines deposition of carbon in lake sediments across wide range of trophic states in order to give insights into carbon sources and sinks in the lakes under different nutrient regimes. The research comprises a comprehensive field study, application of a process-based ecological model to assist with predictions of changes in GHG emissions from lakes under a warming climate and changing nutrient load,

and critical analysis of existing datasets across a group of lakes, to develop an integrated understanding across a diversity of lake trophic states and seasonal mixing patterns. The in-depth analysis of CO_2 and CH_4 emissions was focused on a monomictic eutrophic lake, Okaro, Bay of Plenty, New Zealand, where an active lake restoration program has been in place for more than one decade. The broad-scale analysis over a group of lakes included 11 major lakes from this region.

1.3. Thesis overview

This thesis comprises three main research chapters (Chapters 2 – 4) which have been written in a format suitable for submission to scientific journals. The final chapter of this thesis (Chapter 5) provides a synthesis of the main findings of study in a wider perspective, and identifies some avenues for future research that could be further advanced.

Chapter 2 presents the results of an extensive field study in Lake Okaro in capturing the dynamics of CO_2 and CH_4 over a one-year period. The aim of this chapter was to estimate CO_2 and CH_4 diffusive emissions by combining field observation data and a simple process-based mass balance model. The model was used to calculate rates of internal CO_2 and CH_4 cycling, and diffusive fluxes with the atmosphere that regulate whole-lake CO_2 and CH_4 storage over an annual cycle. Through this approach, it was hypothesised that biological processes in the water column (e.g. phytoplankton uptake and CH_4 oxidation) would reduce the magnitude of CO_2 and CH_4 fluxes from the lake to the atmosphere.

Chapter 3 describes the application of a numerical one-dimensional (1-D) hydrodynamic-ecological model (GLM-AED^2) to simulate CO_2 and CH_4 dynamics in Lake Okaro. The model solves the vertical mass and energy balances in the water column and is integrated with biogeochemical cycles of the lake (Hipsey *et al*. 2014; Hipsey *et al*. 2012). A range of model scenarios with regard to changing climate (represented by increases air temperature) and nutrient regimes (represented by alterations in external

and internal nutrient loading) was simulated in order to assess CO_2 and CH_4 dynamics and emissions from the lake in various future projections.

Chapter 4 synthesizes CO_2 emission dynamics in 11 volcanic lakes of varying trophic states and mixing regime in Rotorua, North Island New Zealand, calculated from pH, temperature and alkalinity (Stumm and Morgan 1996) datasets collected by the Bay of Plenty Regional Council (BOPRC). This synthesis is combined with carbon burial estimates based on a first-order diagenesis model of the deposited carbon (Berner 1980) in the sediment collected by other studies (Pickett, 2008; Trolle *et al.*, 2008). This chapter gives an overview of how the sinks and releases of carbon (as CO_2) from the lake.

1.4. References

Adams D (2005) Diffuse Flux of Greenhouse Gases — Methane and Carbon Dioxide — at the Sediment-Water Interface of Some Lakes and Reservoirs of the World. In: *Greenhouse Gas Emissions — Fluxes and Processes* (ed Tremblay A, Varfalvy L, Roehm C, Garneau M), pp. 129–153. Springer Berlin Heidelberg.

Aufdenkampe AK, Mayorga E, Raymond PA *et al.* (2011) Riverine coupling of biogeochemical cycles between land, oceans, and atmosphere. *Frontiers in Ecology and the Environment*, **9**, 53–60.

Bastviken D, Tranvik LJ, Downing JA, Crill PM, Enrich-Prast A (2011) Freshwater methane emissions offset the continental carbon sink. *Science*, **331**, 50.

Battin TJ, Luyssaert S, Kaplan LA, Aufdenkampe AK, Richter A, Tranvik LJ (2009) The boundless carbon cycle. *Nature Geoscience*, **2**, 598–600.

Berner RA (1980) *Early diagenesis: A theoretical approach*. Princeton University Press.

Bueche T, Vetter M (2015) Future alterations of thermal characteristics in a medium-sized lake simulated by coupling a regional climate model with a lake model. *Climate Dynamics*, **44**, 371–384.

Cole JJ, Caraco NF, Kling GW, Kratz TK (1994) Carbon dioxide supersaturation in the surface waters of lakes. *Science (New York, N.Y.)*, **265**, 1568–1570.

Cole JJ, Pace ML, Carpenter SR, Kitchell JF (2000) Persistence of net heterotrophy in lakes during nutrient addition and food web manipulations. *Limnology and Oceanography*, **45**, 1718–1730.

Cole JJ, Prairie YT, Caraco NF *et al.* (2007) Plumbing the global carbon cycle: Integrating inland waters into the terrestrial carbon budget. *Ecosystems*, **10**, 171–184.

Downing JA, Prairie YT, Cole JJ *et al.* (2006) The global abundance and size distribution of lakes, ponds, and impoundments. *Limnology and Oceanography*, **51**, 2388–2397.

Fernández JE, Peeters F, Hofmann H (2014) Importance of the autumn overturn and anoxic conditions in the hypolimnion for the annual methane emissions from a temperate lake. *Environmental Science and Technology*, **48**, 7297–7304.

Forster P, Ramaswamy V, Artaxo P *et al.* (2007) Changes in atmospheric constituents and in radiative forcing. Chapter 2. In: *Climate Change 2007. The Physical Science Basis*. *Contribution of Working Group I to the Fourth Assessment Report of the Intergovernmental Panel on Climate Change* (ed Solomon, S, Qin D, Manning M *et al.*). Cambridge University Press, Cambridge, United Kingdom and New York, NY, USA.

Gonzalez-Valencia R, Sepulveda-Jauregui A, Martinez-Cruz K, Hoyos-Santillan J, Dendooven L, Thalasso F (2014) Methane emissions from Mexican freshwater bodies: Correlations with water pollution. *Hydrobiologia*, **721**, 9–22.

Hamilton DP, McBride CG, Özkundakci D *et al.* (2013) Effects of climate change on New Zealand lakes. In: *Climate Change and Inland Waters: Impacts and Mitigation for Ecosystems and Societies* (ed Goldman CR, Kumagai M, Robarts RD), pp. 337–366. John Wiley & Sons, Ltd.

Hanson PC, Pollard AI, Bade DL, Predick K, Carpenter SR, Foley JA (2004) A model of carbon evasion and sedimentation in temperate lakes. *Global Change Biology*, **10**, 1285–1298.

Hipsey MR, Bruce LC, Bruggeman J, Bolding K, Hamilton DP (2012) *GLM-FABM v0.9a Model Overview and User Documentation*. The University of Western Australia. Perth, 44 pp.

Hipsey MR, Bruce LC, Hamilton DP (2014) *General Lake Model: Model overview and user information. AED Report #26.* The University of Western Australia. Perth, 42 pp.

IPCC (2007) *Climate change 2007: The Physical Science Basis. Contribution of Working Group I to the Fourth Assessment Report of the Intergovernmental Panel on Climate Change* (ed Solomon S, Qin D, Manning M, *et al.*). Cambridge University Press, Cambridge, United Kingdom and New York, NY, USA, 1-1007 pp.

Kirschke S, Bousquet P, Ciais P *et al.* (2013) Three decades of global methane sources and sinks. *Nature Geoscience*, **6**, 813–823.

Kuivila KM, Murray JW (1984) Organic matter diagenesis in freshwater sediments: The alkalinity and total CO_2 balance and methane production in the sediments of Lake Washington. *Limnology and Oceanography*, **29**, 1218–1230.

Levin I, Naegler T, Heinz R *et al.* (2010) The global SF6 source inferred from long-term high precision atmospheric measurements and its comparison with emission inventories. *Atmospheric Chemistry and Physics*, **10**, 2655–2662.

López Bellido J, Peltomaa E, Ojala A (2011) An urban boreal lake basin as a source of CO_2 and CH_4. *Environmental Pollution*, **159**, 1649–1659.

Maberly SC, Barker PA, Stott AW, Ville D, Mitzi M (2013) Catchment productivity controls CO_2 emissions from lakes. *Nature Climate Change*, **3**, 391–394.

Özkundakci D, Hamilton DP, Gibbs MM (2011) Hypolimnetic phosphorus and nitrogen dynamics in a small, eutrophic lake with a seasonally anoxic hypolimnion. *Hydrobiologia*, **661**, 5–20.

Panneer Selvam B, Natchimuthu S, Arunachalam L, Bastviken D (2014) Methane and carbon dioxide emissions from inland waters in India - implications for large scale greenhouse gas balances. *Global Change Biology*, **20**, 3397–3407.

Pickett RC (2008) *A tephra-dated record of palaeoenvironmental change since ~ 5,500 years ago from Lake Rotorua, North Island, New Zealand*. Master Thesis. The University of Waikato.

Le Quéré C, Moriarty R, Andrew RM *et al.* (2015) Global carbon budget 2014. *Earth System Science Data*, **7**, 47–85.

Rasilo T, Prairie YT, del Giorgio PA (2015) Large-scale patterns in summer diffusive CH_4 fluxes across boreal lakes, and contribution to diffusive C emissions. *Global Change Biology*, **21**, 1124–1139.

Raymond PA, Hartmann J, Lauerwald R *et al.* (2013) Global carbon dioxide emissions from inland waters. *Nature*, **503**, 355–359.

Regnier P, Friedlingstein P, Ciais P *et al.* (2013) Anthropogenic perturbation of the carbon fluxes from land to ocean. *Nature Geoscience*, **6**, 597–607.

Riera JL, Schindler JE, Kratz TK (1999) Seasonal dynamics of carbon dioxide and methane in two clear-water lakes and two bog lakes in northern Wisconsin, U.S.A. *Canadian Journal of Fisheries and Aquatic Sciences*, **274**, 1–10.

Schubert CJ, Diem T, Eugster W (2012) Methane emissions from a small wind shielded lake determined by eddy covariance, flux chambers, anchored funnels, and boundary model calculations: A comparison. *Environmental Science and Technology*, **46**, 4515–4522.

Sobek S, Durisch-Kaiser E, Zurbrügg R, Wongfun N, Wessels M, Pasche N, Wehrli B (2009) Organic carbon burial efficiency in lake sediments

controlled by oxygen exposure time and sediment source. *Limnology and Oceanography*, **54**, 2243–2254.

Stumm W, Morgan JJ. 1996. *Aquatic chemistry: Chemical equilibria and rates in natural waters*. Hoboken, New Jersey: Wiley.

Stets EG, Striegl RG, Aiken GR, Rosenberry DO, Winter TC (2009) Hydrologic support of carbon dioxide flux revealed by whole-lake carbon budgets. *Journal of Geophysical Research: Biogeosciences*, **114**, 1–14.

Striegl RG, Michmerhuizen CM (1998) Hydrologic influence on methane and carbon dioxide dynamics at two north-central Minnesota lakes. *Limnology and Oceanography*, **43**, 1519–1529.

Tranvik LJ, Downing J a., Cotner JB *et al.* (2009) Lakes and reservoirs as regulators of carbon cycling and climate. *Limnology and Oceanography*, **54**, 2298–2314.

Trolle D, Hamilton DP, Hendy C, Pilditch C (2008) Sediment and nutrient accumulation rates in sediments of twelve New Zealand lakes: Influence of lake morphology, catchment characteristics and trophic state. *Marine and Freshwater Research*, **59**, 1067–1078.

Trolle D, Hamilton DP, Pilditch CA, Duggan IC, Jeppesen E (2011) Predicting the effects of climate change on trophic status of three morphologically varying lakes: Implications for lake restoration and management. *Environmental Modelling and Software*, **26**, 354–370.

Weyhenmeyer GA, Kosten S, Wallin MB, Tranvik LJ, Jeppesen E, Roland F (2015) Significant fraction of CO_2 emissions from boreal lakes derived from hydrologic inorganic carbon inputs. *Nature Geoscience*, **8**, 933–936.

Chapter 2 CO_2 and CH_4 emissions from a small eutrophic monomictic lake: a mass balance approach

Abstract

Lakes are known as 'hotspots' on the landscape for CO_2 and CH_4 emissions to the atmosphere and they substantially affect the global carbon cycle. However, process-based estimates of emissions from lakes are rarely undertaken. Here CO_2 and CH_4 emissions are calculated for a small, eutrophic monomictic lake (Okaro, New Zealand) using a mass balance model for CO_2 and CH_4 and monthly water column measurements over a one-year period. To support model computations, I collected sediment porewater concentrations of CO_2 and CH_4 using peepers and took water column profiles of temperature, dissolved oxygen concentration and chlorophyll *a* biomass. A large pulsed emission of CO_2 and CH_4 was predicted in response to the onset of water column turnover in early winter, after these gases had accumulated in the hypolimnion during seasonal stratification. On an annual basis, however, CO_2 was taken up from the atmosphere by the lake, mostly to sustain high rates of phytoplankton productivity. In addition, the lake gained a substantial amount of CO_2 from CH_4 oxidation. Annually, only ca. 31% of CH_4 produced in the sediment escaped to the atmosphere as a diffusive flux. Our study indicates that eutrophic lakes with high rates of primary production may act as net greenhouse gas emitters, although the magnitude of the emission is relatively lower than the average emission from global lakes.

Keywords: diffusive flux, greenhouse gas storage, mass balance, oxidation, thermal stratification.

2.1. Introduction

Recent studies have shown that substantial amounts of carbon dioxide (CO_2) and methane (CH_4) are emitted from inland waters (Raymond et al 2013; Bastviken et al. 2011). CO_2 in lakes is mostly produced within the water column and as a result of sediment respiration (Vachon and del Giorgio 2014; Algesten et al. 2005) as well as from dissolved inorganic carbon (DIC) inputs from the catchment (Maberly et al. 2013; Weyhenmeyer et al. 2015). Methane is mostly produced in the sediment during organic matter mineralization (Huttunen et al. 2006), although hypolimnetic waters can also produce significant amounts of CH_4 (Wand et al. 2006). Atmospheric release is one of the pathways for removal of CO_2 and CH_4 from lakes, but biogeochemical processes can also produce and transform these gases. For example, inorganic carbon dissociation from carbonates may produce CO_2, whilst autotrophic activity may take up CO_2 (Marcé et al. 2015). Methanogenic bacteria contribute substantial amounts of CH_4 to the system under anoxic conditions, while anaerobic methane oxidation is another CH_4 sink (Borrel et al. 2011). It has been estimated that around 50 to 95% of CH_4 produced in the sediment is oxidized to CO_2 at the sediment-water interface, before entering the water column (Bastviken 2009).

In stratified eutrophic lakes where there are high rates of organic matter deposition to lake bed sediments, dissolved oxygen may be completely removed from the hypolimnion. This anaerobic hypolimnion can accumulate large quantities of CH_4 and CO_2 (Huttunen et al. 2003; Juutinen et al. 2009; López Bellido et al. 2011). On the other hand, high nutrient concentrations in these lakes lead to high rates of phytoplankton production, creating supersaturation of dissolved oxygen and undersaturation of CO_2 in the surface layer (Hanson et al. 2003). Hence, as CH_4 is oxidized in the presence of oxygen, the CO_2 is taken up by phytoplankton photosynthesis and the surface layer can be quite efficient in removing CH_4 and CO_2, particularly during the stratified period. However, at the onset of water column mixing, large quantities of CO_2 and

CH_4 stored in the hypolimnion (storage flux; Bastviken 2009) can be released rapidly to the atmosphere (Fernández et al. 2014; Weyhenmeyer et al. 2015), often over a time scale of a few days (Kankaala et al. 2007). Although it was initially assumed that all stored hypolimnetic CH_4 was released to the atmosphere at the onset of water column mixing (Bastviken et al. 2004), a major fraction of the CH_4 can be oxidised, at rates dependent on the availability of oxygen, mixing regime and water column depth (Kankaala et al. 2007; Fernández et al. 2014). There is still considerable debate about the extent that oxidation reduces CH_4 emissions (Schubert et al. 2012; Fernández et al. 2014), which complicates global estimates of greenhouse gas emission potential from lakes, particularly from those that are eutrophic.

In addition to the issue of the intermittent nature of CO_2 and CH_4 emissions from eutrophic lakes, inventories for small lakes remain scarce (Raymond et al. 2013; Bastviken et al. 2011; Ortiz-Llorente and Alvarez-Cobelas 2012). Knowing that inland waters are dominated by small water bodies with surface areas of <1 km^2 (Downing *et al.* 2006) which are prone to eutrophication and organic carbon burial (Downing *et al.* 2008), detailed studies of carbon emission from small lakes are important to determine the greenhouse gas emission estimates from lakes across the globe.

In the present study I applied a simple process-based model that accounts for internal CO_2 and CH_4 cycling, and fluxes with the atmosphere. Through this approach I tested the hypothesis that biological processes in the water column (e.g., phytoplankton uptake and CH_4 oxidation) of a eutrophic lake would reduce the magnitude of CO_2 and CH_4 effluxes to the atmosphere. The magnitude of greenhouse gas emissions (as kg CO_2-eq m^{-2} y^{-1}) estimated from the mass balanced model was examined in relation to current knowledge of the role of lakes in regulating global carbon cycle and climate change (Tranvik et al. 2009; Moss et al. 2011) and specifically in relation to the direction and magnitude of gas fluxes in eutrophic lakes.

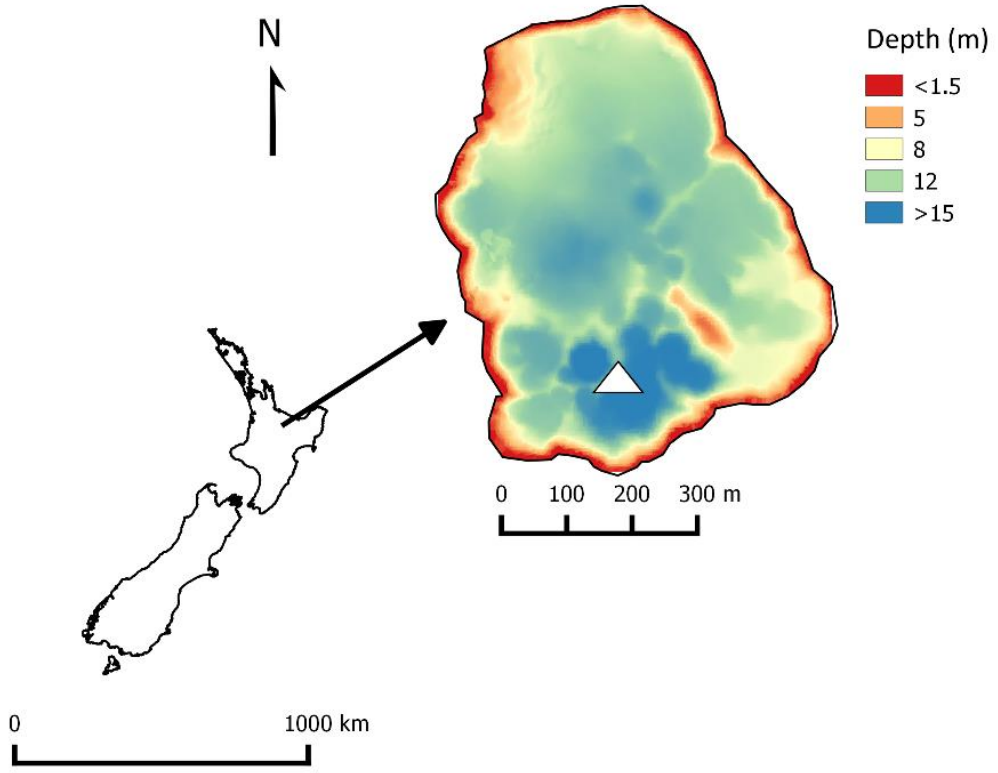

Figure 2.1 Location map and the bathymetry of Lake Okaro, North Island, New Zealand. Sampling site is marked by a white triangle.

2.2. Methods

2.2.1. Study site

The study was Lake Okaro, 27 km south of Rotorua township, North Island of New Zealand (Figure 2.1). The lake is small (0.3 km^2), with a maximum depth of 18 m, and is the most eutrophic of 12 major lakes in the Rotorua region. More than 90% of its catchment area (3.98 km^2) is pasture used for dairy, deer, sheep and beef farming. Water residence time of Lake Okaro is estimated to be ca. 1.5 years, with surface inflows from two unnamed streams entering the lake from the north-west, and one outflow (Haumi Stream) in the south-east. The trophic state of this lake has increased since the 1960s (Forsyth et al. 1988) and the lake has become eutrophic, with periodic blooms of cyanobacteria in spring and summer (Paul et al.

2008). The hypolimnion of the lake is anoxic throughout most of the 9-month stratified period (Özkundakci et al. 2011).

2.2.2. Sampling summary

Water column samples were collected on a monthly basis from September 2013 to October 2014 from the deepest station of the lake (Figure 2.1). In mid-winter (June, southern hemisphere) additional samples were collected on two occasions to capture the abrupt changes in the water column profile due to the onset of annual lake mixing. Water samples were collected at the subsurface (0.5 m) and to a depth of 16 m with a vertical resolution of 2 m using a 10-L Schindler-Patalas water sampler. Subsamples of 60 mL were taken from the sampler using a syringe, for dissolved CO_2 and CH_4 analysis. The aliquot in the syringe was transferred into a 45 mL glass bottle with excess water overflowing the bottle. The bottle was capped with a polypropylene screw cap with a PTFE/silicone septa, leaving no bubbles in the bottle, and stored in the dark and cold (4 ^{o}C) until analysis. Water column profiles of temperature and dissolved oxygen were taken on each sampling occasion using a conductivity-temperature-depth (CTD) profiler (Sea-Bird Electronics 19 plus) with an additional mounted dissolved oxygen (DO, Sea-Bird Electronics) sensor.

Sediment porewater samples were collected from peepers, as described in detail by Hesslein (1976) and Teasdale et al. (1995). Briefly, milli-Q water was added to 15 mL peeper bottles and bottles were placed at 2 cm intervals from the sediment surface to a depth of 50 cm in the sediment. Two peepers were placed in the sediment of the deepest part of the lake for one month (May to June 2014 and August to September 2014). At the end of the incubation, aliquots in the peeper bottle were transferred into the 45 mL glass bottle, kept upside down to avoid gas leakage from the septa, and stored in the dark and cold until analysis.

Dissolved CO_2 and CH_4 concentrations for gas samples from the field were determined in the laboratory by the headspace equilibration method within 24 h of sampling (Striegl and Michmerhuizen, 1998). Briefly, for

water column samples approximately 20 mL of pure N_2 was injected into the 45 mL glass bottle through the PTFE/silicone septa, replacing aliquots in the bottle to create headspace and using a second needle to drain water. The remaining water sample in the bottle was kept at 28 mL. Additional nitrogen gas (5 mL) was added to the bottles to over-pressurise the headspace in the bottle. For porewater samples, 10 mL of ambient air was injected into the 45 mL glass bottle for equilibration. Equilibration was performed by shaking the bottles vigorously for 3 minutes. Bottles were kept upside down to avoid gas leakage from the septa. Subsamples of 5 mL of equilibrated gas were transferred from the headspace into 3.7 mL prevacuumed Labco Exetainer® vials. The CO_2 concentration in the headspace was measured by an infra-red gas analyser (IRGA, LI-COR® LI-6262). A gas chromatograph equipped with a flame ionization detector (GC-FID, Varian CP 3800) was used to determine CH_4 concentrations in the headspace. The concentrations of dissolved gas in the water samples were then calculated based on the solubility function of CO_2 and CH_4 following Weiss and Price (1980) and Wiesenburg and Guinasso (1979), respectively, with temperature adjustment. Chlorophyll *a*, pH and alkalinity were collected either from the lake surface or as an integrated depth sample through the surface mixed layer. All samples were analysed using standard methods based on APHA (1998).

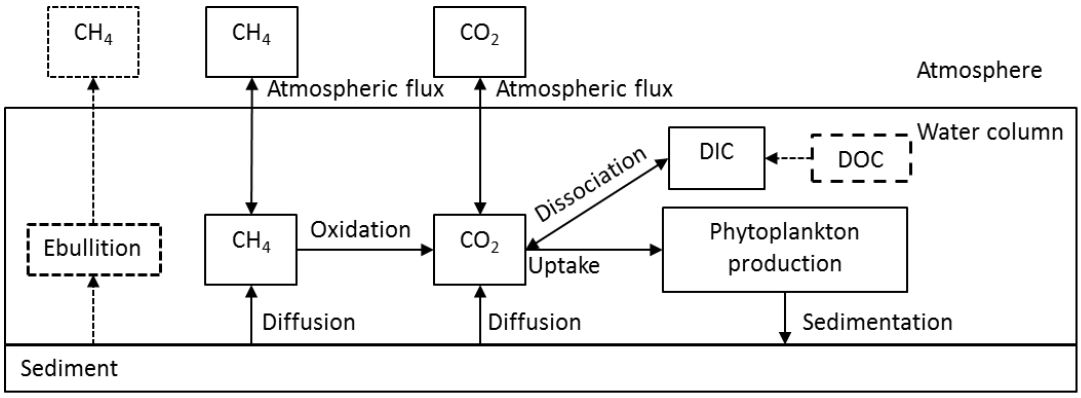

Figure 2.2 Conceptual model of CO_2 and CH_4 annual budget. Ebullition and DOC (dashed box) are not accounted for in the model simulation (see text for details).

2.2.3. Data analysis and the mass balance model

Thermal stratification was indicated by the depth of the thermocline calculated from the CTD temperature profiles. The thermocline depth was defined as the depth of the maximum change in water density calculated from vertical variations in temperature from CTD casts (as salinity is too low to alter density significantly). rLakeAnalyzer (Winslow et al. 2015) was used to compute the thermocline depth (see theoretical basis given by Read et al. 2011).

A conceptual model was developed from which a quantitative model was then used to calculate the whole-lake CO_2 and CH_4 fluxes and mass balance (Figure 2.2). The model calculated rates for processes involved in the loss and gain of CO_2 and CH_4, i.e., 1) diffusion across the sediment-water interface, 2) atmospheric diffusive flux, 3) aerobic oxidation of CH_4, 4) diffusion of CO_2 and CH_4 across the sediment-water interface, 5) CO_2 uptake by phytoplankton, and 6) CO_2 dissociation with from carbonate (Table 2.1). The model assumes that lake sediment is the main source of CO_2 and CH_4. In addition, respiration, CH_4 oxidation and DIC dissociation are expected to supply CO_2 to the water column. Due to the short residence time of the studied lake (1.5 years), it is assumed that that dissolved organic (DOC) mineralization in the lake is low (negligible) (Hanson et al 2011). The occurrence of CH_4 ebullition from the lake sediment was also not included in the model simulation, however, it was assumed that most gas bubbles released rapidly through the water column and thereby escaped CH_4 oxidation. Other processes that may contribute to the whole-lake CO_2 and CH_4 mass balance but were not conceptualized in the model are elaborated upon in the discussion.

The model was used to simulate the whole-lake mass storage of CO_2 and CH_4 over the period of observation (Eq. 1, Table 2.1). The areal mass of CO_2 and CH_4 stored in 2 m depth intervals in the lake was calculated by multiplying concentrations of the gas in each depth by volume and surface area ratio of each layer (Eq. 2, Table 2.1).

Table 2.1 Equations for processes in the CO_2 and CH_4 mass balance estimation. See Table 2.2 for definitions of symbols used in equations.

Equation	Eq. No.	Units	Process definition	Source
$\Delta C_{strg} = \frac{dC_{strg}}{dt}$	(1)	mmol m^{-2} d^{-1}	Observed gas mass change over the sampling period	
$C_{strg} = \sum_{i=1}^{z} \frac{C_{(i)}\ dV_{(i)}}{A_{(i)}}$	(2)	mmol m^{-2}	Whole-lake water column gas storage	1
$J_{gas} = -\emptyset\left(D_{gas}\,\theta^{-2}\right)\left(\frac{dC}{dz}\right)$	(3)	mmol m^{-2} d^{-1}	Sediment-water interface gas diffusion	2
$Rsed_{oxi} = J_{CH4}\,rs$	(4)	mmol m^{-2} d^{-1}	Sediment-water interface CH_4 oxidation	
$Rw_{oxi} = \sum_{i=1}^{z} \frac{K_{CH4-O2}\ CH_{4(i)}\ O_2\ dV_{(i)}}{O_{2sol}\ A_{(i)}}\ e^{Q10\,(temp-20)/10}$	(5)	mmol m^{-2} d^{-1}	Whole lake CH_4 oxidation flux with Arrhenius temperature adjustment	3
$Up = \frac{10.3\ Chl^{1.19}\ V_{surf}}{12.01\ A}(1-ra)$	(6)	mmol m^{-2} d^{-1}	Phytoplankton CO_2 uptake	4
$F_{gas} = corr_k k_{gas}\left(C_{surf} - C_{atm}\right)$	(7)	mmol m^{-2} d^{-1}	Atmospheric gas flux	
$DIC_{diss} = \frac{\sum \Delta HCO_{3-strg}}{n}$	(8)	mmol m^{-2} d^{-1}	Dissociation rate of HCO_3 to CO_2	
$\frac{dCO_{2\_strg}}{dt} = J_{CO2} + Rsed_{oxi} + Rw_{oxi} - F_{CO2} - Up - exDIC_{diss}$	(9)	mmol m^{-2}	CO_2 mass balance model over the sampling period calculated	
$\frac{dCH_{4\_strg}}{dt} = J_{CH4} - Rsed_{oxi} - Rw_{oxi} - F_{CH4}$	(10)	mmol m^{-2}	CH_4 mass balance model over the sampling period calculated	

Sources: [1]Striegl and Michmerhuizen (1998), [2]Berner (1980), [3]Lopes et al. (2011), [4]delGiorgio and Peters (1993).

Table 2.2 Parameters used for CO_2 and CH_4 mass balance calculations.

Symbol	Description	Units	Value	Source
$C_{(i)}$	Concentration of the dissolved gas at layer (i)	µM		
V	Lake volume	m^3		
V_{surf}	Lake volume of 0 to 2 m surface layer	m^3		
A	Lake surface area	m^2		
i	Water column layer			
n	Number of samples			
t	Date of sampling			
D_{gas}	Diffusion coefficient of gas in water at 20°C	cm s^{-1}	CO_2 = 1.42 x 10^{-5}; CH_4 = 1.48 x 10^{-5}	8
θ	Sediment tortuosity		1.1	9
$\emptyset$	Sediment porosity		0.9	10
z	Sediment depth	Cm		
Chl	Chlorophyll *a* concentration	µg L^{-1}		
k_{gas}	Gas exchange coefficient	m d^{-1}		11
C_{surf}	Dissolved gas concentration at the air-water interface	µM		
C_{atm}	Gas solubility concentration calculated from atmospheric molar fraction concentration	µM		12 13
O_2	Dissolved oxygen concentration	µM		
O_{2sol}	Oxygen solubility	µM		14
Parameters used for optimization routine				
$corr_k$	Correction factor for gas exchange coefficient		0.5 – 2.0	
rs	Proportion of dissolved CH_4 sourced from the sediment that is oxidized		0.6 – 0.9	15
$K_{CH4\text{-}O2}$	Aerobic CH_4 oxidation kinetic constant	d^{-1}	0.01 – 6.5	15
ra	Proportion of phytoplankton production that is respired		0.7 – 0.85	16
ex	Dissociation factor		-2 – 2	

Sources: [8]Broecker and Peng (1974), [9] Boudreau (1996), [10] Trolle et al. (2010), [11]Cole and Caraco (1998), [12]Weiss and Price (1980), [13]Wiesenburg and Guinasso (1979), [14]Weiss (1970), [15]Bastviken (2009), [16]Hanson et al. (2004).

The diffusive flux of CO_2 and CH_4 from the sediment to the water column was calculated using Fick's law of diffusion (Eq. 3, Table 2.1) according to Berner (1980). This calculation used the measured vertical concentration gradient in the first 6 cm of the sediment layer. The sediment tortuosity value (θ; Table 2.2) was set to 1.1 (see Boudreau 1996) based on the estimated porosity of sediment ($\emptyset$; Table 2.2) for Lake Okaro of 0.9 (Trolle et al. 2010). Data from Bastviken (2009) suggest that 50 – 95% of CH_4 diffusing out of the sediment (rs; Table 2.2) is oxidized to CO_2 before entering the water column (Eq. 4, Table 2.1). In the water column, CH_4 is oxidized into CO_2 in the presence of dissolved oxygen with an oxidation rate constant ($K_{CH4\text{-}O2}$; Table 2.2) in the range 0.01 – 1.0 d^{-1}, as observed in most eutrophic lakes (Bastviken 2009). In the model, we estimated the water column oxidation rate as a first order reaction following Lopes et al. (2011) with temperature adjustment using a form of the Arrhenius equation (Eq. 5; Table 2.1) with Q_{10} set to 2.2 (Bastviken 2009).

The model was used to calculate CO_2 phytoplankton uptake (Up, Eq. 6; Table 2.1) as the difference between volumetric rate of phytoplankton production and the proportion returned back to the system via autotrophic respiration (ra; Table 2.2). To formulate this, the phytoplankton production estimate (using chlorophyll *a* concentration as a proxy: del Giorgio and Peters, 1993) was multipled by ra. It has been estimated that ra ranged from 50 – 95% (Hanson et al. 2004).

Gas exchange at the air-water interface was calculated using a boundary layer equation (Eq. 7; Table 2.1) with gas exchange coefficient (k_{gas}, Table 2.2) estimated as a function of wind speed (Cole and Caraco 1998). Average monthly speed collected by the National Climate Database (http://cliflo.niwa.co.nz/) was used to feed the calculation. However, due to the uncertainty in the gas transfer coefficient estimates (Dugan et al. in press), a correction factor ($corr_k$; Table 2.2) was added in the gas exchange calculation. It was assumed that the atmospheric CO_2 and CH_4 mole fraction concentrations were constant at 393.5 ppmv and 1.76 ppmv, respectively.

As a soft water lake with alkalinity ~0.6 meq L^{-1} (data not shown), inputs of inorganic carbon from carbonate weathering into Lake Okaro would likely be minor (Marcé et al. 2015). McColl (1972) noted that change in pH in the surface is mostly regulated by phytoplankton productivity while the reduced pH in the hypolimnion is related directly to CO_2 production in the tropholytic zone where decomposition dominates the cycle. Based on this knowledge, I assumed that changes in the whole-lake DIC dynamics are mainly contributed by CO_2 dissociation into the carbonate system. This dissociation and the proportion of CO_2 lost to HCO_3 and vice versa, depend on pH and temperature which may vary on a daily basis. Maberly (1996) recorded that a eutrophic lake had a high diel pH variation (over 2 pH units) during a phytoplankton bloom, while pH values in the mixing period was relatively stable. In the model, a multiplication factor (*ex*; Table 2.2) was introduced to give ranges for the contribution of dissociation to the whole-lake CO_2 mass. This multiplication factor (*ex*) represents the proportion of daily CO_2 mass that dissociates into HCO_3 and vice versa. Therefore, by multiplying *ex* with the whole-lake HCO_3 mass, it was possible to estimate rate of the dissociation (Eq. 6; Table 2.1). Concentrations of HCO_3 were calculated as a function of the observed pH, temperature and CO_2 concentration derived from Stumm and Morgan (1996).

An optimization routine ("L-BFGS-B": R Core Team 2015) was used to derive model parameter values from a given range based on the literature (Table 2.2) by minimizing the residual errors between the modelled whole-lake gas storage (Eqns 9 and 10; Table 2.1) against the calculated gas storage from field observations (Eq. 2; Table 2.1). The performance of the model was tested by calculating the mean absolute error (MAE) between simulation and observation. The cumulative annual storage of gases was estimated based on processes involved in the mass balance (see Table 2.1) by calculating areas under the curve of the modelled process (Eqns 3 to 8) over the period of observation (September 2013 to October 2014). Areas were estimated using the trapezoidal rule (R package Hmisc: Harrell, 2015). Changes in the cumulative annual storage were analyzed

in response to alterations in each model parameter by increasing parameter values derived from model optimization by 10% whilst maintaining all other parameters at their optimized value, and re-calculating CO_2 and CH_4 cumulative annual storage. Finally, the total greenhouse gas emissions (in kg CO_2-eq m^{-2} y^{-1}) was calculated as the sum of modelled annual CO_2 and CH_4 atmospheric diffusive fluxes (Eq. 7) and multiplied each gas flux by its global warming potential (GWP) over a 100 year period (i.e., CO_2 = 1, CH_4 = 34; Myhre et al. 2013; IPCC 2007).

2.3. Results

2.3.1. Thermal stratification and dissolved oxygen concentration

Over the period of September 2013 to October 2014, Lake Okaro started to stratify around September 2013 (spring, southern hemisphere) and was completely mixed (i.e., isothermal) on 25 June 2014 (winter, Figure 2.3A). The shallowest recorded thermocline depth was 3.1 m (10 October 2013) and the thermocline depth gradually increased thereafter. Surface water temperature increased steadily from 11.6 °C (17 September 2013) to a maximum of 23.4 °C (17 December 2013, early summer) and continued to decrease gradually thereafter.

Dissolved oxygen (DO) concentration was relatively low (< 5 mg L^{-1}) throughout water column at the onset of lake turnover (5 June 2014), except in near-bottom water where anoxia (< 1 mg L^{-1}) occurred (Figure 2.3B). After a period of sustained mixing (30 July 2014), the DO concentration in the whole water column was around 8 mg L^{-1}. In the early period of stratification (17 September 2013 and 29 August 2014), supersaturation of DO was observed in the epilimnion and concentrations exceeded 11.0 mg L^{-1}. On the other hand, DO concentrations in the hypolimnion decreased gradually as stratification established (17 September 2013 and 23 September 2014) and the hypolimnion was completely anoxic (< 1 mg L^{-1}) in the middle of summer (18 February 2014) and until complete breakdown of stratification (25 June 2014).

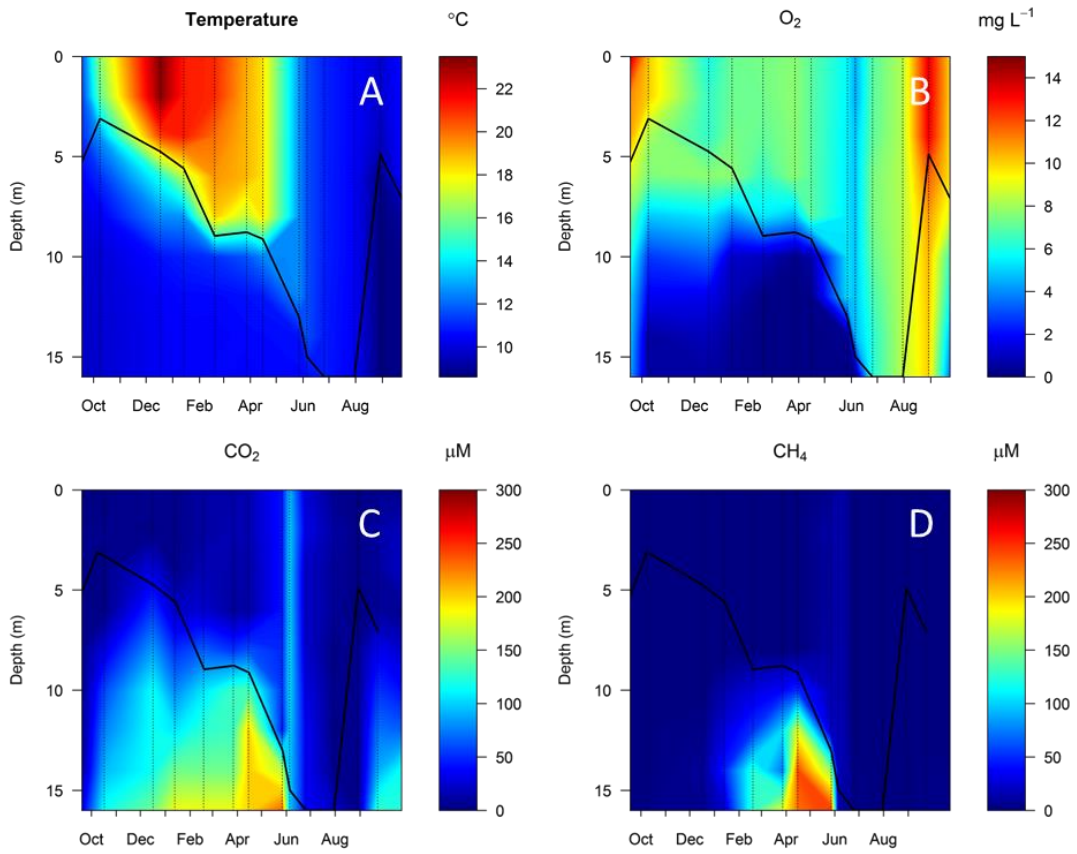

Figure 2.3 Temperature (A) and concentrations of dissolved oxygen (O_2) (B), CO_2 (C) and CH_4 (D) in Lake Okaro over a one-year period (September 2013 to October 2014). Solid black lines indicate calculated thermocline depth, dashed vertical lines indicate day of sampling.

2.3.2. CO_2 and CH_4 concentration and storage dynamics

In general, during the stratification period, concentrations of dissolved CO_2 and CH_4 in the epilimnion were mostly low, <1 – 15.4 µmol L^{-1} and 0.1 – 1.4 µmol L^{-1}, respectively (Figures 2.3C and 2.3D). In contrast, concentrations in the hypolimnion were relatively high, reaching >230 and >240 µmol L^{-1} for CO_2 and CH_4, respectively. While hypolimnetic CO_2 concentrations started to increase following the depletion of DO in the hypolimnion, CH_4 concentrations increased later, as the bottom water became anoxic. The maximum bottom water (16 m depth) concentrations of CO_2 and CH_4 occurred just before stratification break down (27 May 2014). On this sampling day epilimnetic CO_2 and CH_4 concentrations were also high, 43.4 – 52.7 µmol L^{-1} and 6.5 – 19.9 µmol L^{-1}, respectively.

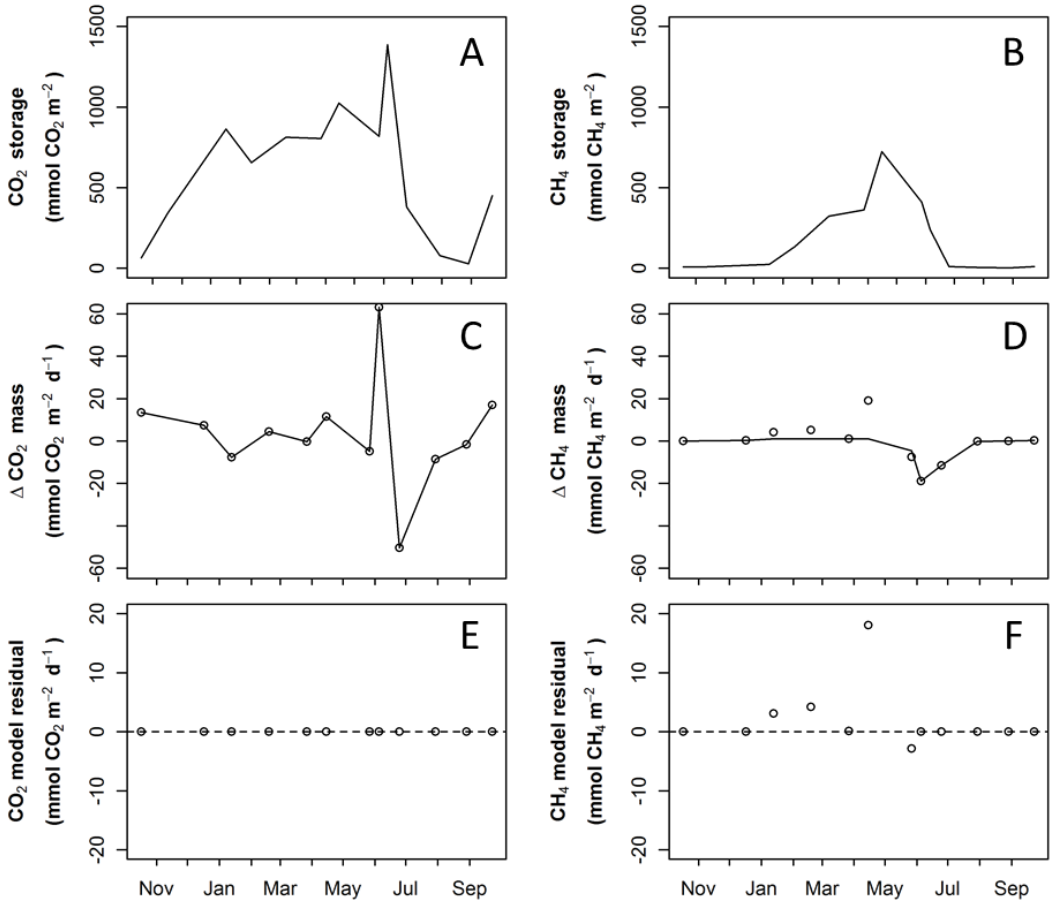

Figure 2.4 Whole-lake mass storage (A and B), whole-lake mass storage change rate (Δ mass) (C and D) and mass balance model residuals against the observation (E and F) of CO_2 and CH_4 in Lake Okaro. Open dots and solid lines in the whole-lake mass storage rate of change (C and D) represent field observations and model output, respectively.

At the onset of the turnover, concentrations of CO_2 and CH_4 in the whole water column were relatively uniform, 93.0 – 102.4 µmol L^{-1} and 15.6 – 20.0 µmol L^{-1}, respectively (Figure 2.3). Porewater concentrations of CO_2 and CH_4 ranged from 2.0 to 5.8 mmol L^{-1} and 0.5 to 3.1 mmol L^{-1}, respectively (Supplementary Information Figure S1). I calculated that 2.24 and 2.22 mmol m^{-2} d^{-1} of CO_2 and CH_4, respectively, were released from the bottom sediment to the water column (see Eq. 3; Table 2.1).

Table 2.3 CO_2 and CH_4 mass balance model over a one-year period in Lake Okaro and its response to model parameter changes. The model yielded estimates of processes involved in mmol m^{-2} y^{-1}. Response of model parameter alterations is presented in percent change of the mass balance.

	CO_2	CH_4
Processes involved		
Sediment flux	832.4	825.0
Atmospheric flux	-4.0	-260.3
CH_4 oxidation at sediment-water interface	NA	-512.4
CH_4 oxidation in the water column	NA	-631.4
Inputs from CH_4 oxidation	1143.8	NA
Phytoplankton uptake	-699.9	NA
DIC exchange	31.6	NA
Mass balance residuals*	1367.6	-571.0
Increasing model parameter by 10%		
$corr_k$	-0.03	-5.7
Rs	3.7	-8.9
$K_{CH4\text{-}O2}$	4.6	-11.0
Ra	14.5	NA
Ex	0.2	NA

Negative and positive values represent loss and gain of gas, respectively, due to one of the identified processes. NA is not available due to the nature of the process. * Mass balance residuals are calculated as mmol m^{-2}.

The dynamics of CO_2 and CH_4 concentrations reflect the temporal variations of storage in the lake. Whole-lake CO_2 mass increased at rate of 3.4 mmol CO_2 m^{-2} d^{-1} as stratification developed, mostly in hypolimnion (Figure 2.4A). An abrupt increase in the rate of whole-lake storage was calculated to occur on 5 June 2014 (63.1 mmol CO_2 m^{-2} d^{-1}) when storage was estimated to be 1412 mmol CO_2 m^{-2}. This change coincided with the deepening of the thermocline depth to 15 m. Within 20 days (by 25 June 2014), CO_2 storage in the lake had fallen to 404 mmol m^{-2} and it continued to drop to 53 mmol m^{-2} while the lake was mixed (to 29 August 2014). At the onset of stratification the rate of loss of CO_2 was 50.3 mmol m^{-2} d^{-1}, reducing progressively to 1.6 mmol m^{-2} d^{-1} as stratification started to develop in September.

Unlike CO_2, the whole-lake mass of CH_4 gradually increased during summer, at a rate c. 2.6 mmol m^{-2} d^{-1}), and reached a peak (723 mmol m^{-2}) in autumn (15 April 2014, Figure 2.4B). As the thermocline deepened nearing the end of summer stratification (27 May 2014), the accumulated CH_4 in the lake started to decline. This loss of CH_4 was calculated to be 7.4 mmol m^{-2} d^{-1} (27 May 2014) and was maximal at 18.8 mmol m^{-2} d^{-1} during the onset of the mixing (5 June 2014; Figure 2.4D). However, during the mixing period (25 June – 29 August 2014) the flux was reduced to <0.1 mmol m^{-2} d^{-1}, and only 2.3 mmol CH_4 m^{-2} remained in the lake by 29 August 2014.

2.3.3. Mass balance model output and the global warming potential

In general, the modelled change in whole-lake mass storage showed relatively good agreement with the field observations (n = 12, Figure 2.4C to 2.4F). The change in the modelled CO_2 mass storage had low mean absolute error (MAE < 10^{-5} mmol m^{-2} d^{-1}, p< 0.001), while for CH_4 the model had a moderate level of error (MAE = 2.3 mmol m^{-2} d^{-1}, p<0.001). The model output for the sediment release rate (to the water column) was 832.4 mmol m^{-2} y^{-1} of CO_2 and 825.0 mmol m^{-2} y^{-1} of CH_4 (Table 2.3). However, it was calculated that 62% of CH_4 flux from the sediment was oxidized at the sediment-water interface. Collectively, oxidation at both the sediment-water interface and in the water column increased CO_2 storage in the lake by 1,143.8 mmol m^{-2} over the annual cycle (September 2013 – October 2014) (Table 2.3).

Increasing one of the optimized model parameter values (Supplementary Information Figure S2) by 10% changed cumulative annual gas storage in the lake (Table 2.3). For ra, that increase would increase whole-lake CO_2 annual storage by around 14.5% while increasing $K_{CH4\text{-}O2}$ by 10% would reduce the whole-lake CH_4 storage by 11.0%.

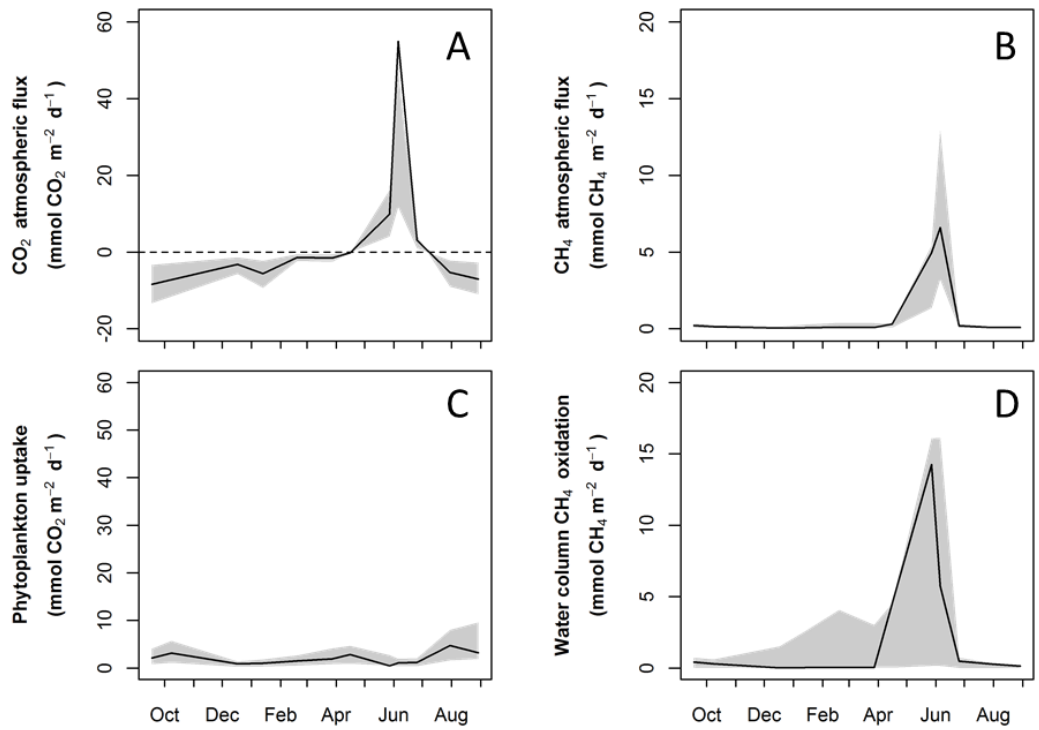

Figure 2.5 Seasonal dynamics of atmospheric flux of CO_2 (A) and CH_4 (B), water column CH_4 oxidation (C) and phytoplankton CO_2 uptake (D) for Lake Okaro calculated from the mass balance model. Shaded areas indicate the range of outputs calculated from literature values (Table 2.2), solid lines represent model outputs. Positive and negative values represent loss and gain of gas, respectively.

The model values indicated that both CO_2 and CH_4 were released to the atmosphere as pulsed emissions of up to 54.9 and 6.6 mmol m^{-2} d^{-1}, respectively (Figures 2.5A and 2.5B). Most of the time the CO_2 flux was from the atmosphere to the lake, nevertheless it was estimated that there was a net annual average emission of 4.0 mmol CO_2 m^{-2} from the lake to the atmosphere. Methane was emitted throughout the year at an annual average emission rate of 260 mmol m^{-2}. Based on these calculations, the total annual greenhouse gas emission (CO_2 and CH_4 combined) from Lake Okaro is 8.8 mol CO_2-eq m^{-2} y^{-1} (~0.39 kg CO_2-eq m^{-2} y^{-1}).

2.4. Discussion

The dynamics of dissolved CO_2 and CH_4 of the lake in this study were strongly seasonally dominated. This pattern was similar to observations in

other monomictic lakes and in dimictic lakes, with at least four distinguishable periods (Striegl and Michmerhuizen, 1998; Riera et al. 1999; López Bellido et al. 2011). These periods relate to, firstly, dissolved gas (CO_2 and CH_4) accumulation in the hypolimnion as stratification begins in spring, secondly, high concentrations of dissolved gas in the hypolimnion and low concentrations in the surface layer during summer stratification, thirdly high dissolved gas concentrations in the surface layer, as well as high atmospheric fluxes at the onset of breakdown of stratification in autumn, and lastly, rapid loss of dissolved gases in the surface water due to evasion, phytoplankton uptake, and CH_4 oxidation during the period of turnover. Additionally, I observed that progressive deepening of the thermocline gradually entrained CO_2 and CH_4 from the hypolimnion prior to complete water column mixing. When fully mixed, high releases of CO_2 and CH_4 to the atmosphere was occurred (Figures 2.3C, 2.3D, 2.5A and 2.5B).

The mass balance model potentially explained the major processes that contribute to the loss and gain of CO_2 and CH_4 from the lake. The bottom sediment flux was identified as the main source of CO_2 and CH_4 to the lake. It arises from high rates of remineralization of organic carbon accumulated in the bottom sediments (Kuivila et al. 1998). The surficial sediment of Lake Okaro has high concentrations of organic carbon compared with other lakes in the same region (Trolle et al. 2008). The sediment carbon consists of two fractions; permanently buried material which is refractory and metabolizable material which is labile (Berner 1980). The latter is readily remineralized and released back into overlying waters as CO_2 and CH_4, as well as dissolved organic carbon (DOC) and dissolved inorganic carbon (DIC).

The model was used to identify that together with water column oxidation, instantaneous oxidation at the sediment-water interface played a major role in CH_4 removal from the lake (Table 3). Annually, only ~ 31% of CH_4 produced in the sediment escapes to the atmosphere via diffusive fluxes. During mixing, dissolved oxygen in the whole water column was sufficient

to remove CH_4 by oxidation at rates almost three times higher than diffusive flux to the atmosphere from the lake (Figure 2.5B and 2.5D). However, statistical analysis of the performance of the model in simulating the whole-lake CH_4 accumulation was modest for the period of summer stratification, and processes such as ebullition of CH_4 were not simulated (see Method). McGinnis et al. (2006) showed that as CH_4 bubbles rise following release from the sediment, a large proportion of the CH_4 in each bubble dissolves into overlying waters. The dissolution rate depends on the bubble size and the concentration of CH_4 in the ambient water. Ebullition may have resulted in additional accumulation of CH_4 in the water column of Lake Okaro. Fluxes to the atmosphere from ebullition can account for >80% of total CH_4 fluxes from the lake to the atmosphere (DelSontro et al. 2010; Martinez and Anderson 2013). On the other hand, while there might be substantial dissolution of CH_4 associated with rising bubbles in the epilimnion, CH_4 might readily be oxidized due to elevated levels of dissolved oxygen (Figure 2.4B). The estimates of CH_4 emissions from Lake Okaro in this study, therefore, should be viewed as conservative and apply only to diffusive fluxes of CH_4.

Lake Okaro was a sink for CO_2 most of the time except for the pulsed emission at the onset of mixing (Figure 2.4). Eutrophic lakes with high rates of primary productivity deplete CO_2 in the surface layer to below atmospheric saturation concentrations (del Giorgio et al. 1999) and it is therefore widely accepted that they are sinks for CO_2 (Balmer and Downing 2011). On the other hand CO_2 generally accumulates in the hypolimnion as a result of the CO_2 sediment flux, and from CH_4 oxidation where there is adequate oxidation status to support this process. McColl (1972) noted that CO_2 dynamics in Lake Okaro is strongly regulated by algal productivity in the surface waters and organic carbon decomposition in the sediment. Although it has been suggested that oxidation of terrestrial-derived DOC may subsidize CO_2 storage (Sobek et al. 2003), however, as the DOC concentration in this lake relatively low (~5.2 mg L^{-1}; Bay of Plenty Regional Council, unpublished data), DOC oxidation would likely provide only a minor CO_2 subsidy. The quality of DOC in Lake Okaro

is considered to be humic-like suggesting that recalcitrant organic matter is dominant (Hartland pers. Comm 2016). This implies that biological remineralization of the DOC in the water column would be very low.

In low-alkalinity lakes, e.g., Lake Okaro < 1 meq L^{-1}, inputs of inorganic carbon from carbonate weathering would also be relatively unimportant (Marcé et al. 2015). Although diel variation of pH in Lake Okaro reaches 2 pH units during spring and summer stratification (see http://monitoring.boprc.govt.nz/), dissociation of DIC species due to pH and temperature variation also seems to be a minor influence for the whole-lake CO_2 mass, as evidenced by changing the parameter ex, where a 10% increase only increased whole-lake CO_2 in the mass balance by 0.2% (Table 3).

This model could also explain changes in the mass of carbon gases due to the alteration of one or more of the processes (Table 3). Increasing CH_4 oxidation (rs and $K_{CH4\text{-}O2}$) efficiently removed CH_4 from the lake but also contributed to a small increase of whole-lake CO_2 storage. Hence, knowing that global warming potential (GWP) of CH_4 over a 100-year horizon is 34 times larger than that of CO_2 (Myhre et al. 2013), greenhouse gas emissions from this lake, as well as from other eutrophic lakes in general, will be reduced by increasing CH_4 oxidation. Hypolimnetic oxygenation (Debroux et al. 2012), for example, can be one alternative to support water column CH_4 oxidation. Future global change predictions include climate warming and increased nutrient loads from land use intensification, which are expected to result in eutrophication, with more frequent and prolonged occurrence of anoxic hypolimnia as thermal stratification is extended (Foley et al. 2012). Hypolimnetic oxygenation may prevent large quantities of CH_4 accumulation and, consequently, reduce the storage flux during lake overturn. Additionally, such a technique might beneficially reduce NH_4 accumulation in the hypolimnion (Liboriussen et al. 2009), as NH_4 plays a role in inhibiting CH_4 oxidation (Bodelier and Steenbergh, 2014).

Based on the mass balance approach, Lake Okaro could be considered as a net carbon emitter and it therefore contributes to global warming. Furthermore, knowing that the lake accumulates a large quantity of NH_4 in the hypolimnion during stratification (Özkundakci et al. 2011) and that a large proportion of this material may only undergo partial nitrification to nitrous oxide (N_2O) during seasonal mixing, it would be expected that nitrous oxide (N_2O) could be an important contributor to greenhouse gas emissions from the lake. Downes (1991) calculated that ~0.6 µmol m^{-2} d^{-1} of N_2O was emitted from Lake Okaro at a time when the lake was in an early phase of stratification (October to December 1981). Emissions of N_2O would be expected to align temporally with those of CH_4, and occur mostly in the early mixing phase preceding overturn (May) and last until re-stratification (October), as N_2O might not be detected in the water column during thermal stratification (Downes 1991), then the total N_2O emission from Lake Okaro could be estimated to occur only in 240 days, yielding 144 µmol m^{-2} y^{-1}. This emission equates to 0.018 kg CO_2-eq m^{-2} y^{-1} (GWP N_2O = 298: Myhre et al. 2013). Thus, by combining this estimate and the carbon emission calculated above, the total greenhouse gas emissions from Lake Okaro is estimated to be 0.408 kg CO_2-eq m^{-2} y^{-1}.

Recently, Holgerson and Raymond (2016) reported that, in global average, small lakes release more CO_2 and CH_4 to the atmosphere. They calculated that lakes which have surface area of 0.1 to 1 km^2 would emit 23.87 mmol CO_2 m^{-2} d^{-1} and 0.16 mmol CH_4 m^{-2} d^{-1}. Within the same surface area, on daily average, Lake Okaro releases 0.01 mmol m^{-2} and 0.71 mmol m^{-2} of CO_2 and CH_4, respectively. This may suggest that in terms of CO_2 emission, eutrophic lake, e.g. Lake Okaro, emit less CO_2 than the global lake average but releasing higher CH_4. Barros et al. (2011) calculated that total CO_2 and CH_4 emissions for lakes as a whole across the globe as 3,743 Tg CO_2-eq y^{-1}. McCrackin and Elser (2011) computed that N_2O release from lakes averages 1.02 Tg N_2O y^{-1}, which equates to 10.9 Tg CO_2-eq y^{-1}. These values yield an areal rates of 0.893 kg CO_2-eq m^{-2} y^{-1} based on the total surface area of the world's lakes of 4.2 x 10^{12} m^2 (Downing et al. 2006). By comparison the areal rate of greenhouse gas

emissions for Lake Okaro of 0.408 kg CO_2-eq m^{-2} y^{-1} is about half of the rate used in the global estimates (Figure 2.6).

In summary, these results show that biological processes (i.e., phytoplankton uptake and CH_4 oxidation) in a eutrophic monomictic lake may remove a substantial amount of CO_2 and CH_4 in the water column. Hence, only a small proportion of CO_2 and CH_4 produced in the sediment escapes to the atmosphere through diffusive flux. However, a substantial amount of the accumulated gases was entrained when the lake mixed. Dissolution of CH_4 from gas bubbles, although not accounted for in the mass balance analysis, is likely to contribute to accumulation of CH_4 in the hypolimnion. These results also underscore the importance of eutrophic lakes in global warming and indicate that further measurements and analysis are required to refine estimates for individual lakes and improve extrapolation estimates relevant to the global scale.

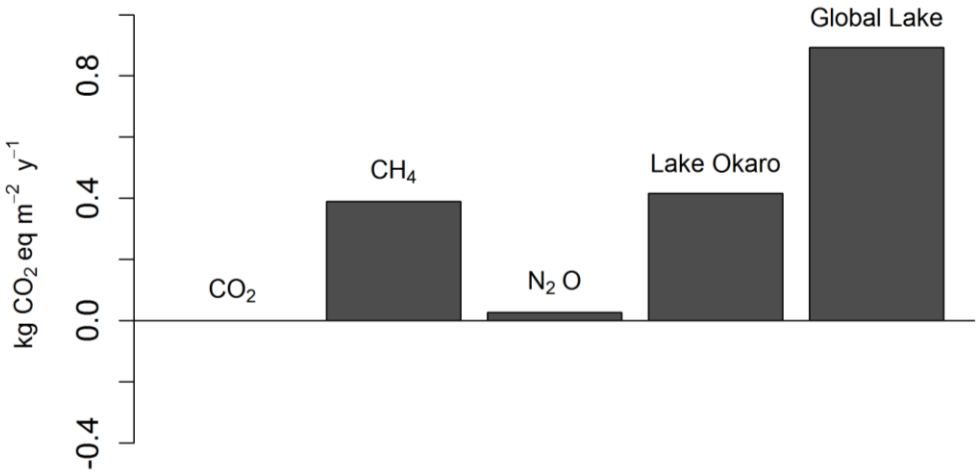

Figure 2.6 Estimated annual areal greenhouse emission rates (CO_2, CH_4 and N_2O combined) from Lake Okaro and for lakes globally (Barros et al. 2011; McCrackin and Elser 2010).

2.5. References

Algesten G, Sobek S, Bergström AK, et al (2005) Contribution of sediment respiration to summer CO_2 emission from low productive boreal and subarctic lakes. Microb Ecol 50:529–535. doi: 10.1007/s00248-005-5007-x

APHA (1998) Standard methods for the examination of water and wastewater, 20th edn. APHA-AWWA-WEF, Washington, D.C.

Balmer MB, Downing JA (2011) Carbon dioxide concentrations in eutrophic lakes : undersaturation implies atmospheric uptake. Inl Waters 125–132. doi: 10.5268/IW-1.2.366

Barros N, Cole JJ, Tranvik LJ, et al (2011) Carbon emission from hydroelectric reservoirs linked to reservoir age and latitude. Nat Geosci 4:593–596. doi: 10.1038/ngeo1211

Bastviken D (2009) Methane. In: Likens GE (ed) Encyclopedia of Inland Waters. Academic Press, Oxford, pp 783–805

Bastviken D, Cole J, Pace M, Tranvik L (2004) Methane emissions from lakes: Dependence of lake characteristics, two regional assessments, and a global estimate. Global Biogeochem Cycles 18:1–12. doi: 10.1029/2004GB002238

Bastviken D, Tranvik LJ, Downing JA, et al (2011) Freshwater Methane Emissions Offset the Continental Carbon Sink. Science 331:50-50.

Berner RA (1980) Early diagenesis: A theoretical approach. Princeton University Press. Princeton. New Jersey

Bodelier PL., Laanbroek HJ (2004) Nitrogen as a regulatory factor of methane oxidation in soils and sediments. FEMS Microbiol Ecol 47:265–277. doi: 10.1016/S0168-6496(03)00304-0

Borrel G, Jézéquel D, Biderre-Petit C, et al (2011) Production and consumption of methane in freshwater lake ecosystems. Res Microbiol 162:833–847. doi: 10.1016/j.resmic.2011.06.004

Boudreau BP (1996) A method-of-lines code for carbon and nutrient diagenesis in aquatic sediments. Comput Geosci 22:479–496. doi: 10.1016/0098-3004(95)00115-8

Cole JJ, Caraco NF (1998) Atmospheric exchange of carbon dioxide in a low-wind oligotrophic lake measured by the addition of SF6. Limnol Oceanogr 43:647–656. doi: 10.4319/lo.1998.43.4.0647

Debroux J-F, Beutel MW, Thompson CM, Mulligan S (2012) Design and testing of a novel hypolimnetic oxygenation system to improve water quality in Lake Bard, California. Lake Reserv Manag 28:245–254. doi: 10.1080/07438141.2012.716501

del Giorgio PA, Cole JJ, Caraco NF, Peters RH (1999) Linking planktonic biomass and metabolism to net gas fluxes in northern temperate lakes. Ecology 80:1422–1431.

del Giorgio PA, Peters RH (1993) Balance between phytoplankton production and plankton respiration in lakes. Can J Fish Aquat Sci 50:282–289. doi: 10.1139/f93-032

DelSontro T, McGinnis DF, Sobek S, et al (2010) Extreme methane emissions from a swiss hydropower reservoir: contribution from bubbling sediments. Environ Sci Technol 44:2419–2425. doi: 10.1021/es9031369

Downes MT (1991) The production and consumption of nitrate in an eutrophic lake during early stratification. Arch für Hydrobiol 122:257–274.

Downing JA, Cole JJ, Middelburg JJ, et al (2008) Sediment organic carbon burial in agriculturally eutrophic impoundments over the last century. Global Biogeochem Cycles 22:1–10. doi: 10.1029/2006GB002854

Downing JA, Prairie YT, Cole JJ, et al (2006) The global abundance and size distribution of lakes, ponds, and impoundments. Limnol Oceanogr 51:2388–2397. doi: 10.4319/lo.2006.51.5.2388

Fernández JE, Peeters F, Hofmann H (2014) Importance of the autumn overturn and anoxic conditions in the hypolimnion for the annual methane emissions from a temperate lake. Environ Sci Technol 48:7297–7304. doi: 10.1021/es4056164

Foley B, Jones ID, Maberly SC, Rippey B (2012) Long-term changes in oxygen depletion in a small temperate lake: Effects of climate change and eutrophication. Freshw Biol 57:278–289. doi: 10.1111/j.1365-2427.2011.02662.x

Forsyth DJ, Dryden SJ, James MR, Vincent WF (1988) The Lake Okaro ecosystem 1. Background limnology. New Zeal J Mar Freshw Res 22:17–27. doi: 10.1080/00288330.1988.9516274

Hanson PC, Hamilton DP, Stanley EH, et al (2011) Fate of allochthonous dissolved organic carbon in lakes: A quantitative approach. PLoS One. doi: 10.1371/journal.pone.0021884

Hanson PC, Pollard AI, Bade DL, et al (2004) A model of carbon evasion and sedimentation in temperate lakes. Glob Chang Biol 10:1285–1298. doi: 10.1111/j.1365-2486.2004.00805.x

Hanson PC, Bade DL, Carpenter SR, Kratz TK (2003) Lake metabolism: Relationships with dissolved organic carbon and phosphorus. Limnol Oceanogr 48:1112–1119. doi: 10.4319/lo.2003.48.3.1112

Harrell FEJ (2015) Hmisc: Harrell miscellaneous. R package version 3.15-0. http://cran.r-project.org/package=Hmisc.

Holgerson MA, Raymond PA (2016) Large contribution to inland water CO_2 and CH_4 emissions from very small ponds. Nature Geosci. doi: 10.1038/NGEO2654

Huttunen JT, Väisänen TS, Hellsten SK, Martikainen PJ (2006) Methane fluxes at the sediment–water interface in some boreal lakes and reservoirs. Boreal Environ Res 11:27–34.

Huttunen JT, Alm J, Liikanen A, et al (2003) Fluxes of methane, carbon dioxide and nitrous oxide in boreal lakes and potential anthropogenic effects on the aquatic greenhouse gas emissions. Chemosphere 52:609–621. doi: 10.1016/S0045-6535(03)00243-1

IPCC (2007) Climate change 2007: The Physical Science Basis. Contribution of Working Group I to the Fourth Assessment Report of the Intergovernmental Panel on Climate Change. Cambridge University Press, Cambridge, United Kingdom and New York, NY, USA

Juutinen S, Rantakari M, Kortelainen P, et al (2009) Methane dynamics in different boreal lake types. Biogeosciences 6:209–223. doi: 10.5194/bg-6-209-2009

Kankaala P, Taipale S, Nykänen H, Jones RI (2007) Oxidation, efflux, and isotopic fractionation of methane during autumnal turnover in a polyhumic, boreal lake. J Geophys Res Biogeosciences 112:1–7. doi: 10.1029/2006JG000336

Kuivila KM, Murray JW, Devol AH, et al (1988) Methane cycling in the sediments of Lake Washington. Limnol Oceanogr 33:571–581. doi: 10.4319/lo.1988.33.4.0571

Liboriussen L, Søndergaard M, Jeppesen E, et al (2009) Effects of hypolimnetic oxygenation on water quality: Results from five Danish lakes. Hydrobiologia 625:157–172. doi: 10.1007/s10750-009-9705-0

López Bellido J, Peltomaa E, Ojala A (2011) An urban boreal lake basin as a source of CO_2 and CH_4. Environ Pollut 159:1649–1659. doi: 10.1016/j.envpol.2011.02.042

Maberly SC, Barker PA, Stott AW, et al (2013) Catchment productivity controls CO_2 emissions from lakes. Nat Clim Chang 3:391–394. doi: 10.1038/nclimate1748

Maberly SC (1996) Diel, episodic and seasonal changes in pH and concentrations of inorganic carbon in a productive lake. Freshw Biol 35:579–598. doi: 10.1111/j.1365-2427.1996.tb01770.x

Marcé R, Obrador B, Morguí J-A, et al (2015) Carbonate weathering as a driver of CO_2 supersaturation in lakes. Nat Geosci 8:107–111. doi: 10.1038/ngeo2341

Martinez D, Anderson MA (2013) Methane production and ebullition in a shallow, artificially aerated, eutrophic temperate lake (Lake Elsinore, CA). Sci Total Environ 454-455:457–465. doi: 10.1016/j.scitotenv.2013.03.040

McColl RHS (1972) Chemistry and trophic status of seven New Zealand lakes. New Zeal J Mar Freshw Res 6:399–447. doi: 10.1080/00288330.1972.9515437

McCrackin ML, Elser JJ (2011) Greenhouse gas dynamics in lakes receiving atmospheric nitrogen deposition. Global Biogeochem Cycles 25:n/a–n/a. doi: 10.1029/2010GB003897

McGinnis DF, Greinert J, Artemov Y, et al (2006) Fate of rising methane bubbles in stratified waters: How much methane reaches the atmosphere? J Geophys Res Ocean 111:1–15. doi: 10.1029/2005JC003183

Moss B, Kosten S, Meerhof M, et al (2011) Allied attack: climate change and eutrophication. Inl Waters 1:101–105. doi: 10.5268/IW-1.2.359

Myhre G, Shindell D, Bréon F-M, et al (2013) Anthropogenic and Natural Radiative Forcing. In: Stocker T.F., Qin D., Plattner G.-K., Tignor M., Allen S.K., Boschung J., Nauels A. , Xia Y. BV and MPM (ed) Climate Change 2013: The Physical Science Basis. Contribution of Working Group I to the Fifth Assessment Report of the Intergovernmental Panel on Climate Change. Cambridge University Press, Cambridge, United Kingdom and New York, NY, USA, pp 659–740

Ortiz-Llorente MJ, Alvarez-Cobelas M (2012) Comparison of biogenic methane emissions from unmanaged estuaries, lakes, oceans, rivers and

wetlands. Atmos Environ 59:328–337. doi: 10.1016/j.atmosenv.2012.05.031

Özkundakci D, Hamilton DP, Gibbs MM (2011) Hypolimnetic phosphorus and nitrogen dynamics in a small, eutrophic lake with a seasonally anoxic hypolimnion. Hydrobiologia 661:5–20. doi: 10.1007/s10750-010-0358-9

Paul WJ, Hamilton DP, Gibbs MM (2008) Low-dose alum application trialled as a management tool for internal nutrient loads in Lake Okaro, New Zealand. New Zeal J Mar Freshw Res 42:207–217. doi: 10.1080/00288330809509949

Raymond PA, Hartmann J, Lauerwald R, et al (2013) Global carbon dioxide emissions from inland waters. Nature 503:355–359. doi: 10.1038/nature12760

Read JS, Hamilton DP, Jones ID, et al (2011) Derivation of lake mixing and stratification indices from high-resolution lake buoy data. Environ Model Softw 26:1325–1336.

Riera JL, Schindler JE, Kratz TK (1999) Seasonal dynamics of carbon dioxide and methane in two clear-water lakes and two bog lakes in northern Wisconsin, U.S.A. Can J Fish Aquat Sci 274:1–10. doi: 10.1139/f98-182

Sobek S, Algesten G, Bergström A-K, et al (2003) The catchment and climate regulation of pCO_2 in boreal lakes. Glob Chang Biol 9:630–641.

Striegl RG, Michmerhuizen CM (1998) Hydrologic influence on methane and carbon dioxide dynamics at two north-central Minnesota lakes. Limnol Oceanogr 43:1519–1529. doi: 10.4319/lo.1998.43.7.1519

Tranvik LJ, Downing JA, Cotner JB, et al (2009) Lakes and reservoirs as regulators of carbon cycling and climate. Limnol Oceanogr 54:2298–2314. doi: 10.4319/lo.2009.54.6_part_2.2298

Trolle D, Hamilton DP, Hendy C, Pilditch C (2008) Sediment and nutrient accumulation rates in sediments of twelve New Zealand lakes: influence of lake morphology, catchment characteristics and trophic state. Mar Freshw Res 59:1067–1078. doi: http://dx.doi.org/10.1071/MF08131

Vachon D, del Giorgio PA (2014) Whole-Lake CO_2 dynamics in response to storm events in two morphologically different lakes. Ecosystems 1338–1353. doi: 10.1007/s10021-014-9799-8

Wand U, Samarkin VA, Nitzsche H-M, Hubberten H-W (2006) Biogeochemistry of methane in the permanently ice-covered Lake Untersee, central Dronning Maud Land, East Antarctica. Limnol Oceanogr 51:1180–1194. doi: 10.4319/lo.2006.51.2.1180

Weiss RF, Price BA (1980) Nitrous oxide solubility in water and seawater. Mar Chem 8:347–359. doi: 10.1016/0304-4203(80)90024-9

Weiss RF (1970) The solubility of nitrogen, oxygen and argon in water and seawater. Deep Sea Res Oceanogr Abstr 17:721–735. doi: 10.1016/0011-7471(70)90037-9

Wiesenburg DA, Guinasso NL (1979) Equilibrium solubilities of methane, carbon monoxide, and hydrogen in water and sea water. J Chem Eng Data 24:356–360. doi: 10.1021/je60083a006

Winslow L, Read J, Woolway R, et al (2015) rLakeAnalyzer: Package for the Analysis of Lake Physics.R package version 1.7.3. http://CRAN.R-project.org/package=rLakeAnalyzer

Supplementary information

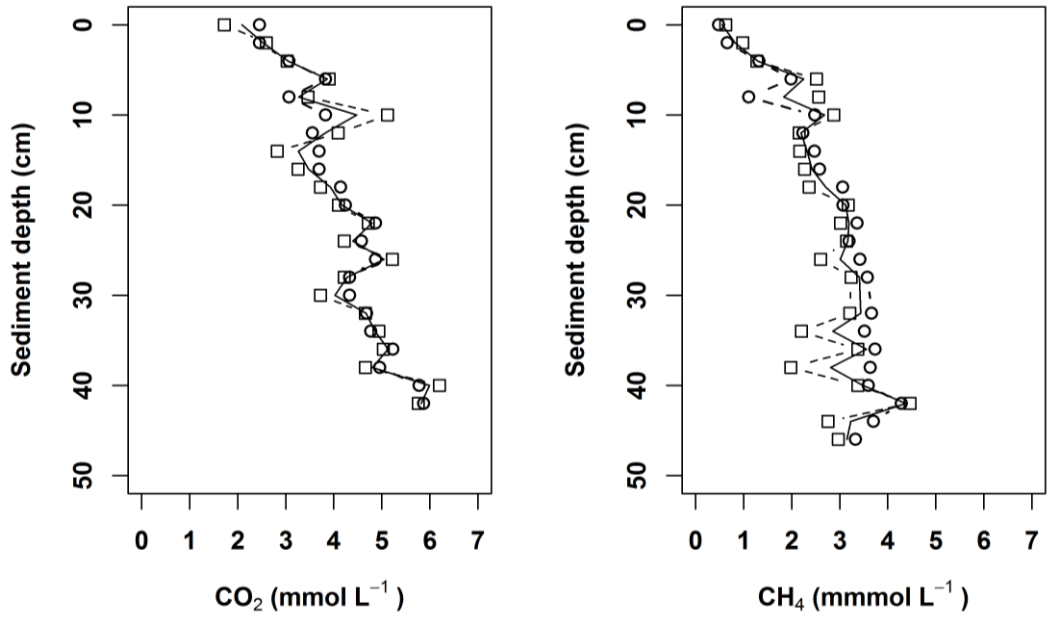

Figure S1. Concentration profile of CO_2 and CH_4 in the lakebed sediments based on peeper incubations over a one-month period, May to June 2014 (○) and August to September 2014 (□). Solid lines indicate mean values of concentrations from the two incubation periods (dashed lines).

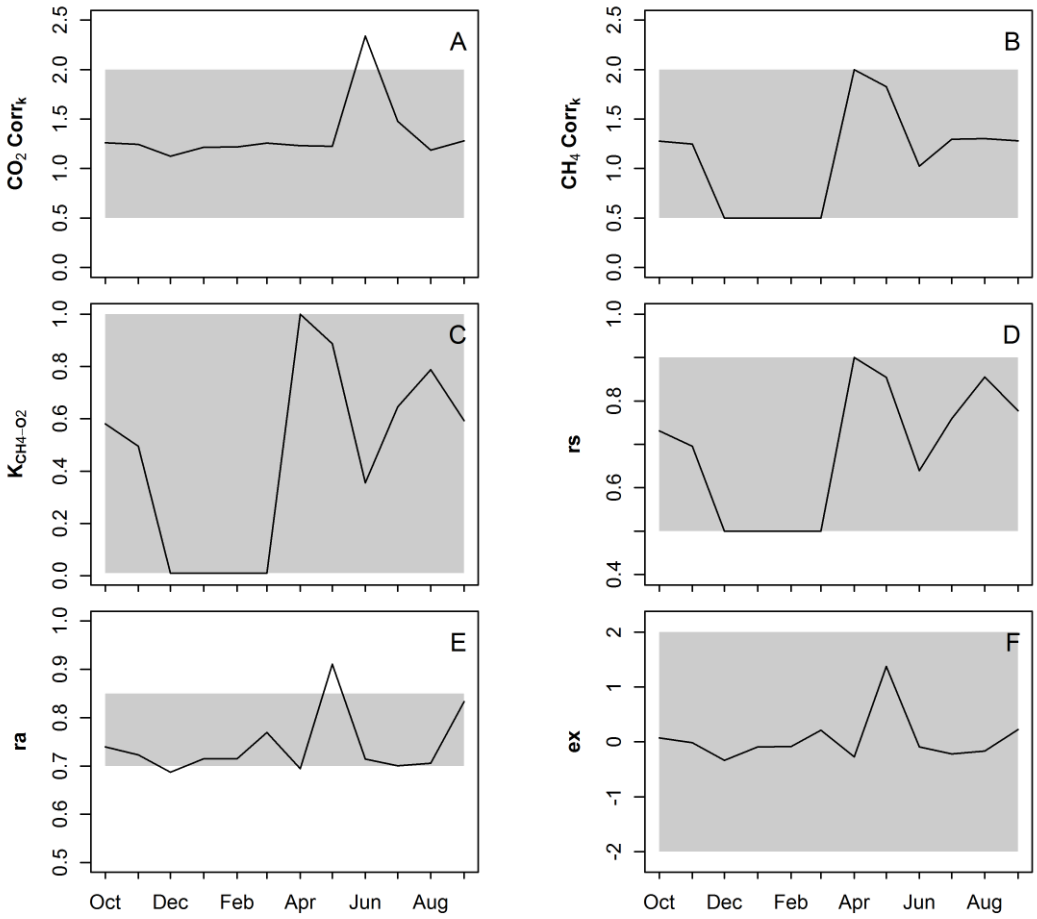

Figure S2. Values of model parameters from optimization routine (solid lines) and ranges of values from the literature (grey shade) (see main text for detail).

Chapter 3 CO_2 and CH_4 emissions from a eutrophic monomictic lake under changing climate and nutrient regimes: a hydrodynamic-ecological model simulation

Abstract

Lakes play an important role in the global carbon cycle, both by sequestering carbon in the sediment and releasing carbon as gases, namely CO_2 and CH_4, to the atmosphere. The extent to which lake trophic state influences global warming or vice versa has not been quantified in detail. A numerical hydrodynamic-ecological model (GLM-AED^2) was applied to a small monomictic eutrophic lake in New Zealand to assess the diffusive emissions of CO_2 and CH_4 in response to changes in climate and nutrient concentrations. Scenarios reflecting changes in climate (increasing air temperature by 2.5°C) and nutrients (halving or increasing by one half internal and external nutrient loads) were applied to a four-year baseline (current condition) period for which the model had been calibrated. The warming climate simulation showed a longer duration of thermal stratification, shallower surface mixed layer and higher level of nutrients in surface waters. Concurrently, annual CO_2 flux from the atmosphere to the lake was estimated to be 4% greater than the baseline, while CH_4 emissions increased by 25%. Together, the total annual greenhouse gas carbon emissions (as kg CO_2-eq m^{-2} y^{-1}) from the lake increased by 27%. Reducing nutrient loads by 50% in a warming climate, would minimize the emission from lake to 19%. This study demonstrates that reducing nutrient loads to eutrophic lakes may mitigate some of the impacts of global warming and could be used to reduce emissions of greenhouse gases from lakes.

Keywords: Lake modelling, greenhouse gas, climate change, water quality, thermal stratification, GLM-AED^2

3.1. Introduction

Freshwaters are now recognized to play an important role in the global carbon balance (Bastviken *et al*., 2011; Raymond *et al*., 2013). Although their total surface area only covers ~3% of the earth's terrestrial land surface (Downing *et al*., 2006), emissions from lakes equate to 20% of carbon dioxide (CO_2) uptake in the global ocean (Bastviken *et al*., 2011; Raymond *et al*., 2013; Battin *et al*., 2011). Inland waters also bury substantial amounts of carbon in the sediments (298 Tg y^{-1}), which is three times that of the global ocean (97 Tg y^{-1}) (Dean & Gorham, 1998). Inland waters are dominated by small water bodies with surface areas of <1 km^2 (Downing *et al*., 2006) and these systems release more CO_2 and methane (CH_4) (Kankaala *et al*., 2013) and have greater areal rates of deposition and accumulation of carbon than larger lakes (Downing *et al*., 2008).

The majority of lakes globally are considered to be CO_2 sources to the atmosphere (Cole *et al*., 1994). However, atmospheric CO_2 fluxes in lakes may vary seasonally, with alternate periods of acting as CO_2 sources and sinks (Trolle *et al*., 2012). Physical processes associated with seasonal overturn (Striegl & Michmerhuizen, 1998) as well as seasonal variations in phytoplankton productivity and community respiration (del Giorgio and Peters 1999) are the main driver of changes in surface water CO_2 concentrations and thereby control the magnitude of CO_2 fluxes in lakes. In addition, nutrient availability (mostly total phosphorus: Hanson *et al*., 2003), as the most common limiting factor for phytoplankton growth, may also indirectly regulate CO_2 emission in lakes (Trolle *et al*., 2012).

Freshwaters represent hot spots for CH_4 emissions (Kirschke *et al*., 2013). Similar to CO_2 fluxes, hydrodynamic processes related to lake mixing have been identified as an important controlling factor in the release of CH_4 to the atmosphere (Fernandez *et al*., 2014). However, there is wide variation among CH_4 emission estimates for lakes due to complexity in the nature of the releases, for example, outgassing and plant mediated releases in the littoral zone (Tranvik *et al*., 2009; Bastviken *et al*., 2011).

In terms of the total carbon content, CH_4 emissions from lakes globally is estimated to be only about 10% that of CO_2 (530 Tg C y^{-1}: Barros *et al*., 2011). However, CH_4 has been calculated to be 34 times more potent in global warming than CO_2 (Myhre *et al*., 2013). This may suggest that both CO_2 and CH_4 are highly important in contributing greenhouse gas emissions from lakes. It has been hypothesised that eutrophication would lead to an increase in autotrophic fixation of CO_2 (Davidson *et al*., 2015), nevertheless, it may also lead to an increase in absolute rates of both productivity and respiration (Yvon-Durocher *et al*., 2010). Furthermore, anoxic bottom waters of eutrophic lakes may store substantial quantities of CH_4 which, if subsequently exposed to the atmosphere, would lead to high rates of greenhouse gas emissions (Bastviken *et al*., 2008; Walter *et al*., 2006).

Changes in climate will lead to changes in the hydrodynamics of lakes (Peeters *et al*., 2002) and increase nutrient availability in the water column (Trolle *et al*., 2011). While there has been considerable theoretical work to identify how climate change may promote eutrophication and vice versa, there have been few quantitative studies to link the two. Furthermore few studies have investigated CO_2 and CH_4 dynamics in lakes simultaneously (e.g. Striegl & Michmerhuizen, 1998; Riera *et al*., 1999; Ojala *et al*., 2011) particularly on time scales that allow understanding to be developed of the interactions amongst climate, seasonal mixing and greenhouse gas emissions.

In this study I applied a dynamic model that integrates physical and biogeochemical processes in order to quantify fluxes of CO_2 and CH_4 in a eutrophic lake (e.g. Bayer *et al*., 2013; Trolle *et al*., 2011; Mooij *et al*., 2007). The numerical model GLM-AED^2 (Hipsey *et al*., 2014; Hipsey *et al*., 2012) was used to simulate CO_2 and CH_4 diffusive emissions from the lake in response to a warming climate and eutrophication from increased nutrient loads. In addition, oligotrophication was simulated to better understand impacts of restoration focused on reducing nutrient loads (e.g. Trolle *et al*., 2012). The model simulations are used to provide insights into

the possible effects of warming climate and eutrophication on carbon gas emissions pattern from a eutrophic lake.

3.2. Methods

3.2.1. Study site

This study was carried out in Lake Okaro, a relatively small (area = 0.3 km^2, maximum depth = 18 m), monomictic lake in the Rotorua lakes group in the North Island of New Zealand (Figure 3.1). Lake Okaro is the most eutrophic lake in the region with more than 90% of its catchment area (3.98 km^2) in pasture and used for dairy, deer, sheep and beef farming. Two small streams enter the lake from the north-west via a constructed wetland which is designed to reduce nutrient loads into the lake. Lake Okaro has only one outflow, Haumi Stream, located in the south-west of the lake. Eutrophication is evidenced in the lake by persistent cyanobacteria blooms during spring and summer and an anoxic hypolimnion throughout summer stratification (Paul *et al*., 2008; Özkundakci *et al*., 2011). Management plans have been undertaken by the regional management authority (Bay of Plenty Regional Council) to attempt to improve water quality of the lake. Nutrient reduction targets have been set for both internal and external loads to the lake and have included catchment restoration planting, a constructed wetland and lake sediment capping (Burns *et al*., 2009; Abell *et al*., 2011).

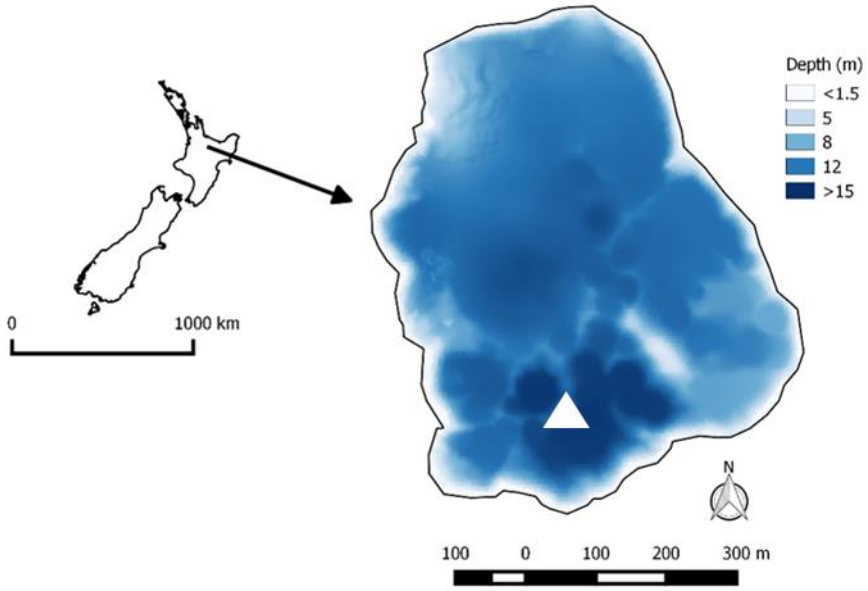

Figure 3.1 Bathymetry map and the location of Lake Okaro in the North Island of New Zealand. Sampling site is indicated by a white triangle.

3.2.2. Model description and conceptualization

A one-dimensional (1D) dynamic model was used to simulate hydrological- and ecological dynamics in Lake Okaro. The General Lake Model version 2.0.2 (GLM) coupled with the Aquatic EcoDynamics module (AED^2) was chosen for this purpose. GLM solves the vertical mass and energy transport equation in the water column using a Lagrangian layer approach which allows layers to change by contracting and expanding in response to inflows, outflows, mixing and surface mass fluxes. Instead of calculating mixing based on vertical velocities in a fixed grid (i.e., a Eulerian procedure), where numerical diffusion tends to be strongly evident at the thermocline, GLM computes mixing processes by merging layers when sufficient energy is available to overcome a density gradient and by adjusting layer sizes to appropriately capture the vertical density gradient. The primary driver of mass transport in the model is the heat flux which is formulated from forcing data inputs of ambient air temperature, wind speed, relative humidity and downwelling long- and shortwave radiation. Biogeochemical properties of the lake and their interactions with ecological state variables are simulated with AED^2. When coupled with the hydrodynamic driver (i.e,. GLM), AED^2 allows a comprehensive simulation

of processes that govern the transport and fate of major water quality attributes which include nutrients, dissolved gases, organic matter (dissolved and particulate), and biological assemblages (e.g., phytoplankton and zooplankton).

The interactions of nutrients and phytoplankton on CO_2 and CH_4 dynamics in the lake are shown conceptually in Figure 3.2 as they relate to simulations with GLM-AED^2. Briefly, CO_2, CH_4 and dissolved inorganic and organic nutrients are released from the bottom sediments depending on temperature and dissolved oxygen (DO) concentrations of the water layer immediately above the sediment surface. Aerobic methane oxidation controls CH_4 dynamics and produces CO_2 as an end product. In the surface layer CO_2 and CH_4 are exchanged with the atmosphere through diffusive fluxes. Concurrently, CO_2 is assimilated and respired by phytoplankton metabolism. Dissolved inorganic nutrients are simulated explicitly and include phosphate (PO_4), ammonium (NH_4) and nitrate (NO_3), which are sourced externally from inflow forcing data inputs and internally from bottom-sediment release and organic nutrient mineralisation in the water column. Two groups of phytoplankton are simulated in the model: non nitrogen-fixing cyanophytes and diatoms. The interaction between nutrient uptake by phytoplankton and mineralisation of the detrital (particulate) and dissolved nutrient constituents, together with the sources of nutrients described above, drives biogeochemical cycling in the model. Most of the algorithms and the computational approaches used for phytoplankton and carbon (C), nitrogen (N), and phosphorus (P) cycles in GLM-AED^2 are similar to other ecological models that have been widely used (DYRESM-WQ: Hamilton & Schladow 1997; CAEDYM: Gal *et al*., 2009). Detailed information on the model equations can be found in Hipsey *et al*. (2014) and Hipsey *et al*. (2012) (for updates see http://aed.see.uwa.edu.au/research/models/). In order to simulate CH_4 dynamics in the model, algorithms were developed for individual processes relating to the major CH_4 mass fluxes. A brief overview of the relevant equations used in the model is given in Table 3.1. Assigned model parameters are presented in Table 3.2.

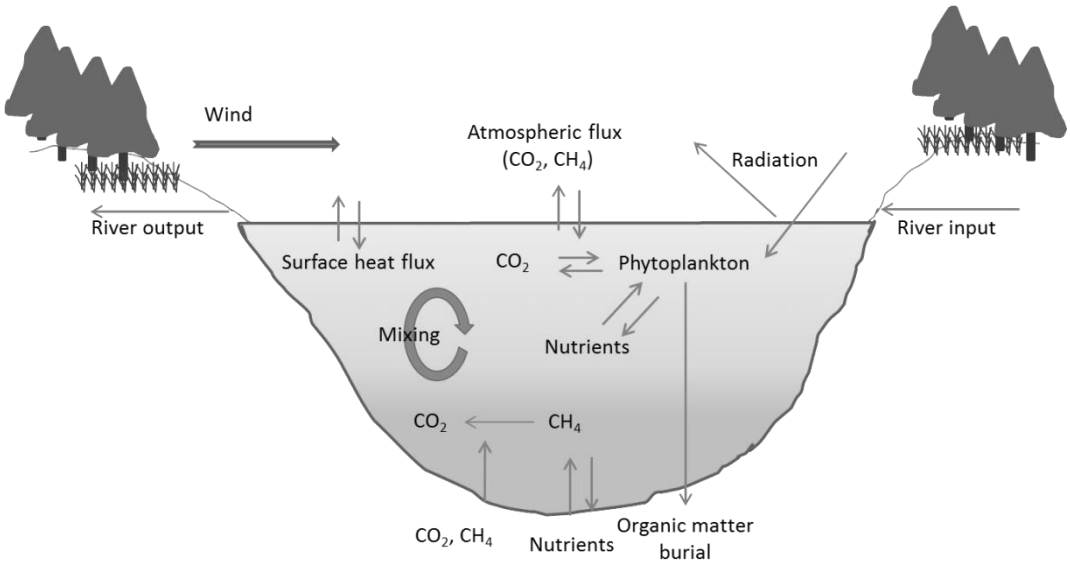

Figure 3.2 A Schematic diagram of ecological and hydrodynamics drivers that control CO_2 and CH_4 dynamics in a lake. The arrows represent either fluxes that were simulated with the model or forcing data inputs.

3.2.3. Model set up and evaluation

Model simulations were configured to run from July 2004 – June 2008, at an hourly internal time-step simulations with daily input forcing data and daily outputs. A static hypsography of the lake was produced to provide the vertical layer dimensions for the lake. Inputs used to drive the model included time series (daily average) meteorological data included wind speed (m s^{-1}), air temperature (°C), relative humidity (%), precipitation (m d^{-1}) and solar (long- and shortwave) radiation (W m^{-2}), in addition to total daily inflows and outflow of stream discharge (m^3 d^{-1}) and temperature. Meteorological data was sourced from the National Climate Data Base for Rotorua Airport climate station, ca. 20 km north of the study site. Linear interpolation of monthly observations of nutrient concentrations in stream inflows was used to calculate external nutrient inputs into the lake as outlined for other model applications (e.g., Trolle *et al.*, 2011; Özkundakci *et al.*, 2011). Outflow discharge was calculated as the residual of the water balance during the simulation period, derived from the change of lake volume due to change in lake level, evaporation, rainfall and the inflow discharge.

Table 3.1 Mass balance of CH_4 in the AED[2] module

Differential equations

$$\frac{\partial CH_4}{\partial t} = f_{sed}^{CH_4} - f_{oxy}^{CH_4} - f_{atm}^{CH_4} \quad (1)$$

$$f_{sed}^{CH_4} = Fsed_{ch4} * \frac{Ksed_{ch4}}{Ksed_{ch4} + oxy} * \emptyset\_sed_{ch4}^{\,temp-20} \quad (2)$$

$$f_{oxy}^{CH_4} = CH_4 * Rox_{ch4} * \frac{oxy}{oxy_{sat}} \quad (3)$$

$$f_{atm}^{CH4} = k_{ch4} * (Surf_{ch4} - Surf_{ch4solub}) \quad (4)$$

State variables

CH_4	Dissolved CH_4 concentration in the water column (mmol m^{-3})
t	Time step (daily)
$f_{sed}^{CH_4}$	Sediment flux of CH_4
$f_{oxy}^{CH_4}$	Water column CH_4 oxidation
$f_{atm}^{CH_4}$	Atmospheric CH_4 exchange
$Fsed_{ch4}$	Maximum CH_4 flux in the water-sediment interface (mmol m^{-2} d^{-1})
$Ksed_{ch4}$	Half saturation of oxygen concentration controlling CH_4 flux from the sediment (mmol m^{-3})
$\emptyset\_sed_{ch4}$	Arrhenius temperature multiplier for sediment CH_4 flux
$temp$	Water temperature (°C)
oxy	Dissolved oxygen concentration (mmol m^{-3})
Rox_{ch4}	Aerobic CH_4 oxidation kinetic constant (d^{-1})
oxy_{sat}	Oxygen saturation concentration (mmol m^{-3}) [b]
k_{ch4}	Gas exchange coefficient for CH_4 (m d^{-1}) [c]
$Surf_{ch4}$	Dissolved CH_4 concentration in air-water interface layer (mmol m^{-3})
$Surf_{ch4solub}$	Methane solubility concentration in air-water interface layer[a]

[a]Wiesenburg & Guinasso (1979).

[b]Benson & Krause (1980).

[c]Cole & Caraco (1998).

Table 3.2 Selected assigned values of model parameters in GLM-AED[2]. For phytoplankton, two generic groups were simulated: cyano = cyanobacteria and diatom = other phytoplankton not included in the cyano selection.

Parameter	Description	Units	Assigned value	Values from literatures*
Hydrodynamics				
Kw	Background light attenuation	m^{-1}	0.72	0.4 – 1.07[q]
coef_mix_conv	Mixing efficiency - convective overturn	-	0.2	0.2[h]
coef_wind_stir	Mixing efficiency - wind stirring	-	0.23	0.23[d]
coef_mix_shear	Mixing efficiency - shear production	-	0.2	0.2[a]
coef_mix_turb	Mixing efficiency - unsteady turbulence (acceleration)	-	0.51	0.51[p]
coef_mix_KH	Mixing efficiency - Kelvin-Helmholtz turbulent billows	-	0.3	0.3[a]
coef_mix_hyp	Mixing efficiency of hypolimnetic turbulence	-	0.5	0.5[c]
cH	Bulk aerodynamic coefficient for latent heat transfer	-	0.0013	0.0013[b]
ce	Bulk aerodynamic coefficient for sensible heat transfer	-	0.0013	0.0013[b]
cD	Bulk aerodynamic coefficient for transfer of momentum	-	0.0013	0.0013[b]
Oxygen				
Fsed_oxy	Maximum sediment oxygen demand at 20 °C	mmol m^{-2} d^{-1}	-10	-6 – -38[i,n]
Carbon				
Fsed_dic	Maximum sediment CO_2 flux at 20 °C	mmol m^{-2} d^{-1}	2.4	0.34 – 3.80[k]
Fsed_ch4	Maximum sediment CH_4 flux at 20 °C	mmol m^{-2} d^{-1}	2.0	0.19 – 3.90[k]
Rch4ox	Aerobic CH_4 oxidation kinetic constant	d^{-1}	0.048	0.01 – 0.21[m]
Fsed_doc	Sediment DOC flux	mmol m^{-2} d^{-1}	2.5	
w_pom	Settling rate of detrital C pool	m d^{-1}	-1.0	
Rpoc_miner	Hydrolysis/breakdown rate of detrital C pool at 20 °C	d^{-1}	0.5	0.1 – 0.3[e]
Rdoc_miner	Mineralisation rate of DOC pool at 20 °C	d^{-1}	0.5	0.5[i]

Table 3.2 Continued

Parameter	Description	Units	Assigned value	Values from literatures*
Nitrogen				
Fsed_amm	Maximum sediment NH_4 flux at 20 °C	mmol m^{-2} d^{-1}	4.0	7.1[o]
Rnitrif	Maximum reaction rate of nitrification at 20 °C	d^{-1}	0.07	0.03 – 0.05[l,n]
Rdenit	Maximum reaction rate of denitrification at 20 °C	d^{-1}	0.05	0.01 – 0.04[l,n]
Rpon_miner	Hydrolysis/breakdown rate of detrital N pool at 20 °C	d^{-1}	0.5	0.05 – 0.3[f]
Rdon_miner	Mineralisation rate of DON pool at 20 °C	d^{-1}	0.5	0.05 – 0.3[†]
Phosphorus				
Fsed_frp	Maximum sediment PO_4 flux at 20 °C	mmol m^{-2} d^{-1}	0.25	0.08 – 0.125[l,n]
Rpop_miner	Hydrolysis/breakdown rate of detrital P pool at 20 °C	d^{-1}	0.03	0.01 – 0.03[i,n]
Rdop_miner	Mineralisation rate of DOP pool at 20 °C	d^{-1}	0.03	0.01 – 0.05[l,n]
Phytoplankton			cyano, diatom	
Ycc	Carbon to chlorophyll ratio	mg C (mg chla)$^{-1}$	50, 50	40[g]
Pmax	Phytoplankton maximum growth rate at 20 °C	d^{-1}	0.7, 3.5	0.5 – 3.36[f,g]
Tstd	Standard temperature	°C	20, 10	13 – 24[n]
Topt	Optimum temperature	°C	28, 15	15 – 29[n]
Tmax	Maximum temperature	°C	35, 28	22 – 35[n]
kr	Phytoplankton respiration/metabolic loss rate at 20 °C	d^{-1}	0.01,0.005	0.001 – 0.125[f]
INmin	Minimum internal nitrogen concentration	mmol N (mmol C)$^{-1}$	0.04, 0.06	0.025 – 0.06[f]

Table 3.2 Continued

Phytoplankton			
INmax	Maximum internal nitrogen concentration	mmol N (mmol C)$^{-1}$	0.10, 0.15
UNmax	Maximum nitrogen uptake	mmol N (mmol C)$^{-1}$ d^{-1}	0.08, 0.05
IPmin	Minimum internal phosphorus concentration	mmol P (mmol C)$^{-1}$	0.008, 0.006
IPmax	Maximum internal phosphorus concentration	mmol P (mmol C)$^{-1}$	0.03, 0.01
UPmax	Maximum phosphorus uptake	mmol P (mmol C)$^{-1}$ d^{-1}	0.009, 0.009

*Values were converted into GLM-AED^2 units
[a]Sherman *et al*. (1978).
[b]Fischer *et al*. (1979).
[c]Weinstock (1981).
[d]Spigel *et al*. (1986).
[e]Connolly & Coffin (1995).
[f]Hamilton & Schladow (1997).
[g]Griffin *et al*. (2001).
[h]Yeates & Imberger (2003).
[i]Obernosterer & Benner (2004).
[j]Romero *et al*. (2004).
[k]Adams (2005).
[l]Bruce *et al*. (2006).
[m]Bastviken (2009).
[n]Gal *et al*. (2009).
[o]Özkundakci *et al*. (2011).
[p]Hipsey *et al*. 2014
[q]Read *et al*. (2014).

Evaluation of the quality of the model simulations in terms of reproducing observed data was performed by visual inspection and quantitative measures of time series plots of model outputs against field observation data collected monthly by Bay of Plenty Regional Council. The monthly data collection included vertical temperature profiles derived from conductivity-temperature-depth (CTD) casts (SBE 19 plus, Seabird Electronics) and water quality variables (DO, chlorophyll *a*, PO_4, NH_4, and NO_3) concentrations sampled at the deep-water site (Figure 3.1). All water quality variables were analysed using standard analytical methods (APHA 1998). Four different stratification indices, namely: thermocline depth; Schmidt stability; surface (0 m); and bottom water (16 m) temperature, and water quality variables were used to assess the model performance. The thermocline was defined as the depth of the maximum gradient in water density calculated from vertical temperature profiles from the CTD casts (as density was not impacted significantly by changes in salinity). Schmidt stability, the aerial amount of energy required to theoretically completely mix the lake, was calculated as a function of water density, acceleration due to gravity and bathymetry. Thermocline depth and Schmidt stability were computed using rLakeAnalyzer package (Winslow *et al*., 2015) for which the computation algorithms are described in Read *et al*. (2011).

A supplementary field campaign was conducted from September 2013 to October 2014 to collect data on CO_2 and CH_4. Water sampling was conducted monthly from the deepest station of the lake (Figure 3.1). Water samples were collected at the subsurface (0.5 m) to a depth of 16 m with a vertical resolution of 2 m using a 10-L Schindler-Patalas water sampler. Subsamples of 60 mL were taken from the sampler using a syringe, transferred into a 45 mL glass bottle with excess water overflowing the bottle. Dissolved CH_4 concentrations in the samples were measured by gas chromatograph (GC-FID, Varian CP 3800) using the headspace equilibration technique (needs reference here). The dissolved CO_2 concentration was also measured from the headspace by an infra-red gas analyser (IRGA, LI-COR® LI-6262). Details on dissolved gas determination can be found in Chapter 2.

The coefficient of determination (R^2) between model output and field observations was calculated to provide insight into how the model reproduced the dynamics of fluctuations in the state variables for the observed data. In addition, to calculate the error of the model fit, the root mean squared error (RMSE) was used:

$$RMSE = \sqrt{\frac{\sum_t^n (Sim_t - Obs_t)^2}{n}} \quad (5)$$

where *Sim* and *Obs* are model simulation output and field observation, respectively, at time *t* and *n* is the number of observations. Model simulation output was daily, at noon, and was compared with the field observations for the same date but which were mostly collected in late morning (09:00 to 12:00 h). For CO_2 and CH_4, however, monthly averages over the period of simulation (July 2004 to June 2008) were compared with field observations (September 2013 to October 2014). The model simulation was calibrated by adjusting parameter values manually within literature ranges (e.g., Hamilton & Schladow 1997; Gal *et al*., 2009) until there was negligible improvement in RMSE and R^2 values. Selected assigned model parameter values and their ranges from the literature are presented in Table 3.1. All nutrient (PO_4, NH_4 and NO_3) and DO concentrations units in simulation outputs (mmol m^{-3}) were converted into mg L^{-1} for model evaluations against the observed data.

3.2.4. Climate change and water quality scenarios

Under the IPCC A1B scenario, the global mean surface air temperature is predicted to increase by 2.8 °C by 2090 (Meehl *et al*., 2007). For New Zealand, this scenario projects a smaller temperature change for the same period (2.1 °C; Ministry for the Environment, 2008). Furthermore, water quality improvement as a result of a lake restoration program might be expected within this time due to recent regional government actions (Environment Bay of Plenty 2006) and the National Policy Statement for Freshwater Management (Ministry for the Environment 2014). Özkundacki *et al*. (2011) suggested that reductions of both internal and external loads of nitrogen and phosphorus by 75 – 90% would shift the trophic state of

Lake Okaro from highly eutrophic to mesotrophic. Hence, in order to quantify the impact of warming climate and water quality changes on CH_4 and CO_2 emissions from the lake, variations of air temperature and nutrient loadings were simulated in the model set up. The best calibrated model simulation result (i.e., with overall highest R^2 and lowest *RMSE* values) over the period of July 2004 – June 2008 was used to represent the base simulation (i.e., no perturbations of climate or nutrient management regimes). Scenarios were then run over the same time period with modified forcing files as follows. For the global warming scenarios, air temperature was increased by 2.5 °C for each day following the approach of Trolle *et al.* (2011). External nutrient loadings were modified by halving or increasing by one half the daily inputs of dissolved and particulate concentrations of nitrogen and phosphorus in the inflows. Internal load adjustment was performed by halving or increasing by one half internal the maximum sediment release of PO_4 (Fsed_frp) and NH_4 (Fsed_amm) relative to their default values (see Table 3.2). Model outputs from these simulations with the unadjusted set up (base scenario). The percentage of change in concentrations relative to the base scenario was used as a quantitative measure of the impact of the alterations. Seasonal patterns in the daily simulation output were analysed by calculating a monthly median value and its 95% confidence interval and plotting the series of median values as an annual cycle. Mann-Whitney-tests were run to evaluate the significance difference between scenarios. The net cumulative CO_2 and CH_4 emissions annual from each simulation were calculated by summing the daily flux model outputs at one year intervals. Total annual greenhouse gas emissions of carbon (in kg CO_2-eq m^{-2} y^{-1}) from the lake were calculated as the sum of annual CO_2 and CH_4 emissions multiplied by their global warming potential (GWP) over a 100 year period (i.e., CO_2 = 1, CH_4 = 34: Myhre *et al*., 2013; IPCC 2007).

3.3. Results

3.3.1. Model simulation and field observation

The four stratification indices derived from the model simulation output satisfactorily reproduced the dynamics and magnitude of field observation measurements (Figures 3.3A – 3.3D, and Table 3.3). The model simulated surface (0 m) water temperature very well (R^2 = 0.98), but bottom (16 m) water was slightly underestimated (R^2 = 0.85). The variation (*RMSE*) between simulated and observed values of surface and bottom water temperature was ~0.6 °C. The timing and duration of the onset of stratification and mixing events were generally well simulated, but there was slight overestimation of the observed thermocline depth at some stages (*RMSE* ~3.2 m). Schmidt Stability indicated a close match of simulated stratification against the model simulation, with an R^2 of 0.97. These results provided confidence in the hydrodynamic simulations as a prerequisite to simulating mass transfer of material across the water layers of the lake.

In general, dissolved oxygen and nutrient dynamics in the model behaved as expected in terms of the timing and magnitude of seasonal variability (Figures 3.4A – 3.4H), however, statistical fit of simulated variables to the observed ones were generally lower than those for the hydrodynamics variables (Table 3.3). During summer stratification, bottom water deoxygenation and oxygen supersaturation in the surface water were reproduced in the model simulations (Figures 3.4A and 3.4B). Subsequently, hypolimnetic PO_4 and NH_4 accumulation were evidenced in the simulation (Figures 3.4D and 3.4F). During winter mixing (around July), the nutrients accumulated in bottom waters were simulated to diffuse with less concentrated nutrients in the surface water, resulting in relatively homogeneous concentrations of PO_4 and NH_4 across water column. At the same time, oxygen rich surface water was also simulated to mix with the anoxic bottom water, creating relatively low DO concentrations throughout the water column (Figures 3.4A and 3.4B). Rapid increases in NO_3 throughout the water column occurred with seasonal mixing were

associated with rapid reductions in NH_4 in bottom waters following seasonal build up of this nutrient during stratification (Figures 3.4G and H).

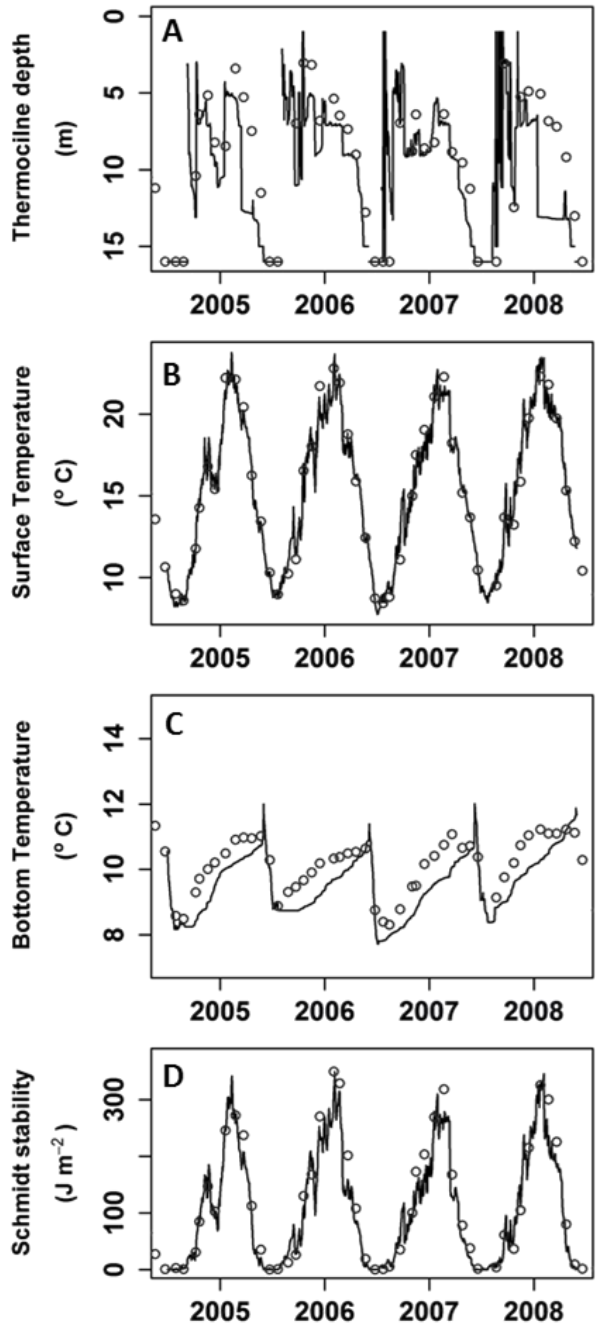

Figure 3.3 Model outputs (solid lines) and field observation (open circles) of stratification indices: A. thermocline depth (m), B. surface water (0 m) temperature, C. bottom water (16 m) temperature, and D. Schmidt stability.

Table 3.3 Coefficient of determination (R^2) and root mean squared error (*RMSE*) between model outputs and field observations.

State variable	R^2	RMSE
Hydrodynamics		
Surface temperature (°C)	0.984	0.611
Bottom temperature (°C)	0.855	0.650
Thermocline depth (m)	0.403	3.244
Schmidt stability (J m^{-2})	0.969	24.999
Water quality		
Surface water (0 m)		
DO (mg L^{-1})	0.167	3.330
Chlorophyll *a* (µg L^{-1})	0.024	51.685
PO_4 (mg P L^{-1})	0.226	0.023
NO_3 (mg N L^{-1})	0.124	0.079
NH_4 (mg N L^{-1})	0.185	0.307
CH_4 (µmol L^{-1})	0.474	2.084
CO_2 (µmol L^{-1})	0.224	17.795
Bottom water (16 m)		
DO (mg L^{-1})	0.495	2.735
PO_4 (mg P L^{-1})	0.411	0.139
NO_3 (mg N L^{-1})	0.016	0.120
NH_4 (mg N L^{-1})	0.337	1.065
CH_4 (µmol L^{-1})	0.936	51.374
CO_2 (µmol L^{-1})	0.735	39.595

The statistical fit of the model for chlorophyll *a* was less satisfactory (Table 3.3), but most peaks were captured (Figure 3.5A) and typical seasonal succession patterns were reproduced of dominance and blooms of cyanophytes in spring and summer, and dominance of diatoms in winter (Figure 3.5B). The magnitude and timing of this succession contributed substantially to the cycling of C, N and P in the model through biogeochemical processes. High primary productivity, indicated by high chlorophyll *a* biomass (Figure 3.5), contributed to periods of DO supersaturation (Figure 3.4A) and CO_2 undersaturation (Figure 3.6A).

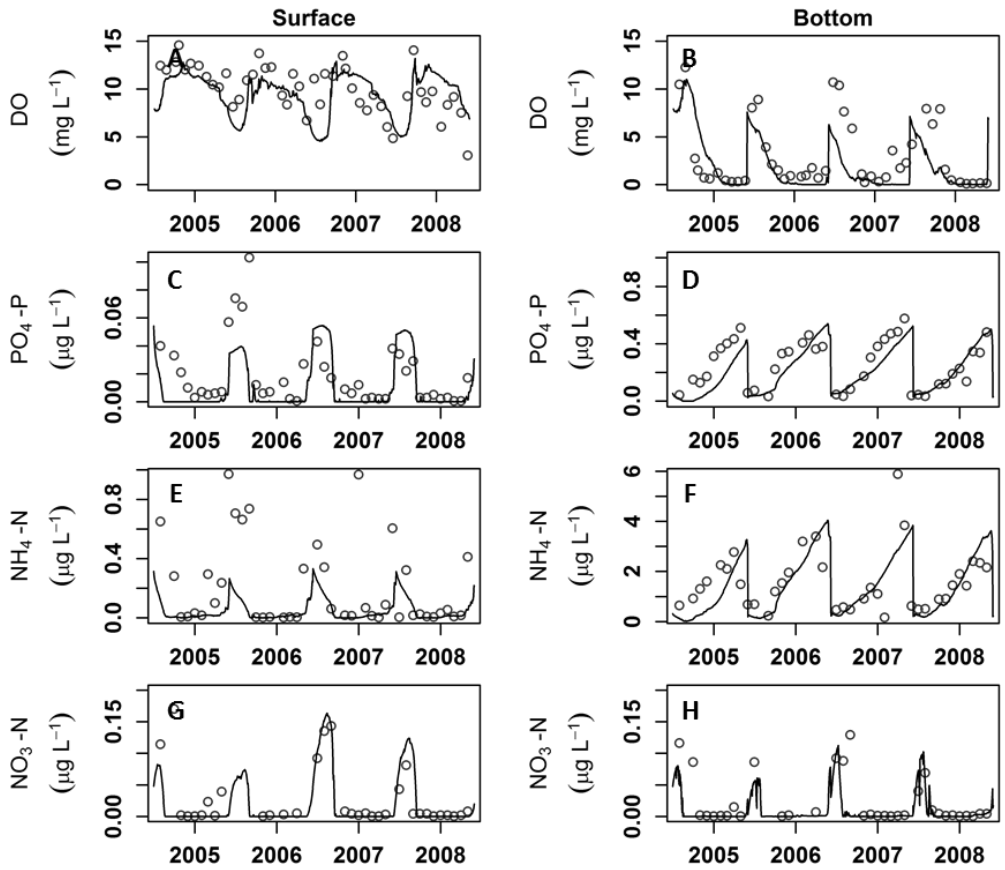

Figure 3.4 Model outputs (solid lines) and field measurements (open circles) of water quality variables: A-B. dissolved oxygen (DO), C-D. soluble reactive phosphorus as PO_4-P, E-F. ammonium as NH_4-N, G-H. nitrate as NO_3-N. Left hand panel (A, C, E, G) indicates surface water (0 m), right hand panel (B, D, F, H) indicates bottom water (16 m).

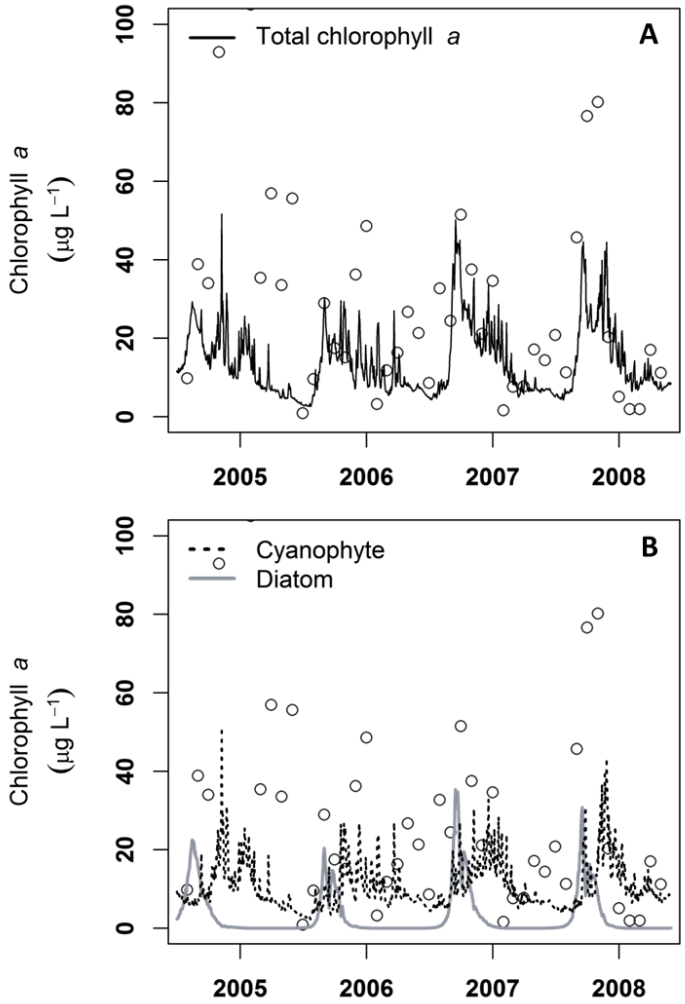

Figure 3.5 Model outputs (solid black line) and field measurements (open circle) of surface water (0 m) total chlorophyll *a* (A) and chlorophyll a contributed from the two simulated phytoplankton groups (B).

The model was able to satisfactorily reproduce water column measurements of CO_2 and CH_4 from 2014 field observations (Table 3.3, Figures 3.6A – 3.6D). Distinguishing features which were simulated by the model included the accumulation of dissolved CO_2 and CH_4 in the hypolimnion during stratification and increases in carbon dioxide concentrations in the hypolimnion following formation of stratification at the same time as there was an increase in CH_4 concentrations as anoxia formed in the bottom layer. The model simulation was also able to reproduce vertical transport of this accumulated CO_2 and CH_4 during lake turnover.

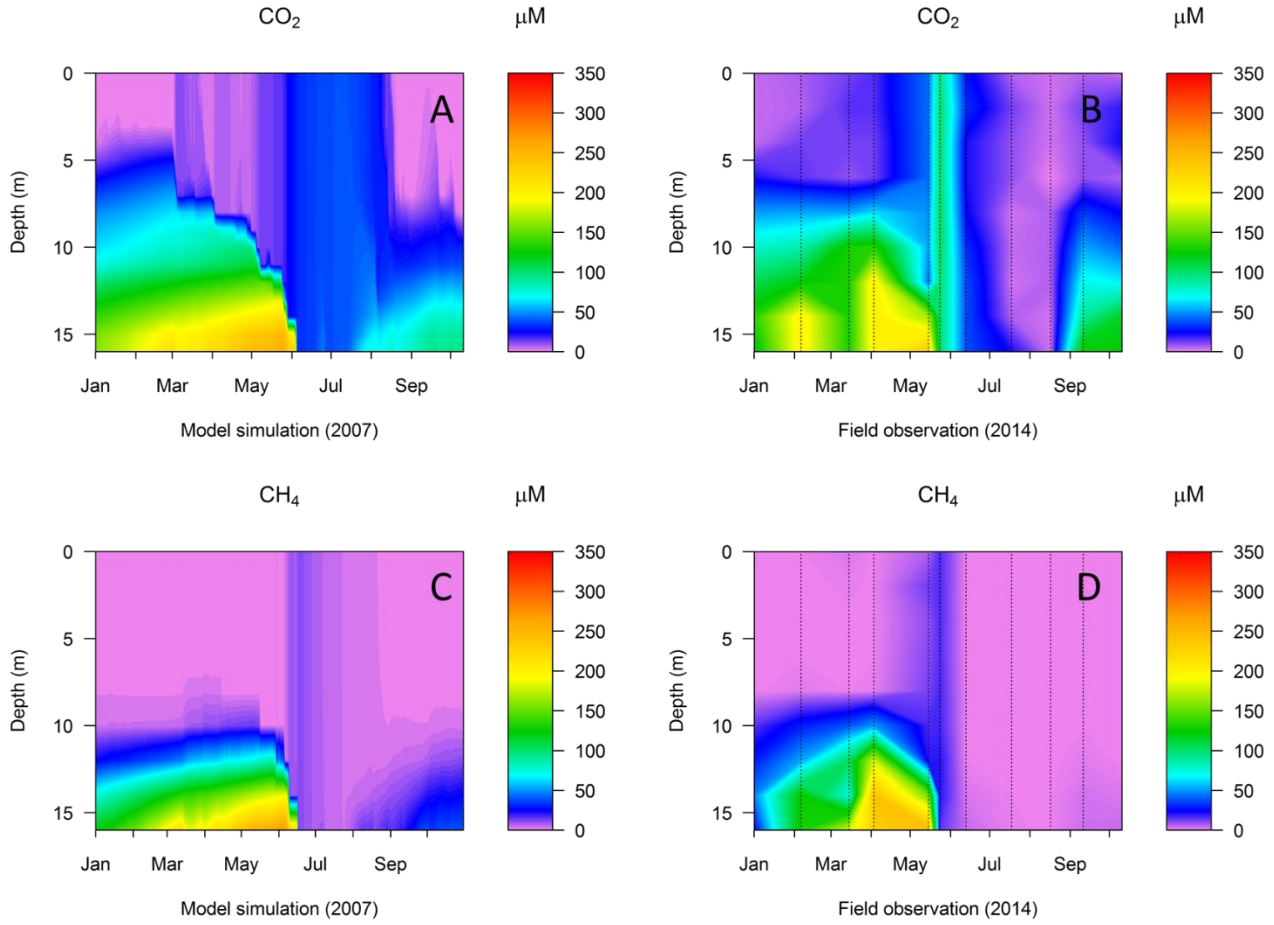

Figure 3.6 Model simulations in 2007 (A, C) and field observations in 2014 (B, D) of CO_2 and CH_4 concentrations, respectively, through the water column. Vertical dashed lines indicate day of sampling.

3.3.2. Warming climate and water quality simulations

Model simulation of the climate change scenario showed that increased air temperature would not only increase surface water temperature but also have a strong effect on lake hydrodynamics and the mixing regime (Figure 3.7). Lake stratification was more persistent and also shallower than the base scenario condition. A prolonged stratification period from July (mid-winter) until March (late-summer) and a shorter window of winter mixing (July) were observed in the climate change scenario (Figure 3.7A). When coupled with climate change, the nutrient load reduction produced weaker stratification than the climate change scenario alone, however, winter re-stratification still occurred. The effect of the nutrient load reduction in the absence of air temperature increase had little impact on water temperature and hydrodynamics of the lake (Figure 3.7B).

Warming climate was simulated to have a strong effect on surface water chlorophyll *a* and nutrient concentrations. Annual average concentrations were increased by 20 – 40% relative to base scenario concentrations (Figure 3.8A). Interestingly, there was no additional change in water quality variables in the warming scenario when nutrients were increased. The model simulated an increasing duration of anoxia in the hypolimnion (data not shown) due to longer stratification which, in turn, enhanced sediment release of CH_4, NH_4 and PO_4. On the other hand, reducing nutrient load in the warmer climate was simulated to reduce chlorophyll *a* and nutrient concentrations by ~2% and ~10%, respectively, relative to the base scenario.

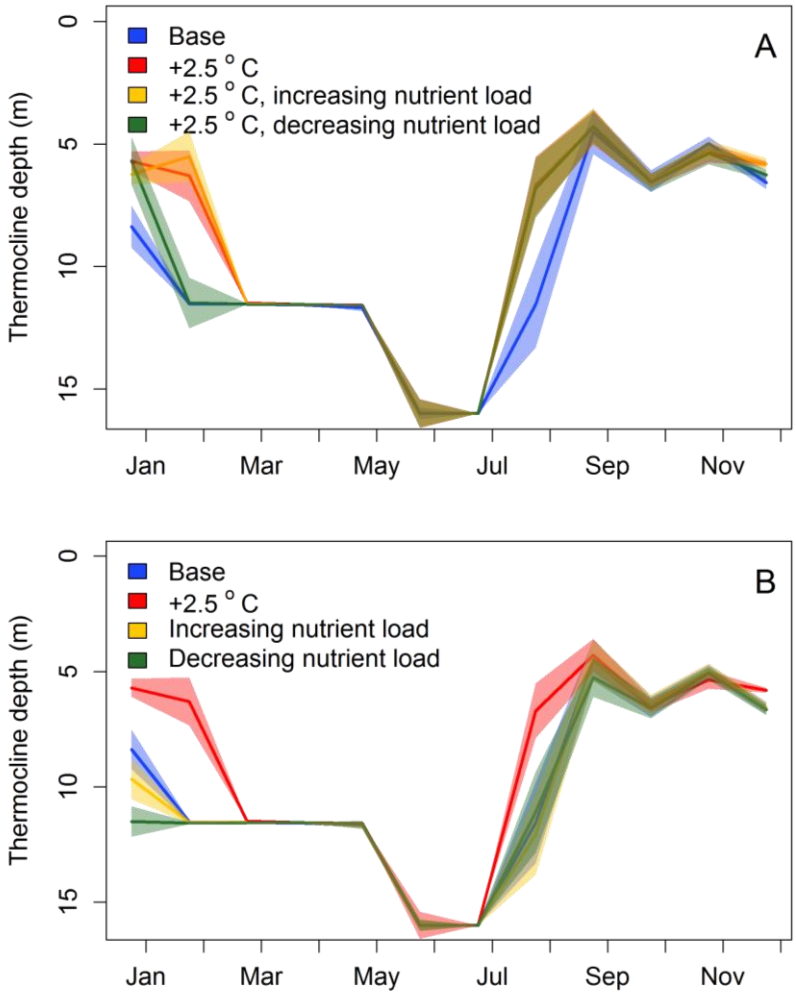

Figure 3.7 Median monthly thermocline depth calculated from four years of model simulation under (A) warming climate and, (B) without warming climate. Shaded areas indicate 95% confidence interval derived from daily model output.

Without increasing air temperature, adding more nutrients was simulated to increase annual average chlorophyll *a* and nutrient concentrations by around 10% and 20%, respectively, relative to the base scenario (Figure 3.8B). Nutrient load reductions in the non-warming climate scenario were simulated to reduce chlorophyll *a* by 9% and nutrient concentrations by 8 – 14% relative to the base scenario.

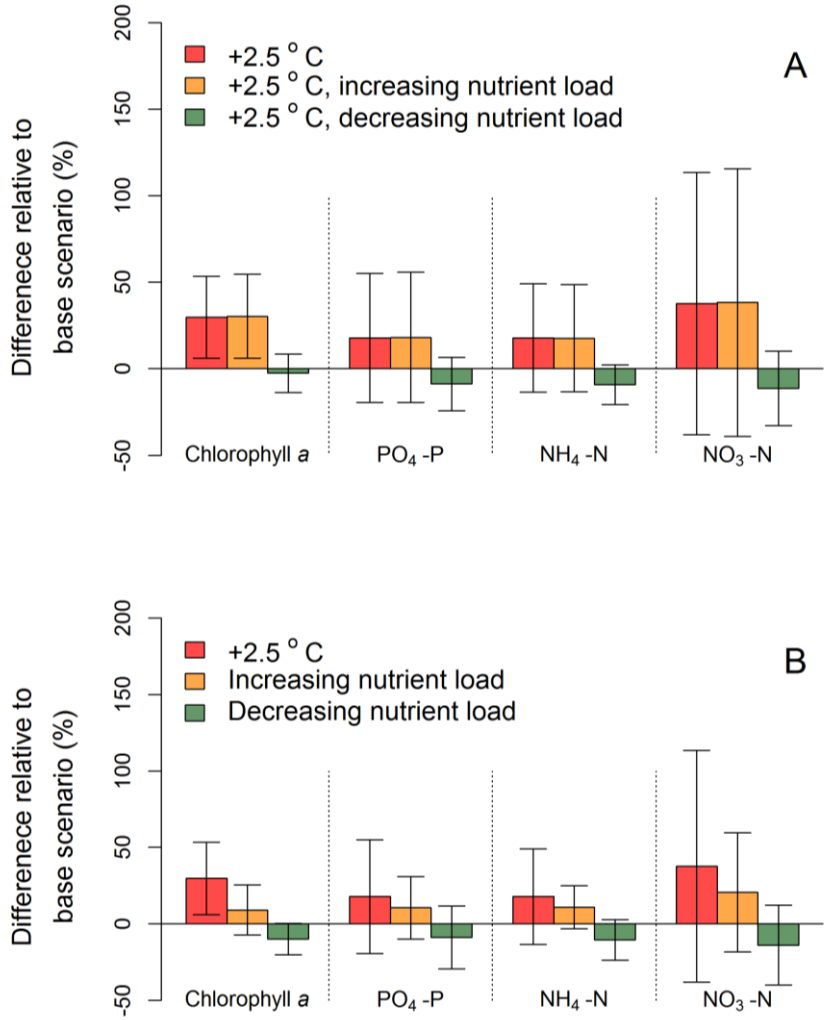

Figure 3.8 The mean difference of chlorophyll *a*, PO_4-P, NH_4-N, and NO_3-N concentrations in surface water (0 m) relative to present (base scenario): A. Under warming climate scenario, B. Without warming climate scenario. Error bars indicate standard deviation of the relative difference.

3.3.3. CO_2 and CH_4 dynamics and emissions under warming climate and water quality change simulations

The model simulations revealed that hydrodynamics and water quality changes due to climate warming and nutrient load alterations would result in changes in the magnitude of surface water CO_2 and CH_4 concentrations relative to the base scenario (Figure 3.9). Under the climate warming scenario, surface water CO_2 would decrease by ~15%, while reduced nutrient concentrations would result in a ~25% increase in CO_2 (Figure 3.9A). Without climate warming, the increased nutrient scenario reduced

CO_2 by ~11%, while the nutrient reduction scenario increase CO_2 by ~57% (Figure 3.9B). There was a close and inverse correspondence between chlorophyll *a* (Figure 3.8A) and CO_2 concentrations in the surface waters across the simulations.

Climate warming had a greater effect on CH_4 concentrations than for CO_2, particularly during winter mixing (Figures 3.9C and 3.9D). During mixing, climate warming increased monthly median CH_4 concentrations by ~66%, but concentrations were largely unaltered by increasing nutrient load. Reducing nutrient load, however, resulted in a smaller CH_4 increase of ~27% under the climate warming scenario (Figure 3.9C). Without climate warming, changes in nutrients did not produce a substantial change to surface water CH_4 concentrations in any of the seasons (Figure 3.9D).

In the model, Lake Okaro was simulated to take up CO_2 from the atmosphere from spring to autumn (August – May, see Figure 3.7) when the lake was stratified, and release CO_2 during winter mixing (end of May – August). Simulations showed that the monthly median value of CO_2 emission from the lake during mixing in the base simulation was up to 6.6 mmol m^{-2} d^{-1}, while up to 7.0 mmol m^{-2} d^{-1} of CO_2 diffused into the lake during stratification from spring to autumn. Reducing nutrient loads under a climate warming scenario led to a monthly median emission of 7.9 mmol CO_2 m^{-2} d^{-1} during mixing, while the release rate was 6.7 mmol CO_2 m^{-2} d^{-1} for the same period in the non-warming climate scenario (Figures 3.10A and 3.10B). A prolonged period of CO_2 emission was also observed in the nutrient reduction scenarios. In the warming climate, reducing nutrient concentrations led to release of CO_2 from the period of mixing in July to the onset of stratification in early September, while in the non-climate warming simulation CO_2 release would persist until October.

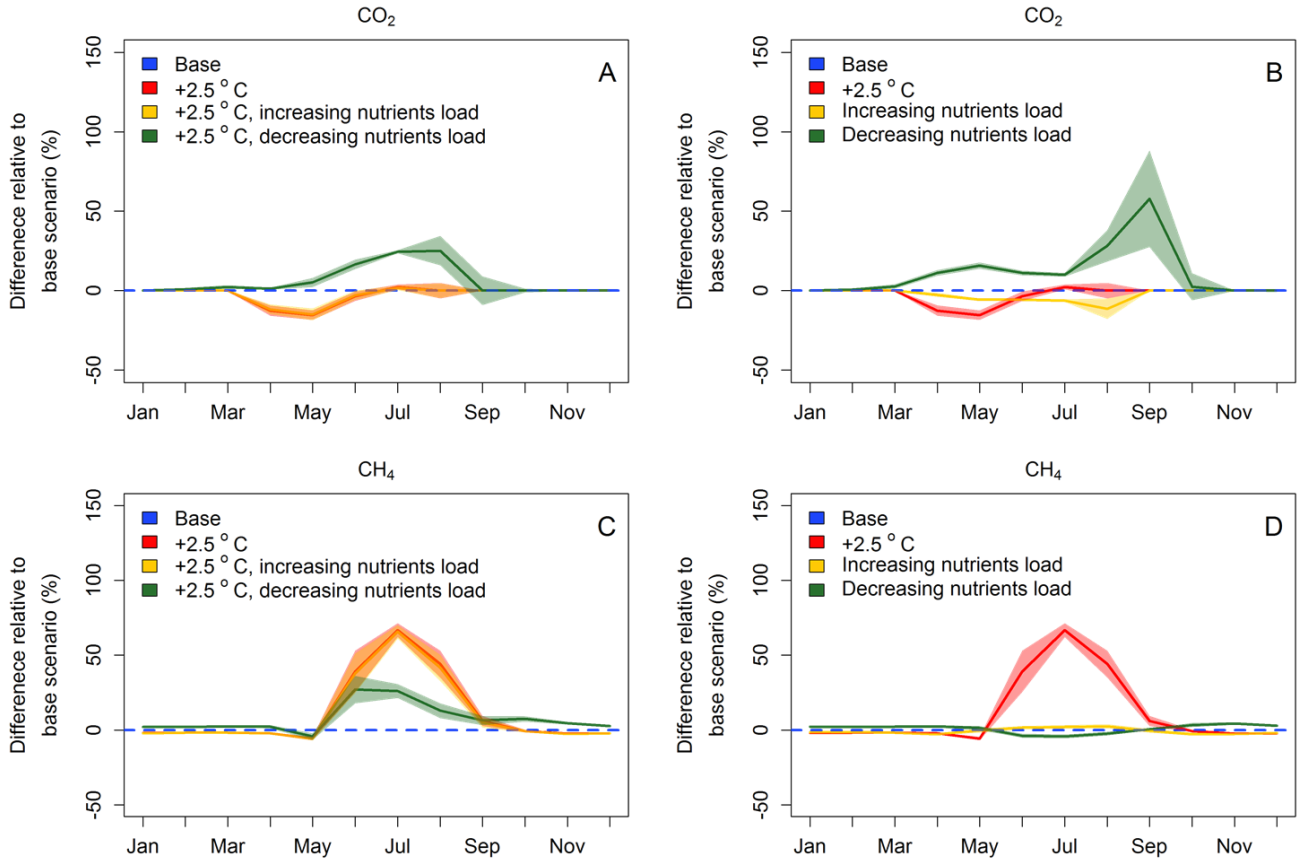

Figure 3.9 Monthly difference of CO_2 (A and B) and CH_4 (C and D) concentrations in the surface water (0 m) relative to present (base scenario) under warming climate scenario (A, C) and without warming climate scenario (B, D). Solid lines indicate the medians of the monthly difference, shaded areas indicate the 95% confidence interval of the medians.

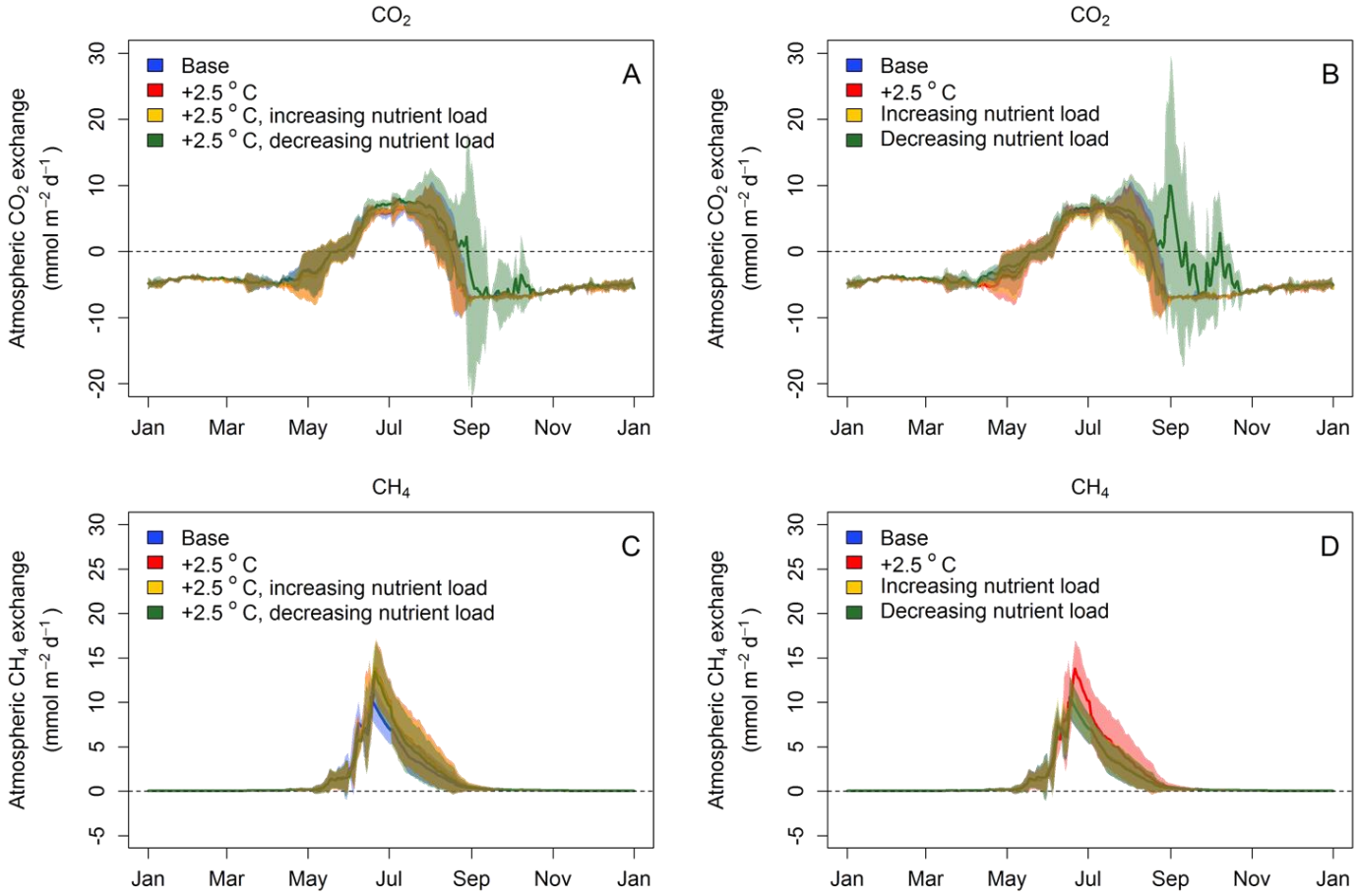

Figure 3.10 Daily CO_2 (A and B) and CH_4 (C and D) emissions from model simulations, with warming climate influence (A, C) and without warming climate influence (B, D). Solid lines indicate the medians from daily output over the four years of the simulation, shaded areas indicate the 95% confidence interval of the medians. Positive values indicate flux from lake to the atmosphere, negative indicate the reverse.

Similar to the CO_2 flux to the atmosphere, a large diffusive emission of CH_4 was simulated during winter mixing (end of May – August) (Figures 3.10C and 3.10D). In the base scenario the CH_4 winter release (median) was estimated to be 10.6 mmol m^{-2} d^{-1}. However, the CH_4 emission was higher in the climate warming scenario, with a median rate of 13.9 mmol CH_4 m^{-2} d^{-1}. Without climate warming, winter CH_4 emissions in all nutrient load scenarios reached a peak of 10.5 mmol m^{-2} d^{-1}.

The model revealed substantial variations of CO_2 and CH_4 diffusive emissions due to climate warming and large changes in the cumulative annual fluxes (Table 3.4). Under the base scenario Lake Okaro had an atmospheric CO_2 uptake rate of 993.3 mmol m^{-2} y^{-1} and a release rate of 435.6 mmol m^{-2} y^{-1} CH_4. With higher productivity under the scenarios of climate warming and additional nutrients, the net annual CO_2 flux to the lake was simulated to be ~4% to ~7% higher than the base scenario. When nutrient loads were reduced and the lake became less productive, atmospheric CO_2 uptake was also reduced. Under warming climate conditions, reducing nutrient loads decreased the annual CO_2 uptake to ~23% of the base scenario, while nutrient reductions alone decreased atmospheric CO_2 uptake by ~46%. The effect of climate warming on the annual emission rate of CH_4 was more prominent than that of CO_2. Climate warming, in addition to increased nutrient load, would increase CH_4 emissions by ~25%. Without climate warming nutrient additions would result in only a 1% increase in CH_4 emissions.

Table 3.4 Annual atmospheric fluxes of CO_2 and CH_4 (mmol m^{-2} y^{-1}) and total greenhouse gas emissions (kg CO_2-eq m^{-2} y^{-1}) in Lake Okaro for base conditions and scenarios of air temperature increase and changes in nutrient loads. Positive values indicate flux from lake to the atmosphere, negative indicate the reverse.

Scenario	Annual flux (mmol m^{-2} y^{-1})		Total emission (kg m^{-2} y^{-1})
	CO_2	CH_4	CO_2-eq
Base (present condition)	-993.3	435.6	0.608
2.5 °C air temperature increase (climate)	-1035.7	545.8	0.771
Climate + increase nutrients load	-1036.4	545.0	0.770
Climate + reduce nutrients load	-767.9	507.3	0.725
Increase nutrients load	-1063.5	439.4	0.611
Reduce nutrients load	-534.5	431.3	0.622

3.4. Discussion

3.4.1. Model performance and constraints

The hydrodynamic-ecological lake model GLM-AED^2 was in general successful in simulating the hydrodynamics and seasonal variability of geochemical and ecological state variables in the study lake. Many of the state variables in GLM-AED^2 have a direct or indirect impact on the diffusive emissions of CO_2 and CH_4. In terms of the hydrodynamic simulation, the model reproduced most aspects of the thermal structure observed in the field data (Figure 3.3) and the model performance was comparable to that of other studies (e.g. Özkundakci *et al*., 2011; Bayer *et al*., 2013). In general, the model performed relatively well in simulating epilimnion and hypolimnion temperatures, with RMSE = 0.61 °C and 0.65 °C, respectively (Table 3.3). Using an earlier version of GLM (version 1.2.0) to simulate hydrodynamics of a large group of lakes (2368 lakes in the conterminous United States), Read *et al*. (2014) produced overall epilimnion and hypolimnion temperature RMSE of 1.74°C and 3.33°C, respectively. However, the model performance for simulation of thermocline depth in Lake Okaro (Figure 3.3A) was relatively poor (RMSE = 3.24 m; Table 3.3). This discrepancy can be attributed partly to inaccuracies in the meteorological forcing data due to the distance of the meteorological station from Lake Okaro (20 km). Lake mixing is highly

sensitive to wind (Hipsey et al., 2014) but small lakes are also relatively sensitive to convective mixing for which variations in air temperature are highly important in the parameterization of this process, with air temperature also likely to be influenced by the distance separating the meteorological station from Lake Okaro (Read *et al.*, 2014; Markfort *et al.*, 2010).

The model was generally also able to simulate interactions within and amongst the biogeochemical and ecological variables. Simplifications in the conceptualizations and formulations of these processes in GLM-AED^2 are a potential source of error in the simulation output but increases in complexity need to be balanced by the requirements for increased parameterization and higher levels of user skill. One simplification in GLM-AED^2 is the release of dissolved compounds from the sediment into the water column. The releases of PO_4 and NH_4, as well as CH_4 in the model, are regulated by oxygen concentration and temperature in the specific model water layer immediately adjacent to the bottom sediments. Releases therefore reflect the relevant water layer variables and not changes in sediment composition that result from mineralization processes (Søndergaard *et al*., 2003; Boudreau 1996). In reality CH_4 production associated with sediment diagenesis is followed by diffusion through pore waters and gas bubble formation (see Boudreau *et al*., 2001), and then by methane bubbles that rise through the water column (see McGinnis *et al*., 2006). These processes have not been formulated in GLM-AED^2. The latter process can account for >80% of the total CH_4 atmospheric flux from lakes (DelSontro *et al*., 2010; Martinez and Anderson 2013). Simplifications of the model are also inherent in the community structure representation (Özkundakci *et al*., 2011), including trophic interactions. In this study the only biota simulated explicitly was phytoplankton and there were limited data for other community groups which can influence CO_2 dynamics in lakes through, for example, respiratory processes (Cole *et al*., 2000).

Another source of error may be the variability of model parameters. Improved parameter estimations and model calibration through optimization techniques may further enhance model performance (Janssen *et al*., 2015). However, the model optimisation was considered satisfactory based on comparison with other similar modelling studies in the international literature (Schladow & Hamilton 1997) and it was considered suitable to meet the objectives of this study.

3.4.2. CO_2 and CH_4 emissions from lakes in a warming climate and with changes in nutrient loading

Although complex process based models like GLM-AED^2 have limitations and should be used with caution in predicting environmental scenarios, numerical models of this type provide some of the most advanced tools to understand lake functioning and how lakes respond to alterations in environmental forcing. In this study, simulations were used to understand the possible effects of climate warming and water quality changes on diffusive emissions of CO_2 and CH_4. By altering only air temperature to simulate climate warming, the model may not reflect future climatic conditions as other meteorological variables such as cloud cover, solar radiation and rainfall are likely to be also be affected, and they will influence the heat budget and thermal structure of the lake (Bueche & Vetter 2014), while stratification is also highly sensitive to changes in wind (de Stasio *et al.,* 1996). It has been reported that increased air temperature could contribute to long term hypolimnetic warming, however, a longer simulation run (40 – 50 years) may be required to capture this effect (Peeters *et al*., 2002). Similar approaches of evaluating effects of increased air temperature on model simulation output against a baseline simulation using present-day meteorological input data have previously been used to simulate the effect of future climate change on lakes (Trolle *et al*., 2011; Bayer *et al*., 2013).

This study demonstrated that a 2.5 °C increase in air temperature would prolong lake thermal stratification and produce a shallower thermocline depth (Figure 3.7). A warming climate on its own was simulated to

increase lake productivity (Figure 3.8). Longer periods of thermal stratification due to warmer air temperature have also been predicted in model simulations for other lakes (e.g., Bueche and Vetter 2014; Hetherington *et al*., 2014) and may enhance cyanobacteria dominance because of their higher optimum temperatures for growth and ability of cells or colonies to float (Trolle *et al*., 2011; Mooij *et al*., 2007; Kosten *et al*., 2012). Higher abundance of phytoplankton may result in greater CO_2 influxes to lakes (Davidson *et al*., 2015). However, heterotrophic respiration might also be enhanced with higher availability organic carbon as well as warmer water temperature (Yvon-Durocher *et al*., 2010). Therefore, while climate warming may increase CO_2 fluxes to lake due to increasing phytoplankton biomass, this outcome should be treated with a degree of caution as ecosystem respiration may effectively counter this change and only a singly community component (phytoplankton) is represented in the model.

Lake restoration, simulated in this study by reducing internal and external nutrient loads, was demonstrated through model simulations to reduce phytoplankton productivity (Figure 3.8) which in turn increased release of CO_2 to the atmosphere (Figure 3.10). Observations of Danish lakes undergoing water quality improvement (reduced nutrients and chlorophyll *a* concentrations) over two decades, found annual increases in CO_2 emissions of up to 32% (Trolle *et al*., 2012). This observation is comparable to the model results for Lake Okaro, where reducing nutrient loads would reduce CO_2 uptake from the atmosphere by 46% (Table 3.4). However, under climate warming conditions, the effect of reduced nutrient loads on CO_2 emission rates is likely to be lower as the lake will be more productive due to warmer temperatures.

In mono- and dimictic lakes a very large diffusive emissions of CH_4 occur early on in the mixing phase (e.g. Fernandez *et al*., 2014). It has been hypothesised that a warming climate would increase these temporally discrete emissions (Bastviken *et al*., 2008, Rasilo *et al*., 2015). Model estimates of lake CH_4 diffusive emissions indicate a 25% increase with a

climate warming scenario of 2.5°C (Table 3.4, Figure 3.10). This scenario was associated with a longer duration of stratification which created a longer extent and duration of anoxic hypolimnion which sustained higher rates of CH_4 release from the sediment. Hypolimnetic warming due to climate change (Peeters *et al.*, 2002), additionally, might increase CH_4 as well as CO_2 fluxes from the sediment by increasing microbial activity (e.g., methanogenic metabolism). Marrota *et al*. (2014) proposed that increasing temperature, as projected by a 2100 climate (IPCC, 2007), would increase biological production of CO_2 and CH_4 in anaerobic sediment by 9 – 61% over present rates. Increasing temperature may also enhance emission via ebullition (DelSontro *et al.,* 2010). Therefore, model predictions of CH_4 emissions in this study may be conservative and future work will need to consider methods to quantify the highly heterogeneous ebullition fluxes of greenhouse gases from lakes.

3.4.3. Implication for lake restoration and greenhouse gas emission

The model simulations demonstrated that warming climate and changes in water quality affect CO_2 and CH_4 diffusive emissions from a small monomictic eutrophic lake. In terms of total carbon gas emissions (kg CO_2-eq m^{-2} y^{-1}), the model revealed that eutrophic lakes may act as net emitters, and continuation of a warming climate may magnify the scale of the emissions (Table 3.4). In this regard, CH_4 emissions were larger than CO_2 influxes in the total emission inventory due to greater greenhouse warming potential for CH_4 over CO_2. It is striking to note that the enhanced CO_2 atmospheric sink from the lake due to warming climate, in combination with nutrient enrichment, is overwhelmed by the release of CH_4 which is more strongly influenced by warming temperature than CO_2. The scenario used in the model simulations of reduced nutrients under a warming climate would still result in increased carbon emissions. In the case without a warming climate, increasing CO_2 uptake due to nutrient addition is still offset by the increased emission of CH_4, resulting in the lake still being a net carbon emitter to the atmosphere. These results suggest that CH_4 is a particularly important component in the total greenhouse gas emissions in eutrophic lakes. They also confirm that

eutrophication may promote climate change, and a warming climate would enhance greenhouse gas emissions from eutrophic lakes. Improving lake water quality under the influence of a warming climate could be used as a strategy to reduce the magnitude of greenhouse gas emissions.

3.5. References

Abell JM, Özkundakci D, Hamilton DP, Miller SD (2011) Relationships between land use and nitrogen and phosphorus in New Zealand lakes. *Marine and Freshwater Research*, **62**, 162–175.

Adams D (2005) Diffuse flux of greenhouse gases — methane and carbon dioxide — at the sediment-water interface of some lakes and reservoirs of the world. In: *Greenhouse Gas Emissions — Fluxes and Processes* (eds Tremblay A, Varfalvy L, Roehm C, Garneau M), pp. 129–153. Springer Berlin Heidelberg.

Barros N, Cole JJ, Tranvik LJ *et al*. (2011) Carbon emission from hydroelectric reservoirs linked to reservoir age and latitude. *Nature Geoscience*, **4**, 593–596.

Bastviken D (2009) Methane. In: *Encyclopedia of Inland Waters*, pp. 783–805.

Bastviken D, Tranvik L, Downing J, Crill PM, Enrich-prast A (2011) the Continental Carbon Sink. *Science*, **331**, 50.

Battin TJ, Luyssaert S, Kaplan LA, Aufdenkampe AK, Richter A, Tranvik LJ (2009) The boundless carbon cycle. *Nature Geoscience*, **2**, 598–600.

Bayer TK, Burns CW, Schallenberg M (2013) Application of a numerical model to predict impacts of climate change on water temperatures in two deep, oligotrophic lakes in New Zealand. *Hydrobiologia*, **713**, 53–71.

Benson BB, Krause D (1980) The concentration and isotopic fractionation of gases dissolved in freshwater in equilibrium with the atmosphere. 1. Oxygen. *Limnology and Oceanography*, **25**, 662–671.

Boudreau BP (1996) A method-of-lines code for carbon and nutrient diagenesis in aquatic sediments. *Computers and Geosciences*, **22**, 479–496.

Boudreau BP, Gardiner BS, Johnson BD (2001) Rate of growth of isolated bubbles in sediments with a diagenetic source of methane. *Limnology and Oceanography*, **46**, 616–622.

Bruce LC, Hamilton D, Imberger J, Gal G, Gophen M, Zohary T, Hambright KD (2006) A numerical simulation of the role of zooplankton in C, N and P cycling in Lake Kinneret, Israel. *Ecological Modelling*, **193**, 412–436.

Bueche T, Vetter M (2014) Future alterations of thermal characteristics in a medium-sized lake simulated by coupling a regional climate model with a lake model. *Climate Dynamics*, **44**, 371–384.

Burns N, McIntosh J, Scholes P (2009) Managing the lakes of the Rotorua District, New Zealand. *Lake and Reservoir Management*, **25**, 284–296.

Cole JJ, Caraco NF (1998) Atmospheric exchange of carbon dioxide in a low-wind oligotrophic lake measured by the addition of SF6. *Limnology and Oceanography*, **43**, 647–656.

Cole JJ, Caraco NF, Kling GW, Kratz TK (1994) Carbon dioxide supersaturation in the surface waters of lakes. *Science (New York, N.Y.)*, **265**, 1568–1570.

Cole JJ, Pace ML, Carpenter SR, Kitchell JF (2000) Persistence of net heterotrophy in lakes during nutrient addition and food web manipulations. *Limnology and Oceanography*, **45**, 1718–1730.

Connolly JP, Coffin RB (1995) Model of carbon cycling in planktonic food webs. *Journal of Environmental Engineering,* **121**, 682–690.

Davidson TA, Audet J, Svenning JC *et al*. (2015) Eutrophication effects on greenhouse gas fluxes from shallow-lake mesocosms override those of climate warming. *Global Change Biology*, **21**, 4449–4463.

Dean WE, Gorham E (1998) Magnitude and significance of carbon burial in lakes, reservoirs, and peatlands. *Geology*, **26**, 535–538.

del Giorgio PA, Cole JJ, Caraco NF, Peters RH (1999) Linking planktonic biomass and metabolism to net gas fluxes in northern temperate lakes. *Ecology*, **80**, 1422–1431.

DelSontro T, McGinnis DF, Sobek S, Ostrovsky I, Wehrli B (2010) Extreme methane emissions from a swiss hydropower reservoir: contribution from bubbling sediments. *Environmental Science & Technology*, **44**, 2419–2425.

de Stasio BT, Hill DK, Kleinhans JM, Nibbelink NP, Magnuson JJ (1996) Potential effects of global climate change on small north-temperate lakes: Physics, fish, and plankton. *Limnology and Oceanography*, **41**, 1136–1149.

Downing JA, Prairie YT, Cole JJ *et al*. (2006) The global abundance and size distribution of lakes, ponds, and impoundments. *Limnology and Oceanography*, **51**, 2388–2397.

Downing JA, Cole JJ, Middelburg JJ *et al*. (2008) Sediment organic carbon burial in agriculturally eutrophic impoundments over the last century. *Global Biogeochemical Cycles*, **22**, 1–10.

Environment Bay of Plenty (2006) *Lake Okaro Action Plan*. Rotorua, New Zealand.

Fernández JE, Peeters F, Hofmann H (2014) Importance of the autumn overturn and anoxic conditions in the hypolimnion for the annual methane emissions from a temperate lake. *Environmental Science and Technology*, **48**, 7297–7304.

Fischer HB EJ List, RCY Koh, J. Imberger, and NH Brooks, 1979: *Mixing in Inland and Coastal Waters*. Academic Press. NY.

Gal G, Hipsey MR, Parparov A, Wagner U, Makler V, Zohary T (2009) Implementation of ecological modeling as an effective management and investigation tool: Lake Kinneret as a case study. *Ecological Modelling*, **220**, 1697–1718.

Griffin SL, Herzfeld M, Hamilton DP (2001) Modelling the impact of zooplankton grazing on phytoplankton biomass during a dinoflagellate bloom in the Swan River Estuary, Western Australia. *Ecological Engineering*, **16**: 373-394

Hamilton DP, Schladow SG (1997) Prediction of water quality in lakes and reservoirs. Part I — Model description. *Ecological Modelling*, **96**, 91–110.

Hanson PC, Bade DL, Carpenter SR, Kratz TK (2003) Lake metabolism: Relationships with dissolved organic carbon and phosphorus. *Limnology and Oceanography*, **48**, 1112–1119.

Hetherington AL, Schneider RL, Rudstam LG, Gal G, DeGaetano AT, Walter MT (2015) Modeling climate change impacts on the thermal dynamics of polymictic Oneida Lake, New York, United States. *Ecological Modelling*, **300**, 1–11.

Hipsey MR, Bruce LC, Bruggeman J, Bolding K, Hamilton DP (2012) *GLM-FABM v0.9a Model Overview and User Documentation*. The University of Western Australia. Perth, 44 pp.

Hipsey MR, Bruce LC, Hamilton DP (2014) *General Lake Model: Model overview and user information. AED Report #26.* The University of Western Australia. Perth, 42 pp.

Janssen ABG, Arhonditsis GB, Beusen A *et al*. (2015) Exploring, exploiting and evolving diversity of aquatic ecosystem models: a community perspective. *Aquatic Ecology*, **49**, 513–548.

Kankaala P, Huotari J, Tulonen T, Ojala A (2013) Lake-size dependent physical forcing of carbon dioxide and methane effluxes from lakes in a boreal landscape. *Limnology and Oceanography*, **58**, 1915–1930.

Kirschke S, Bousquet P, Ciais P *et al*. (2013) Three decades of global methane sources and sinks. *Nature Geoscience*, **6**, 813–823.

Kosten S, Huszar VLM, Bécares E *et al*. (2012) Warmer climates boost cyanobacterial dominance in shallow lakes. *Global Change Biology*, **18**, 118–126.

Markfort CD, Perez ALS, Thill JW, Jaster DA, Porté-Agel F, Stefan HG (2010) Wind sheltering of a lake by a tree canopy or bluff topography. *Water Resources Research*, **46**, 1–13.

Marotta H, Pinho L, Gudasz C (2014) Greenhouse gas production in low-latitude lake sediments responds strongly to warming. *Nature Climate Change*, **4**, 11–14.

Martinez D, Anderson MA (2013) Methane production and ebullition in a shallow, artificially aerated, eutrophic temperate lake (Lake Elsinore, CA). *Science of the Total Environment*, **454-455**, 457–465.

McGinnis DF, Greinert J, Artemov Y, Beaubien SE, Wüest a. (2006) Fate of rising methane bubbles in stratified waters: How much methane reaches the atmosphere? *Journal of Geophysical Research: Oceans*, **111**, 1–15.

Meehl GA, Stocker TF, Collins WD *et al*. (2007) 2007: Global Climate Projections. *Climate Change 2007: Contribution of Working Group I to the Fourth Assessment Report of the Intergovernmental Panel on Climate Change*, 747–846.

Ministry for the Environment (2014) *National Policy Statement for Freshwater Management 2014*. Wellington, New Zealand.

IPCC (2007) *Climate change 2007: The Physical Science Basis. Contribution of Working Group I to the Fourth Assessment Report of the Intergovernmental Panel on Climate Change* (eds Solomon S, Qin D, Manning M, Chen Z, Marquis M, Averyt KB, Tignor M, Miller HL). Cambridge University Press, Cambridge, United Kingdom and New York, NY, USA, 1-1007 pp.

Mooij WM, Janse JH, De Senerpont Domis LN, Hülsmann S, Ibelings BW (2007) Predicting the effect of climate change on temperate shallow lakes with the ecosystem model PCLake. *Hydrobiologia*, **584**, 443–454.

Ministry for the Environment (2008) *Climate Change Effects and Impacts Assessment: A Guidance Manual for Local Government in New Zealand. 2nd Edition*. Mullan B; Wratt D; Dean S; Hollis M; Allan S; Williams T, Kenny G and Ministry for the Environment, Wellington.

Myhre G, Shindell D, Bréon F-M *et al*. (2013) 2013: Anthropogenic and Natural Radiative Forcing. In: *Climate Change 2013: The Physical Science Basis. Contribution of Working Group I to the Fifth Assessment Report of the Intergovernmental Panel on Climate Change* (ed Stocker T.F., Qin D., Plattner G.-K., Tignor M., Allen S.K., Boschung J., Nauels A. , Xia Y. BV and MPM), pp. 659–740. Cambridge University Press, Cambridge, United Kingdom and New York, NY, USA.

Obernosterer I, Benner R (2004) Competition between biological and photochemical processes in the mineralization of dissolved organic carbon. *Limnology and Oceanography*, **49**, 117–124.

Ojala A, Bellido JL, Tulonen T, Kankaala P, Huotari J (2011) Carbon gas fluxes from a brown-water and a clear-water lake in the boreal zone during a summer with extreme rain events. *Limnology and Oceanography*, **56**, 61–76.

Özkundakci D, Hamilton D, Trolle D (2011) Modelling the response of a highly eutrophic lake to reductions in external and internal nutrient loading. *New Zealand Journal of Marine and Freshwater Research*, **45**, 165–185.

Paul WJ, Hamilton DP, Gibbs MM (2008) Low-dose alum application trialled as a management tool for internal nutrient loads in Lake Okaro, New Zealand. *New Zealand Journal of Marine and Freshwater Research*, **42**, 207–217.

Peeters F, Livingstone DM, Goudsmit G-H, Kipfer R, Forster R (2002) Modeling 50 years of historical temperature profiles in a large central European lake. *Limnology and Oceanography*, **47**, 186–197.

Rasilo T, Prairie YT, del Giorgio PA (2015) Large-scale patterns in summer diffusive CH4 fluxes across boreal lakes, and contribution to diffusive C emissions. *Global Change Biology*, **21**, 1124–1139.

Raymond PA, Hartmann J, Lauerwald R *et al*. (2013) Global carbon dioxide emissions from inland waters. *Nature*, **503**, 355–359.

Read JS, Hamilton DP, Jones ID *et al*. (2011) Derivation of lake mixing and stratification indices from high-resolution lake buoy data. *Environmental Modelling & Software*, **26**, 1325–1336.

Read JS, Winslow LA, Hansen GJA, Van Den Hoek J, Hanson PC, Bruce LC, Markfort CD (2014) Simulating 2368 temperate lakes reveals weak coherence in stratification phenology. *Ecological Modelling*, **291**, 142–150.

Riera JL, Schindler JE, Kratz TK (1999) Seasonal dynamics of carbon dioxide and methane in two clear-water lakes and two bog lakes in northern Wisconsin, U.S.A. *Canadian Journal of Fisheries and Aquatic Sciences*, **274**, 1–10.

Romero JR, Antenucci JP, Imberger J (2004) One- and three-dimensional biogeochemical simulations of two differing reservoirs. *Ecological Modelling*, **174**, 143–160.

Schladow SG, Hamilton DP (1997) Prediction of water quality in lakes and reservoirs: Part II - Model calibration, sensitivity analysis and application. *Ecological Modelling*, **96**, 111–123.

Sherman FS, Imberger J, Corcos GM (1978) Turbulence and Mixing in Stably Stratified Waters. *Annual Review of Fluid Mechanics*, **10**, 267–288.

Søndergaard M, Jensen JP, Jeppesen E (2003) Role of sediment and internal loading of phosphorus in shallow lakes. *Hydrobiologia*, **506**, 135–145.

Spigel RH, Imberger J, Rayner KN (1986) Modeling the diurnal mixed layer. *Limnology and Oceanography*, **31**, 533–556.

Striegl RG, Michmerhuizen CM (1998) Hydrologic influence on methane and carbon dioxide dynamics at two north-central Minnesota lakes. *Limnology and Oceanography*, **43**, 1519–1529.

Tranvik LJ, Downing JA, Cotner JB *et al*. (2009) Lakes and reservoirs as regulators of carbon cycling and climate. *Limnology and Oceanography*, **54**, 2298–2314.

Trolle D, Hamilton DP, Pilditch CA, Duggan IC, Jeppesen E (2011) Predicting the effects of climate change on trophic status of three morphologically varying lakes: Implications for lake restoration and management. *Environmental Modelling and Software*, **26**, 354–370.

Trolle D, Staehr PA, Davidson TA, Bjerring R, Lauridsen TL, Søndergaard M, Jeppesen E (2012) Seasonal dynamics of CO_2 flux across the surface of shallow temperate lakes. *Ecosystems*, **15**, 336–347.

Walter KM, Zimov SA, Chanton JP, Verbyla D, Chapin FS (2006) Methane bubbling from Siberian thaw lakes as a positive feedback to climate warming. *Nature*, **443**, 71–75.

Walter KM, Chanton JP, Chapin FS, Schuur EAG, Zimov SA (2008) Methane production and bubble emissions from arctic lakes: Isotopic implications for source pathways and ages. *Journal of Geophysical Research: Biogeosciences*, **113**, G3, doi:10.1029/2007JG000569.

Weinstock J (1981) Vertical turbulence diffusivity for weak or strong stable stratification. *Journal of Geophysical Research: Oceans*, **86**, 9925–9928.

Wiesenburg DA, Guinasso NL (1979) Equilibrium solubilities of methane, carbon monoxide, and hydrogen in water and sea water. *Journal of Chemical & Engineering Data*, **24**, 356–360.

Winslow L, Read J, Woolway R, Brentrup J, Leach T, Zwart J (2015) rLakeAnalyzer: Package for the Analysis of Lake Physics.

Yeates PS, Imberger J (2003) Pseudo two dimensional simulations of internal and boundary fluxes in stratified lakes and reservoirs. *International Journal of River Basin Management*, **1**, 297–319.

Yvon-Durocher G, Jones JI, Trimmer M, Woodward G, Montoya JM (2010) Warming alters the metabolic balance of ecosystems. *Philosophical Transactions of the Royal Society of London. Series B, Biological Sciences*, **365**, 2117–2126.

Chapter 4 Carbon dioxide emissions and sediment organic carbon burial across a gradient of trophic state gradient in eleven New Zealand lakes

Abstract

Lakes are known to be important to the global carbon balance as they are both CO_2 sources to the atmosphere and also accumulate large amounts of carbon in their sediment. Dissolved CO_2 dynamics in 11 lakes of varying trophic state in the Rotorua region, New Zealand, were examined. Organic carbon content in bottom sediments was used to derive estimates of the effects of sediment accumulation and diagenesis on carbon burial, and to provide insights into net accumulation of sediment carbon. Lakes may shift from being atmospheric CO_2 sources to sinks due to seasonal changes in phytoplankton productivity and lake mixing dynamics. Decreases in trophic state (i.e., improved water quality) in some of the lakes over the eight-year monitoring period were associated with increased surface water CO_2 concentrations and as a consequence, increasing CO_2 flux to the atmosphere. Lakes with high phytoplankton productivity, indicated by high chlorophyll *a* biomass, generally had high rates of carbon deposition to the sediments, but not all deposited carbon was permanently buried. This study suggests that greenhouse gases produced during carbon remineralization in the sediment may potentially be released to the atmosphere and their quantification is critical to establishing the role of lakes in the global carbon cycle.

Keywords: CO_2 flux, sediment carbon accumulation, seasonal variation, lake restoration, carbon balance.

4.1. Introduction

Lakes play an important role in processing organic carbon (OC) derived from their catchments and within the waterbody itself (i.e., allochthonous

and autochthonous production, respectively). This carbon is either stored in lake sediments or released as carbon dioxide (CO_2) and methane (CH_4) to the atmosphere (Cole *et al.* 2007; Tranvik *et al.* 2009). The vast majority of world's lakes are considered to be CO_2 sources to the atmosphere (Cole *et al.* 1994), largely due to respiration of OC derived from terrestrial sources, which subsidises lake community respiration (Hanson *et al.* 2003; Sobek *et al.* 2005) and inputs of dissolved inorganic carbon derived from carbonate weathering in the watershed (Marcé *et al.* 2015). Carbon dioxide fluxes vary seasonally (López Bellido *et al.* 2009), and as a result lakes may alternate between being highly heterotrophic (CO_2 source) and highly autotrophic (CO_2 sink: Trolle *et al.* 2012). Physical processes associated with water column mixing and overturn (Striegl and Michmerhuizen 1998), storm loads of organic and inorganic carbon (Ojala *et al.* 2011; Vachon and del Giorgio 2014), as well as seasonal variations in phytoplankton productivity and community respiration (del Giorgio and Peters 1999) influence the concentration of dissolved CO_2, and thereby alter the magnitude of CO_2 lake-atmosphere exchanges. Nutrient availability (Hanson *et al.* 2003; Trolle *et al.* 2012) also plays a role in regulating CO_2 in lakes, as it is an important determinant of autochthonous production. The highest rates of lake CO_2 influx tend to occur in eutrophic lakes, but can vary with the structure of the food web, which in turn regulates primary production (Cole *et al.* 2000; Marotta *et al.* 2012). In contrast, oligotrophication can lead to an increase in CO_2 emissions from lakes (Trolle *et al.* 2012).

The progression of eutrophication is characterised by rates of OC burial in lake sediments that exceed rates of carbon emission from the water surface (Hanson *et al.* 2004). However, the burial efficiency of OC (i.e., the ratio of burial to mineralization rate) in eutrophic lakes can be low, as sedimentary OC is mainly sourced from phytoplankton and is readily decomposed. High decomposition rates result in less accumulated carbon in the sediment (Burdige 2007), often despite relatively high sedimentation rates (Downing *et al.* 2008). Less productive lakes receive a higher

relative load of allochthonous refractory carbon, leading to higher carbon burial efficiency (Sobek *et al.* 2009).

Inland waters (including ponds, lakes, wetlands, reservoirs, streams and rivers) cover approximately 3% of the Earth's surface (Downing *et al.* 2006) and have been estimated to be a sink for 0.23 – 0.6 Pg y^{-1} of carbon (Cole *et al.* 2007; Tranvik *et al.* 2009; Reigner *et al.* 2013). This estimate is the same order of magnitude as the global oceanic carbon sink (0.29 Pg y^{-1}, Le Quéré *et al.* 2015). This shows that, although there is some degree of uncertainty in the estimates, lakes are important in regulating the global carbon cycle. In addition, small water bodies with surface areas of <1 km^2 (Downing *et al.* 2006) are prone to eutrophication and OC burial, a process which may increase the influence that freshwaters have on the global carbon cycle (Downing *et al.* 2008).

In this study, a combined analysis of CO_2 flux dynamics and sediment carbon deposition from 11 lakes of varying trophic state (oligotrophic to eutrophic) and mixing regime (monomictic to polymictic) was used to determine the fate of carbon. This analysis synthesized monthly water quality data collected over an eight-year period from 2002 to 2010 to capture the seasonal variability and annual CO_2 flux from the lakes. In addition, it was hypothesised that reductions in nutrients, leading to decreases in chlorophyll *a* concentration, would increase CO_2 concentrations in surface waters and as a consequence would also increase CO_2 evasion from the lakes. Therefore, as eutrophic lakes act as a sink for atmospheric CO_2 due to high autotrophic activity, I hypothesised that these lakes would also have higher rates of net carbon deposition than oligotrophic lakes.

4.2. Methods

4.2.1. Study sites and parameter of interest

The Rotorua lakes (Figure 4.1) lie in the Central Volcanic Plateau of the North Island, New Zealand. Many of the lakes were formed around 140,000 y BP by a series of volcanic eruptions (Lowe and Green, 1987). Several of the lakes are influenced by surface geothermal inflows (Vincent and Forsyth 1987). Mazot *et al.* (2014) identified that Lake Rotomahana has been an active hydrothermal area since Tarawera eruption in 1886 and might massively release 29.5 mol CO_2 m^{-2} d^{-1} through ebullition. Anthropogenic activities, i.e. urbanisation and agriculture (McColl 1972; Hamilton 2005), also threaten lakes in this area while others remain largely unaffected by human influence, resulting in variation in trophic state from oligotrophic to highly eutrophic (Table 4.1). Action Plans developed by the regional council have been put in place to remediate a number of the Rotorua lakes from excess of nutrient loading (Burns *et al.* 2009; Abell *et al.* 2011).

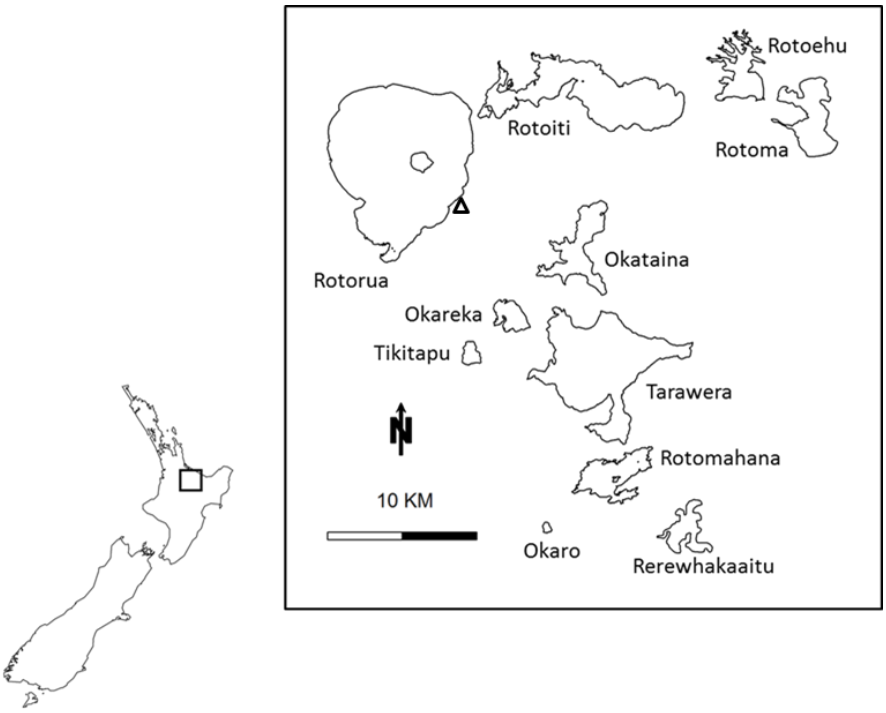

Figure 4.1 Location of the 11 Rotorua lakes in the North Island of New Zealand. The triangle indicates location of Rotorua Airport climate station

Water column variables used in this study were compiled from monthly measurements taken by Bay of Plenty Regional Council (BOPRC) at a deep-water station of each lake during the period of 2002 to 2010. Measurements included chlorophyll *a* (Chl), total nitrogen (TN) and total phosphorus (TP) at the surface (1 m depth) and pH at both surface and bottom water (~1 m above the sediment). Vertical profiles of temperature and dissolved oxygen were also measured from CTD casts (SBE 19 plus, Seabird Electronics). Alkalinity was measured from the surface water at least twice a year by BOPRC. All water quality parameters (Chl, TN, TP and alkalinity) were analysed using standard methods based on APHA (1998) and described by Burns *et al.* (2000). Relevant morphological and water quality parameters for each lake are given in Table 4.1. Sediment carbon content data was sourced from Pickett (2008) for Lake Rotorua and from Trolle *et al.* (2008) for the remaining lakes. Intact sediment cores were taken between 2006 and 2007 from the deepest basin of the lakes using a piston corer for Lake Rotorua (Pickett 2008) or a cylindrical gravity corer for the other lakes (Trolle *et al.* 2008). McColl (1977) reported that sediments of Rotorua lakes are mostly non-calcareous with total carbon (TC) content contributed mostly in organic form. The cores were sliced at 1-2 cm intervals and the slices were dried and analysed for percentage OC content using a LECO TruSpec CN Determinator. The Mt Tarawera eruption of 1886 provided a distinctive tephra layer in the core which was used to calculate annual mean sedimentation rate for the period of 1886 – 2006 (see Trolle *et al.* 2008).

4.2.2. Thermal stratification

The depth of thermocline was defined as greatest rate of density change with depth, determined from vertical variations in temperature from CTD casts. The rLakeAnalyzer software (Winslow *et al.* 2015) was used to assist with calculations of thermocline depth (see theoretical basis given by Read *et al.* 2011).

Table 4.1 Physical and chemical properties of the study lakes. Values of CO_2, chlorophyll *a* (Chl), total nitrogen, total phosphorus (TP) are the mean of long term measurements and numbers in parentheses indicate the range of values. Trophic state categories are oligotrophic (oligo), mesotrophic (meso) and eutrophic (eu). Mixing regimes are monomictic (mono) and polymictic (poly).

Lake	Max depth (m)	Mean depth (m)	Surface area (km^2)	Surface CO_2 ($\mu mol\ C\ L^{-1}$)	Bottom CO_2 ($\mu mol\ C\ L^{-1}$)	CO_2 flux ($mmol\ C\ m^{-2}\ d^{-1}$)	Net annual CO2 flux ($mmol\ C\ m^{-2}\ y^{-1}$)	Chl ($\mu g\ L^{-1}$)	TN ($\mu g\ L^{-1}$)	TP ($\mu g\ L^{-1}$)	Alk ($\mu mol\ L^{-1}$)	Trophic state (-trophic)	Mixing regime (-mictic)
Okareka	33.5	20	3.3	5.26	25.87	0.82	37.72	3.8	206.6	7.7	290	meso	mono
				(0.43-19.81)	(2.8-90.76)	(-5.86-25.1)		(1.3-9.2)	(48.5-323.5)	(0.5 - 24)			
Okaro	18	12.5	0.3	4.77	41.49	-0.53	-327.16	29.3	875.3	65.3	320	eu	mono
				(0-30.68)	(1.6-126.62)	(-7.56-27.88)		(0.9-283)	(202-2940.5)	(11 - 161)			
Okataina	78.5	39.4	10.8	7.00	30.51	3.85	1049.97	2.4	134.7	8.3	310	oligo	mono
				(1.9-20.7)	(3.42-187.82)	(-4.41-30.56)		(0.3-7.2)	(40.5-438)	(0.5 - 49)			
Rerewhakaaitu	15.8	7	5.8	6.20	9.98	2.70	684.67	3.5	389.3	9	230	meso	poly
				(1.16-22.63)	(1.69-48.42)	(-5.95-33.75)		(1-9.8)	(65-708)	(1 - 21)			
Rotoehu	13.5	8.2	8.1	4.97	6.98	0.52	69.78	10.6	400.1	37.2	630	eu	poly
				(0.74-15.61)	(0.76-31.5)	(-6.54-19.87)		(2.8-28.7)	(120-809)	(10 - 118)			
Rotoiti	124	31.5	34.6	12.13	46.79	14.73	5428.98	9.7	298.3	24.1	198	meso	mono
				(0.37-37.17)	(5.96-184.03)	(-7.72-53.7)		(2.4-38.6)	(82-573)	(4 - 51)			
Rotoma	83	36.9	11.2	6.73	21.09	3.70	908.48	1.3	151.2	4.7	210	oligo	mono
				(1.08-19.75)	(5.19-101.48)	(-7.88-28.04)		(0.3-3.5)	(36.5-425)	(0.5 - 13)			
Rotomahana	125	60	9	88.15	333.62	148.73	57255.50	4.3	215.9	33.3	1800	meso	mono
				(17.83-321.79)	(41.7-1277.32)	(27.65-542.47)		(1.3-13.7)	(72.5-366)	(6 - 98)			
Rotorua	11	44.8	80.8	7.06	10.55	5.33	1867.03	21.2	452.6	35.9	75	eu	poly
				(0.15-22.03)	(1.19-36.48)	(-9.66-31.43)		(0.1-78.1)	(215-1810.5)	(9 - 70)			
Tarawera	87.5	50	41.7	11.32	25.81	13.03	4625.26	1.5	127.4	9.5	1120	oligo	mono
				(4.51-24.06)	(12.59-55.48)	(1.35-45.48)		(0.4-3.6)	(18-657.5)	(2 - 25)			
Tikitapu	27.5	18	1.5	7.51	41.84	4.11	1476.21	2	206.7	5.9	41	oligo	mono
				(0.21-20.82)	(1.61-323.53)	(-7.14-33.41)		(0.3-5.6)	(53-483)	(0.5 - 27)			

4.2.3. Dissolved CO_2 calculation

Concentrations of CO_2 (µmol C L^{-1}) in the water column were calculated from the dissociation of dissolved inorganic carbon in freshwater according to pH and alkalinity values at a given temperature (Stumm and Morgan 1996). Due to the limited number of alkalinity measurements, CO_2 was calculated by increasing the alkalinity value by 20% from the measured data to give a range of possible of CO_2 concentrations. This range corresponds to the variations of alkalinity values in Rotorua lakes reported by Timperley and Vigor-Brown (1986) and McColl (1972).

4.2.4. CO_2 air-water exchange estimation

Air-water exchange of CO_2 was computed using Fick's law of gas diffusion:

$$FCO_2 = k_{CO2} (CO_{2aq} – CO_{2sat}) \quad (1)$$

where FCO_2 is the CO_2 flux across the air-water interface (mmol C m^{-2} d^{-1}), CO_{2aq} is the concentration of dissolved CO_2 atmosphere in the surface water (µmol C L^{-1}), k_{CO2} is the gas exchange coefficient (cm d^{-1}) and CO_{2sat} is the CO_2 saturation concentration (µmol C L^{-1}) for a given temperature and atmospheric CO_2 mole fraction in dry air (Weiss and Price, 1980). A monthly average atmospheric CO_2 dataset from 2001 to 2010 was obtained from Baring House Station, Wellington, New Zealand (Dlugokencky *et al.* 2013). Values of k_{gas} were determined from k_{600} standardized to a Schmidt number of 600 (Jähne et al.1987):

$$k_{CO2} = k_{600} (SC_{CO2} / 600)^{-n} \quad (2)$$

where SC_{CO2} is the Schmidt number for CO_2 at given water temperature (Wanninkhof 1992). A value of n of 0.67 and 0.5 was assigned for a wind speed below and above 3 m s^{-1}, respectively (Crusius and Wanninkhof 2003). Values of k_{600} were derived from a wind-based model that accounts for lake size (Vachon and Praire 2013):

$$k_{600} = 2.51 + 1.14U_{10} + 0.39U_{10}\log_{10}LA \quad (3)$$

where U_{10} is the wind speed (m s^{-1}) at 10 m elevation and LA is lake area in km^2. Wind data were obtained from the National Climate Data Base for the Rotorua Airport climate station (see Figure 4.1).

4.2.5. Sediment deposition and burial

Sediment carbon deposition and burial were calculated based on a first-order diagenesis model for labile organic matter (Berner 1980; Klump *et al.* 2009). The composition of OC deposited on the sediment surface was assumed to initially consist of two fractions: permanently buried and metabolizable material. The latter is remineralized and released back to the hypolimnetic layer. The model calculates percentage of OC content in the dry mass of sediment:

$$G_z = G_m \exp[(-k_m\, \omega^{-1})/z] + G_{inf} \qquad (4)$$

where G_z is OC content (%) at depth z (cm) in the sediment column, G_m is the metabolizable carbon (%) in the initially deposited carbon in the sediments, G_{inf} is the non-metabolizable residual (%), and k_m and ω are the first-order rate constant (y^{-1}) and mass accumulation rate (kg m^{-2} y^{-1}), respectively. Published values of ω were used for each lake from Trolle *et al.* (2008). This value was based on an assumption that deposition rates were constant after the Tarawera eruption in 1886. The model was fitted with the measured carbon profile in the sediment using a Nelder-Mead optimization algorithm to estimate the values of G_m, k_m and G_{inf}, minimizing negative log-likelihood errors and maximizing the Pearson correlation coefficient (r). The carbon fluxes (mol m^{-2} y^{-1}) for carbon deposition (J_{in}), burial (J_{bur}) and remineralization (J_{rec}) were calculated by multiplying the %C of the estimated sedimentary matter fractions with ω:

$$J_{in} = \omega\,(G_m + G_{inf}) \qquad (5)$$

$$J_{bur} = \omega\,(G_{inf}) \qquad (6)$$

$$J_{rec} = \omega\,(G_m) \qquad (7)$$

Using the observed tephra depth, the recent areal OC stock (from 1886 to 2006) in the lake sediment was estimated by summing the OC content

down to the tephra layer. The total %C concentration in that layer was multiplied by the annual mass accumulation rate (ω) and the age of the tephra (120 years). Knowing that lake sediments do not accumulate uniformly over the lake's surface but are influenced by sediment focusing, I then calculated the mean thickness of the sediment above the tephra layer and spread it over the entire lake basin based on Ferland *et al.* (2014) as:

$$Z_{mean\_sed} = Z_{max\_sed} /(q + 1) \quad (8)$$

where Z_{mean_sed} is mean depth at which tephra was located, Z_{max_sed} is the maximum depth of the tephra layer and q is exponent value describing the shape of the lake. Following Ferland *et al.* (2014) q was estimated based on the hypsometric relationship between surface area and water depth (Imboden 1973) as:

$$A_z = A_0 (1 – Z / Z_{max})^q \quad (9)$$

where A_z is the planar area at depth Z, A_0 is the surface area of lake and Z_{max} is the maximum lake depth. The value q was solved using a Nelder-Mead optimization algorithm by minimizing negative log-likelihood errors between A_z and the lake's planar area from the hypsometric curve.

4.2.6. Data analysis

Monthly patterns for dissolved CO_2 concentration, fluxes and other measured variables in each lake were developed using a bootstrapping and decomposition technique to examine seasonal and long-term dynamics in water column variables. The extracted median and 95% confidence interval of the bootstrapped data were then plotted to depict seasonal patterns. Pearson's correlation coefficient was used to examine the relationship between CO_2 flux and water quality variables (Chl, TP and TN). A seasonal Mann-Kendall test was used to determine the trend of change (units y^{-1}) in each variable over the entire period of study (Jassby and Cloern 2014). To calculate cumulative annual CO_2 flux, I calculated the areas under the curve of the median bootstrapped flux using the trapezoidal rule (R package Hmisc: Harrell, 2015). All computations and

analyses were performed in the R statistical package (R Core Team 2014; Version 3.1.2).

4.3. Results

Atmospheric CO_2 flux and surface water quality parameters (Chl, TP and TN) in the 11 Rotorua lakes ranged widely (Table 4.1) but there was a strong seasonal pattern in water temperature and mixing regimes, which were either monomictic or dimictic (see Table 4.1). In addition, the pattern of carbon deposition to the sediment was distinguishable by lake trophic state. To further illustrate seasonal variations in CO_2 flux and water quality variables, as well as sediment carbon profiles, three exemples (Tarawera, Okaro and Rotoehu) representing different mixing regimes and trophic states are presented below. Lakes Tarawera and Okaro are oligotrophic and eutrophic, respectively, and both are monomictic, while Lake Rotoehu is eutrophic and polymictic.

4.3.1. Seasonal variation of CO_2 flux

There were strong seasonal variations in CO_2 concentrations among the lakes in association with thermal stratification dynamics (Figure 4.2). In the monomictic lakes (see Table 4.1), surface water CO_2 concentrations increased as the thermocline started to deepen in autumn (around May) and reached maximum levels during the winter mixing period. As this group of lakes stratified, surface CO_2 concentrations decreased. Concentrations varied from under- to over-saturation seasonally (Figure 4.2) apart from Lakes Rotomahana and Tarawera, which were usually supersaturated and therefore released CO_2 to the atmosphere (Table 4.1). Bottom water CO_2 concentrations showed an inverse pattern to the surface concentrations in the monomictic lakes, with concentrations highest in late summer. In the polymictic lakes (see Table 4.1), thermal stratification only occurs in 2 – 3 months during summer (January to February), hence, CO_2 concentrations in surface and bottom waters were relatively similar throughout the year (Figure 4.2).

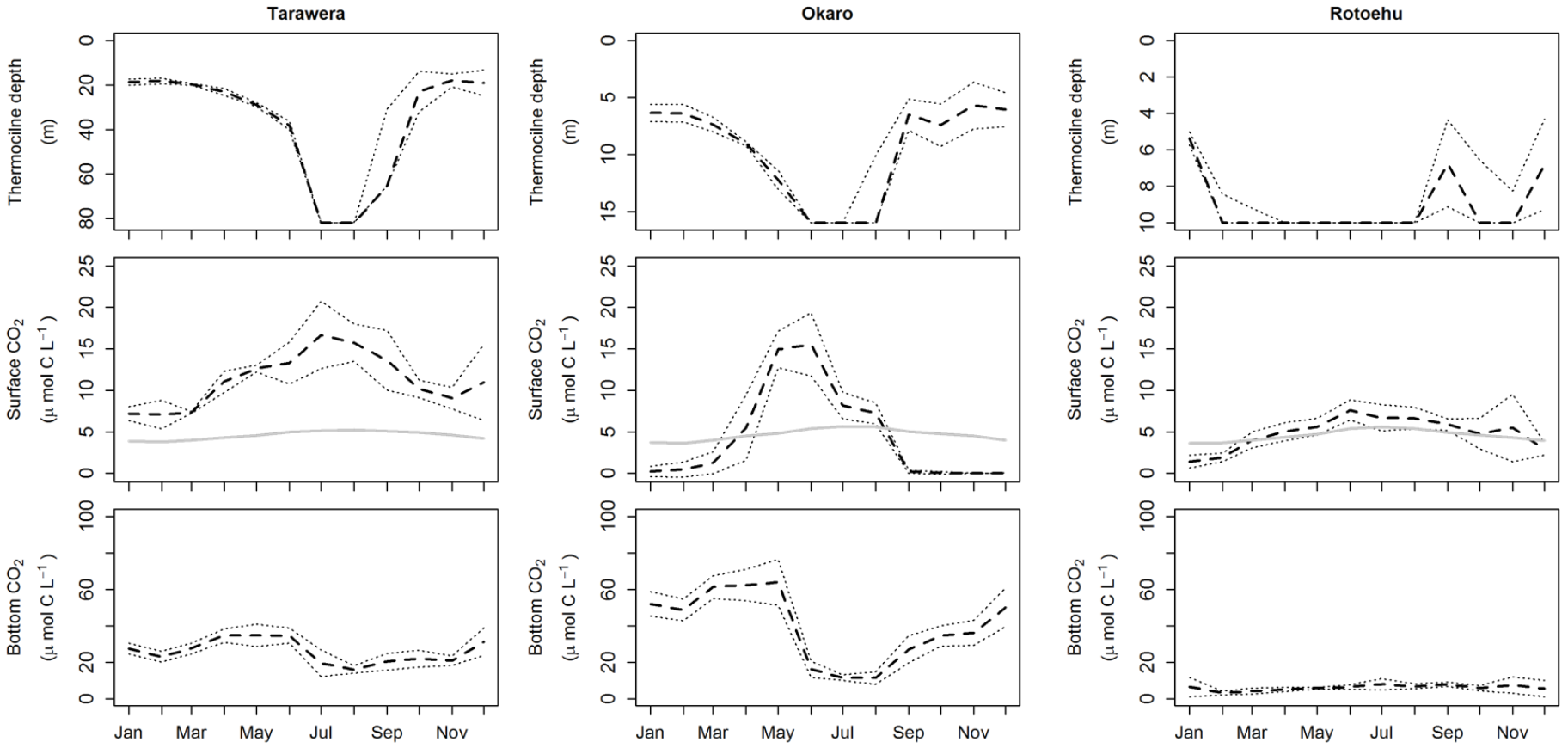

Figure 4.2 Seasonal variation of thermocline depth and CO_2 concentration in Lakes Tarawera, Okaro and Rotoehu. Dashed lines and dotted lines indicate the median of the bootstrapped monthly data over the period of 2002 – 2010 and the 95% confidence interval, respectively. Solid gray lines indicate CO_2 saturation concentrations.

Apart from highly eutrophic Lake Okaro, the Rotorua lakes were calculated to be annual net CO_2 emitters to the atmosphere (Table 4.1). However, there was no distinct pattern of net annual CO_2 emission with regard to trophic state. Eutrophic (Lake Rotorua) and mesotrophic lakes (Lakes Rotoiti and Rotomahana) were calculated to emit more CO_2 annually than the oligotrophic lakes (Table 4.1).

4.3.2. Correlations and long-term trends of CO_2 and water quality variables

Influences of Chl, TP and TN concentrations on CO_2 fluxes in the lakes were examined using annual average values. Lake Rotomahana was excluded from the analysis because of its extreme CO_2 fluxes associated with geothermal emissions (see Table 4.1). Fluxes of CO_2 were significantly negatively correlated with Chl, TP and TN (Table 4.2). Chlorophyll *a* showed a significant positive correlation with nutrients (TP and TN). Therefore lakes with higher concentrations of Chl and nutrients tended to have low surface water CO_2 concentrations. However, while lakes undergoing restoration programmes showed declining trends of chl (~2 – 6% per year) and nutrients, this was not always reflected in increasing CO_2 emissions. Only Lakes Okaro and Rotoma showed a significantly increasing (12 and 19% per year, respectively) CO_2 emissions following a decrease in Chl concentrations (Table 4.3).

Table 4.2 Pearson correlation matrix of surface water CO_2 and water quality parameters for Rotorua lakes.

	Chlorophyll *a*	Total phosphorus	Total nitrogen
Total phosphorus	0.87***		
Total nitrogen	0.89***	0.85***	
CO_2 flux	-0.29**	-0.34**	-0.37***

Lake Rotomahana was excluded in the analysis due to its extreme CO_2 concentration compared with the other lakes (See Table 4.1) and log transformation did not yield a substantial improvement in strength of the correlation. n = 90, ** significant at $p<0.01$, *** significant at $p<0.001$.

Table 4.3 Trends in eight-year (2002 – 2010) of CO_2 flux and water quality in selected Rotorua lakes calculated by seasonal Mann-Kendall tests where there is active management to reduce nutrient loads. Numbers in parentheses indicate percentage change calculated from the long term mean concentration.

Lake	CO_2 flux	TP	TN	Chl
	mmol m^{-2} y^{-1}	µg L^{-1} y^{-1}	µg L^{-1} y^{-1}	µg L^{-1} y^{-1}
Okareka	0.56	0	-0.1	0.06
	(-18.75)	(0)	(-0.05)	-1.48
Okaro	0.38*	-4.38***	-18.24***	-1.00***
	(19.40)*	(-6.71)	(-2.08)	(-3.40)
Rotoehu	-0.79	1	-17.05***	-0.34
	(-41.45)	(-2.69)	(-4.26)	(-3.18)
Rotoiti	-0.28	-0.69	-20.37***	-0.57***
	(-0.52)	(-3.52)	(-6.83)	(-5.95)
Rotoma	1.72*	-0.16	-1.5	-0.03*
	(12.68)*	(-3.52)	(-0.99)	(-2.16)*
Rotorua	2.04	-2.45***	-8.19	-1.34***
	(10.44)	(-6.82)	(-1.81)	(-6.29)

* significant at *p*<0.05, ** significant at *p*<0.01, *** significant at p<0.001

4.3.3. Sediment organic carbon

A diagenetic model was used to reconstruct the observed sediment carbon profile in the 11 Rotorua lakes based on the accumulated sediment between 1886 and 2006. The model reproduced sediment carbon profiles based on an exponential decrease of carbon involving deposition, remineralization, and burial (Table 4.4). There was an exponential pattern of decay of total carbon (TC) through the profile in the core, as visualized by the three example lakes (Tarawera, Okaro, Rotoehu; Figure 4.3). Deposition rates (J_{in}) of carbon ranged from 0.31 to 2.82 mol C m^{-2} y^{-1}, with meso- to eutrophic lakes having higher deposition fluxes than the oligotrophic lakes (Table 4.4). However, the lowest carbon burial rate (J_{bur}) was calculated to be in the most eutrophic lake, Okaro (0.8×10^{-3} mol C m^{-2} y^{-1}), while the highest was in eutrophic Lake Rotorua (0.19 mol C m^{-2} y^{-1}) (Table 4.4). By using the diagenetic model to sumthe carbon content to the tephra layer in the sediment core, the recent areal carbon stock (1886 to 2006) was determined for the lake sediment. Eutrophic lakes were calculated to have higher areal carbon stock (e.g., Lake Okaro: 3.65×10^{3} mol C mol^{-2}) while oligotrophic lakes stored less carbon (e.g., Lake Tikitapu: 0.29×10^{3} mol C mol^{-2}) (Table 4.4).

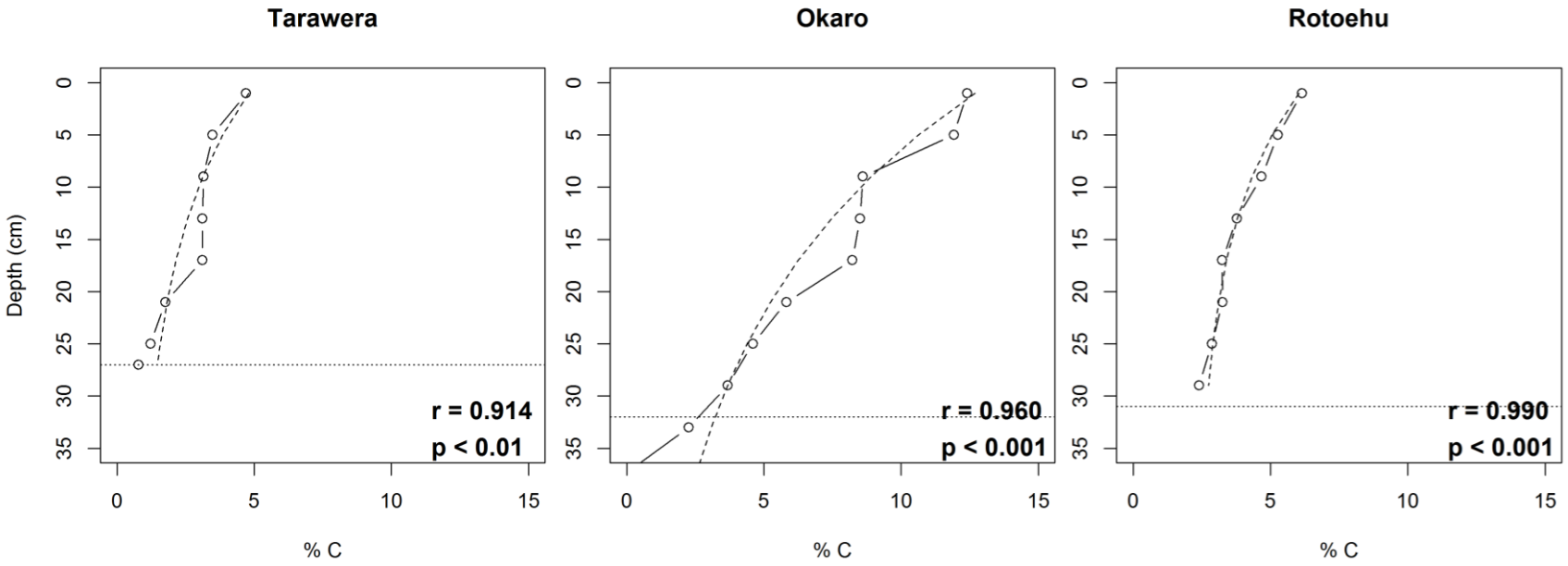

Figure 4.3 Organic carbon profile in the sediment of Lakes Tarawera, Okaro and Rotoehu. Open circles-lines indicate field measurements, dashed lines indicate model output, horizontal dashed lines indicate the depth of the 1886 Tarawera tephra.

Table 4.4 Sediment accumulation rates and organic carbon diagenesis model outputs for 11 Rotorua lakes for the period 1886 -2016.

Lake	Mass accumulation rate ω (kg m^{-2} y^{-1})	First order rate constant k_m (y^{-1})	Mineralizable organic carbon G_m (%C)	Non-mineralizable organic carbon G_{inf} (%C)	Organic carbon deposition rate J_{in} (mol m^{-2} y^{-1})	Organic carbon remineralization rate J_{rec} (mol m^{-2} y^{-1})	Organic carbon burial rate J_{bur} (mol m^{-2} y^{-1})	Organic carbon stock (mol m^{-2})	Fitness of the model: Pearson correlation coefficient
Okareka	0.26	0.03	5.54	0.70	1.35	1.20	0.15	1030	0.989***
Okaro	0.21	0.01	13.26	0.01	2.32	2.32	<0.01	3650	0.960***
Okataina	0.21	0.02	3.61	0.64	0.74	0.63	0.11	580	0.936**
Rerewhakaaitu	0.21	0.03	15.59	0.51	2.82	2.73	0.09	1350	0.960**
Rotoehu	0.36	0.01	5.92	0.62	1.96	1.78	0.18	3360	0.943***
Rotoiti	0.2	0.03	7.72	0.69	1.40	1.29	0.12	670	0.982**
Rotoma	0.27	0.03	5.17	0.78	1.34	1.16	0.18	1130	0.956*
Rotomahana	0.08	0.02	3.83	0.78	0.31	0.25	0.05	140	0.860*
Rotorua	0.35	0.04	4.51	0.66	1.51	1.31	0.19	1500	0.894***
Tarawera	0.21	0.01	4.31	0.76	0.89	0.75	0.13	1220	0.914**
Tikitapu	0.11	0.01	4.06	0.57	0.42	0.37	0.05	290	0.973**

* significant at $p<0.05$, ** significant at $p<0.01$, *** significant at $p<0.001$.

4.4. Discussion

Lake hydrodynamics are known to control the seasonal patterns of CO_2 concentrations in lakes (Striegl and Michmerhuizen 1998; Riera *et al.* 1999; López Bellido *et al.* 2009). In mono- and dimictic lakes, CO_2 produced by decomposition accumulates in the hypolimnion during summer stratification while surface water CO_2 concentrations become depleted due to photosynthetic uptake. Under these conditions CO_2 fluxes are from the atmosphere into the surface water of lakes (del Giorgio *et al.* 1999). Once in the water column, the dissolved CO_2 is assimilated by phytoplankton and converted into biomass, although 50 – 95% of phytoplankton production is respired back to the water column (Quay *et al.* 1986; Cole *et al.* 2002). When monomictic lakes become fully mixed in winter, the accumulated hypolimnetic CO_2 is released, causing supersaturation and CO_2 emissions to the atmosphere. This pattern was observed in all 11 Rotorua lakes, including those that are polymictic (Rotorua, Rotoehu and Rerewhakaaitu). Large hypolimnetic accumulations of CO_2 were not observed in polymictic lakes as they frequently mix. Thus the timing of mixing and stratification events plays an important role in the extent, timing and duration of pulses of greenhouse gases release to the atmosphere (e.g. Figure 4.3).

Lake CO_2 concentrations are influenced by four processes including: 1) external carbon inputs (Maberly *et al.* 2013; Marce *et al.* 2015), 2) lake hydrodynamics (Striegl and Michmerhuizen 1998), 3) internal carbon processing including metabolism and carbon mineralisation (del Giorgio *et al.* 1999; Klump *et al.* 2009), and 4) dissociation with carbonate species which is controlled by pH and alkalinity (Stets *et al.* 2009). The Rotorua lakes lie in an active volcanic zone and many were formed by volcanic eruptions (Lowe and Green, 1987). The volcanic geology may influence lake CO_2 concentrations as bicarbonate is the predominant salt for lakes in this region (McColl 1972; Timperley and Vigor-Brown 1986) and a decrease in pH due to the influence of geothermal inputs strongly modulates the carbonate equilibrium towards high CO_2 concentrations (Stumm and Morgan 1996). Surface waters at times became highly

supersaturated in CO_2 in Lakes Rotomahana, Rotoiti, Rotorua and Tarawera; each subject to varying levels of geothermal influence (Timperley and Vigor-Brown 1986). A special case is Lake Rotomahana, which emits a large amount of CO_2 (Table 4.1). Mazot *et al.* (2014) reported that Lake Rotomahana is an active hydrothermal area, even prior to the eruption of Mt Tarawera in 1886. Substantial CO_2 emissions were related to eruption craters observed in their study. High OC mineralization, supported by allochthonous (OC) inputs, may also yield CO_2 supersaturation (Sobek *et al.* 2005) when respiration dominates over primary production (del Giorgio *et al.* 1999). With a relatively low range of dissolved organic carbon (DOC) in the water column (1.2 – 5.2 mg L^{-1}: BOPRC unpublished data), it is possible that the contribution of water column OC mineralization to CO_2 supersaturation is minimal, as also found in other studies (e.g., Stets *et al.* 2009). Except for the geothermally influenced lakes, mineralization of OC in lake sediment is likely to be associated with CO_2 emissions from the Rotorua lakes as sediment carbon mineralization was of the same magnitude as CO_2 atmospheric emissions (Figure 4.4).

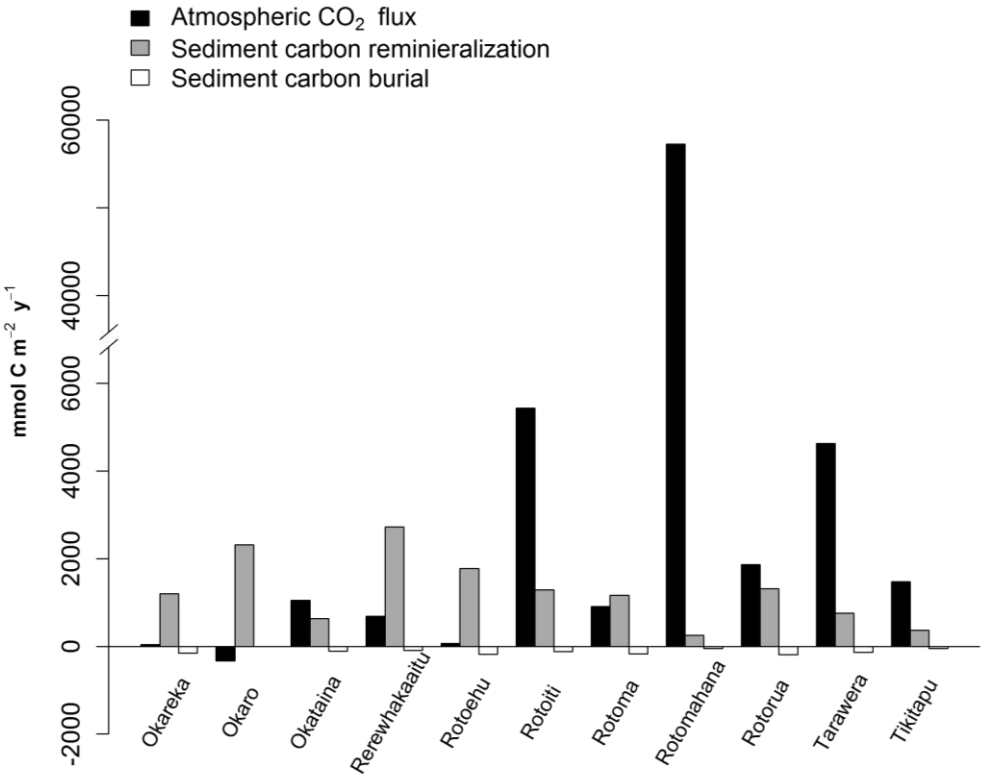

Figure 4.4 Atmospheric carbon flux (FCO_2) and sediment carbon diagenesis rate in 11 Rotorua lakes. Negative values of atmospheric flux represent flux into the lake. Sediment carbon remineralization (J_{rec}) is presented as positive values to indicate release of carbon from the sediment. Permanent burial of carbon in the sediment (J_{bur}) is presented by negative value to indicate sink of carbon in the sediment.

Eutrophication and oligotrophication processes have been shown to influence surface water CO_2 by reducing and increasing the concentration, respectively (Pacheco *et al.* 2013; Schindler 1997; Cole *et al.* 2000; Marotta *et al.* 2012; Trolle *et al.* 2012). In this study, apart from Lake Rotomahana, the negative correlation between surface water CO_2 and TN and TP across all lakes (Table 4.2) is in agreement with previous findings. However, in response to decreasing Chl concentrations through the period of this study, only Lakes Okaro and Rotoma exhibited significant increases in CO_2 emissions (Table 4.2). Primary production either in the watershed or in the water body itself is the ultimate route for OC production, therefore, it follows that more productive systems accumulate more carbon in the sediment. Such accumulation represents short- to long-term sequestration of atmospheric CO_2 in lake sediment (Tranvik *et al.* 2009). The sediment carbon analysis for the Rotorua lakes showed that Chl has a

significant positive relationship with areal storage of carbon in sediment for the period 1886 to 2006 (Figure 4.5A). This result indicates that phytoplankton productivity is the dominant process contributing to carbon deposition in the sediment. It is also in agreement with a recent study by Trolle *et al.* (2008) showing that the carbon to nitrogen ratio (C/N: 4.8 – 10.1) of the surficial sediment organic matter in these lakes is sourced from an autochthonous base (C/N <10: Meyer 1994).

Downing *et al.* (2008) estimated that eutrophic lakes with fertile agricultural catchments accumulate more organic carbon than those in undeveloped catchments. Thus, due to the high lake primary production fed by high nutrient concentrations, as well as high rates of terrestrial carbon input through erosion, eutrophic lakes might act as active organic carbon sinks. Moreover, the study by Sobek *et al.* (2009) showed that sediment receiving high inputs of autochthonous material (more labile organic carbon) would have a lower burial efficiency (low buried OC: deposited OC) than that of allochthonous material (high buried OC: deposited OC). Although not showing a strong statistical fit, the organic carbon burial efficiency of the Rotorua lakes was negatively correlated with Chl (Figure 4.5B). This result agrees with the study by Sobek *et al.* (2009) and confirms that although productive lakes store more carbon in the sediment (Figure 4.5A), only a small proportion of the deposited carbon is permanently buried. The remainder is remineralized, producing dissolved organic and inorganic carbon as well as CO_2 and CH_4 which re-enters the water column (Klump *et al.* 2009). Anoxic bottom waters, typical in stratified eutrophic lakes, may accumulate CH_4 in a large amounts since methanogenesis in the sediments is greatly increased (Borrel *et al.* 2011). In addition to emissions through gas ebullition (McGinnis *et al.* 2006), lakes may entrain the deepest highly enriched (with CO_2 and CH_4) waters during overturn yielding large gas releases to the atmosphere over relatively discrete time periods (Striegl and Michmerhuizen 1998; Riera *et al.*1999; López Bellido *et al.* 2009). Therefore, eutrophication in lakes does increase carbon accumulation in the sediment, but release of carbon

gases, particularly methane, is likely to increase as well, contributing to global warming.

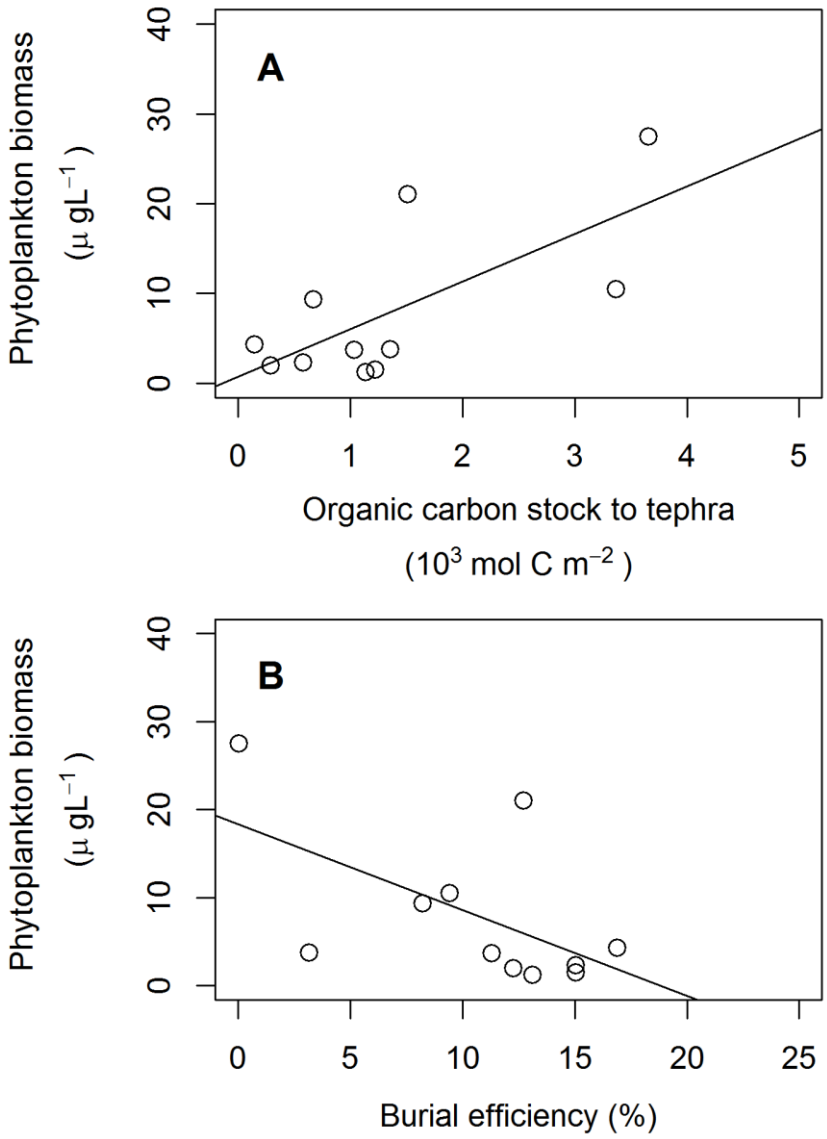

Figure 4.5 Phytoplankton productivity and sedimentary organic carbon where solid lines indicate linear regression relationships. (A) Relationship between phytoplankton biomass and sediment organic carbon stock to the 1886 tephra layer (R^2 = 0.485, $p<0.05$). (B) Relationship between phytoplankton biomass and organic carbon burial efficiency (R^2 = 0.332, $p<0.1$).

4.5. Conclusion

This study demonstrated that CO_2 fluxes in lakes are driven by an interplay between chlorophyll *a,* nutrient availability and hydrodynamic processes. Geothermal activity may also directly contribute to elevated CO_2 concentrations and supersaturation in lakes. Surface water CO_2 concentrations were low during the summer and high in winter in all 11 study lakes. These seasonal variations, except in geothermally influenced lakes, result in atmospheric CO_2 uptake in the summer and CO_2 emissions in the winter. Nutrient concentrations and chlorophyll *a* were negatively correlated with CO_2 atmospheric fluxes. However, reductions in chlorophyll *a* and nutrient concentrations in lakes undergoing restoration were not necessarily matched by increasing CO_2 emissions.

Results of this study confirm that productive lakes, indicated by chlorophyll *a* concentrations, accumulate more carbon in sediment than less productive lakes. However, the burial efficiency in productive lakes is low. The deposited organic carbon in the bottom sediments of the Rotorua lakes was mostly sourced from autotrophic production, and was remineralized to carrying extents in the lakes, resulting in the production of CO_2 and CH_4 which can be released to the atmosphere as greenhouse gases.

4.6. References

Abell JM, Hamilton DP, Paterson J (2011) Reducing the external environmental costs of pastoral farming in New Zealand: experiences from the Te Arawa lakes, Rotorua. *Australasian Journal of Environmental Management*, **18**, 139–154.

APHA (1998) *Standard methods for the examination of water and wastewater*. 20th edn. Washington, DC: American Public Health Association.

Berner RA (1980) *Early diagenesis: A theoretical approach*. Princeton University Press. New Jersey.

Borrel G, Jézéquel D, Biderre-Petit C *et al.* (2011) Production and consumption of methane in freshwater lake ecosystems. *Research in Microbiology*, **162**, 833–847.

Burdige DJ (2007) Preservation of organic matter in marine sediments : controls, mechanisms, and an imbalance in sediment organic carbon budgets? *Chemical Reviews*, **107**, 467–485.

Burns N, McIntosh J, Scholes P (2009) Managing the lakes of the Rotorua District, New Zealand. *Lake and Reservoir Management*, **25**, 284–296.

Cole JJ, Caraco NF, Kling GW, Kratz TK (1994) Carbon dioxide supersaturation in the surface waters of lakes. *Science*, **265**, 1568–1570.

Cole JJ, Pace ML, Carpenter SR, Kitchell JF (2000) Persistence of net heterotrophy in lakes during nutrient addition and food web manipulations. *Limnology and Oceanography*, **45**, 1718–1730.

Cole JJ, Carpenter SR, Kitchell JF, Pace ML (2002) Pathways of organic carbon utilization in small lakes: Results from a whole-lake 13C addition and coupled model. *Limnology and Oceanography*, **47**, 1664–1675.

Cole JJ, Prairie YT, Caraco NF *et al.* (2007) Plumbing the global carbon cycle: Integrating inland waters into the terrestrial carbon budget. *Ecosystems*, **10**, 171–184.

Crusius J, Wanninkhof R (2003) Gas transfer velocities measured at low wind speed over a lake. *Limnology and Oceanography*, **48**, 1010–1017.

Dlugokencky EJ, Lang PM, Masarie KA, Crotwell AM, and Crotwell MJ (2013) Atmospheric carbon dioxide dry air mole fractions from the NOAA ESRL carbon cycle cooperative global air sampling network, 1968-2012. Version: 2013-08-28.

Downing JA, Prairie YT, Cole JJ *et al.* (2006) The global abundance and size distribution of lakes, ponds, and impoundments. *Limnology and Oceanography*, **51**, 2388–2397.

Downing JA, Cole JJ, Middelburg JJ *et al.* (2008) Sediment organic carbon burial in agriculturally eutrophic impoundments over the last century. *Global Biogeochemical Cycles*, **22**, 1–10.

Ferland ME, Prairie YT, Teodoru C, Del Giorgio PA (2014) Linking organic carbon sedimentation, burial efficiency, and long-term accumulation in boreal lakes. *Journal of Geophysical Research: Biogeosciences*, **119**, 836–847.

del Giorgio PA, Cole JJ, Caraco NF, Peters RH (1999) Linking planktonic biomass and metabolism to net gas fluxes in northern temperate lakes. *Ecology*, **80**, 1422–1431.

Hamilton D (2005) Land use impacts on nutrient export in the Central Volcanic Plateau, North Island. *New Zealand Journal of Forestry*, **49**, 27–31.

Hanson PC, Bade DL, Carpenter SR, Kratz TK (2003) Lake metabolism: Relationships with dissolved organic carbon and phosphorus. *Limnology and Oceanography*, **48**, 1112–1119.

Hanson PC, Pollard AI, Bade DL, Predick K, Carpenter SR, Foley JA (2004) A model of carbon evasion and sedimentation in temperate lakes. *Global Change Biology*, **10**, 1285–1298.

Harrell FEJ (2015) Hmisc: Harrell miscellaneous. R package version 3.15-0. http://cran.r-project.org/package=Hmisc.

Jähne BJ, Münnich KOM, Bösinger R, Dutzi A, Huber W, Libner P (1987) On the parameters influencing air-water gas exchange. *Journal of Geophysical Research*, **92**, 1937–1949.

Jassby AD, Cloern JE (2014) wq: Some tools for exploring water quality monitoring data. R package version 0.4-1. URL:http://cran.r-project.org/package=wq.

Klump JV, Fitzgerald SA, Waples JT (2009) Benthic biogeochemical cycling, nutrient stoichiometry, and carbon and nitrogen mass balances in a eutrophic freshwater bay. *Limnology and Oceanography*, **54**, 692–712.

López Bellido J, Tulonen T, Kankaala P, Ojala A (2009) CO_2 and CH_4 fluxes during spring and autumn mixing periods in a boreal lake (Pääjärvi, southern Finland). *Journal of Geophysical Research: Biogeosciences*, **114**, 1–12.

Lowe DJ, Green JD (1987) Origins and development of the lakes. In: Viner AB. Eds. *Inland Waters of New Zealand*. pp. 1–64. DSIR Bulletin 241. DSIR Science Information Publishing Centre, Wellington.

Maberly SC, Barker PA, Stott AW, Ville D, Mitzi M (2013) Catchment productivity controls CO_2 emissions from lakes. *Nature Climate Change*, **3**, 391–394.

MacIntyre S, Jonsson A, Jansson M, Aberg J, Turney DE, Miller SD (2010) Buoyancy flux, turbulence, and the gas transfer coefficient in a stratified lake. *Geophysical Research Letters*, **37**, 2–6.

Marcé R, Obrador B, Morguí J-A, Lluís Riera J, López P, Armengol J (2015) Carbonate weathering as a driver of CO_2 supersaturation in lakes. *Nature Geoscience*, **8**, 107–111.

Marotta H, Duarte CM, Guimarães-Souza BA, Enrich-Prast A (2012) Synergistic control of CO_2 emissions by fish and nutrients in a humic tropical lake. *Oecologia*, **168**, 839–847.

Mazot A, Schwandner FM, Christenson B *et al.* (2014) CO_2 discharge from the bottom of volcanic Lake Rotomahana, New Zealand. *Geochemistry, Geophysics, Geosystems*, **15**, 577–588.

McColl RHS (1972) Chemistry and trophic status of seven New Zealand lakes. *New Zealand Journal of Marine and Freshwater Research*, **6**, 399–447.

McColl RHS (1977) Chemistry of sediments in relation to trophic condition of eight Rotorua Lakes. *New Zealand Journal of Marine and Freshwater Research*, **11**, 509–523.

Meyers PA (1994) Preservation of elemental and isotopic source identification of sedimentary organic matter. *Chemical Geology*, **114**, 289–302.

Ojala A, Bellido JL, Tulonen T, Kankaala P, Huotari J (2011) Carbon gas fluxes from a brown-water and a clear-water lake in the boreal zone during a summer with extreme rain events. *Limnology and Oceanography*, **56**, 61–76.

Pacheco FS, Roland F, Downing JA (2013) Eutrophication reverses whole-lake carbon budgets. *Inland Waters*, **4**, 41–48.

Pickett RC (2008) *A tephra-dated record of palaeoenvironmental change since ~ 5,500 years ago from Lake Rotorua, North Island, New Zealand*. Master Thesis. The University of Waikato.

Quay PD, Emerson S (1986) The carbon cycle for Lake Washington - a stable isotope study. *Limnology and Oceanography*, **31**, 596–611.

Le Quéré C, Moriarty R, Andrew RM *et al.* (2015) Global carbon budget 2014. *Earth System Science Data*, **7**, 47–85.

R Core Team (2014) R: A language and environment for statistical computing. R Foundation for Statistical Computing, Vienna, Austria. URL: http://www.R-project.org/.

Read JS, Hamilton DP, Jones ID *et al.* (2011) Derivation of lake mixing and stratification indices from high-resolution lake buoy data. *Environmental Modelling & Software*, **26**, 1325–1336.

Regnier P, Friedlingstein P, Ciais P *et al.* (2013) Anthropogenic perturbation of the carbon fluxes from land to ocean. *Nature Geoscience*, **6**, 597–607.

Riera JL, Schindler JE, Kratz TK (1999) Seasonal dynamics of carbon dioxide and methane in two clear-water lakes and two bog lakes in northern Wisconsin, U.S.A. *Canadian Journal of Fisheries and Aquatic Sciences*, **274**, 1–10.

Schindler DE (1997) Influence of food web structure on carbon exchange between lakes and the atmosphere. *Science*, **277**, 248–251.

Sobek S, Tranvik LJ, Cole JJ (2005) Temperature independence of carbon dioxide supersaturation in global lakes. *Global Biogeochemical Cycles*, **19**, 1–10.

Sobek S, Durisch-Kaiser E, Zurbrügg R, Wongfun N, Wessels M, Pasche N, Wehrli B (2009) Organic carbon burial efficiency in lake sediments controlled by oxygen exposure time and sediment source. *Limnology and Oceanography*, **54**, 2243–2254.

Stets EG, Striegl RG, Aiken GR, Rosenberry DO, Winter TC (2009) Hydrologic support of carbon dioxide flux revealed by whole-lake carbon budgets. *Journal of Geophysical Research: Biogeosciences*, **114**, 1–14.

Striegl RG, Michmerhuizen CM (1998) Hydrologic influence on methane and carbon dioxide dynamics at two north-central Minnesota lakes. *Limnology and Oceanography*, **43**, 1519–1529.

Stumm W, Morgan JJ. 1996. *Aquatic chemistry: Chemical equilibria and rates in natural waters*. Hoboken, New Jersey: Wiley.

Timperley MH, Vigor-Brown RJ (1986) Water chemistry of lakes in the Taupo Volcanic Zone, New Zealand. *New Zealand Journal of Marine and Freshwater Research*, **20**, 173–183.

Tranvik LJ, Downing JA, Cotner JB *et al.* (2009) Lakes and reservoirs as regulators of carbon cycling and climate. *Limnology and Oceanography*, **54**, 2298–2314.

Trolle D, Hamilton DP, Hendy C, Pilditch C (2008) Sediment and nutrient accumulation rates in sediments of twelve New Zealand lakes: Influence of lake morphology, catchment characteristics and trophic state. *Marine and Freshwater Research*, **59**, 1067–1078.

Trolle D, Staehr PA, Davidson TA, Bjerring R, Lauridsen TL, Søndergaard M, Jeppesen E (2012) Seasonal dynamics of CO_2 flux across the surface of shallow temperate lakes. *Ecosystems*, **15**, 336–347.

Vachon D, del Giorgio PA (2014) Whole-lake CO_2 dynamics in response to storm events in two morphologically different lakes. *Ecosystems*, **17**, 1338–1353.

Vachon D, Prairie YT (2013) The ecosystem size and shape dependence of gas transfer velocity versus wind speed relationships in lakes. *Canadian Journal of Fisheries and Aquatic Sciences*, **70**, 1757–1764.

Vincent WF, Forsyth DJ (1987) Geothermally influenced waters. In: Viner AB. Eds. *Inland Waters of New Zealand.* pp. 349–377. DSIR Bulletin 241. DSIR Science Information Publishing Centre, Wellington.

Wanninkhof R (1992) Relationship between wind speed and gas exchange. *Journal of Geophysical Research*, **97**, 7373–7382.

Weiss RF, Price BA (1980) Nitrous oxide solubility in water and seawater. *Marine Chemistry*, **8**, 347–359.

Winslow L, Read J, Woolway R, Brentrup J, Leach T, Zwart J (2015) rLakeAnalyzer: R package for the analysis of lake physics. R package version 1.7.3. URL: http://CRAN.R-project.org/package=rLakeAnalyzer

Chapter 5 Conclusion

5.1. Overview

This thesis has examined the diffusive emissions of CO_2 and CH_4 in a monomictic eutrophic lake and explored the dynamic interactions of physical and biological processes which govern the emissions, as well as identifying the sinks and sources of these gases in 11 lakes in close proximity. A combination of field research and process-based mathematical modelling has been used to supplement current knowledge of how lakes, particularly eutrophic monomictic lakes, regulate these two greenhouse gases. Projections of future emissions from lakes in response to a warming climate and changes in nutrient regime performed using model simulations in this study also provides support for the hypothesis that lakes and inland waters, should be factored into the global greenhouse gas emission accounting schemes. The remainder of this chapter synthesizes key findings of the study presented in each research chapter (Chapter 2-4), and provides brief concluding remarks and outlooks for future research to improve the knowledge gained in this thesis.

5.2. Diffusive emissions of CO_2 and CH_4 from a eutrophic monomictic lake

Using a simple mechanistic mass balance model based on dynamics of CO_2 and CH_4 observed over a one-year period (2013 – 2014) this study examined the diffusive emissions of these two greenhouse gases in monomictic eutrophic Lake Okaro. Both CO_2 and CH_4 accumulated in the hypolimnion when the lake stratified in early spring, while concentrations in the epilimnion remained low. The progressive deepening of thermocline in late autumn gradually entrained the deeper highly enriched (with CO_2 and CH_4) waters. The mass balance model gave rates for processes involved in the loss and gain of CO_2 and CH_4, i.e., 1) diffusion across the sediment-water interface, 2) atmospheric flux, 3) aerobic oxidation of CH_4, 4) diffusion of CO_2 and CH_4 across the sediment-water interface, 5) CO_2

uptake by phytoplankton, and 6) CO_2 dissociation from carbonate, solved using algorithms and parameter optimization derived from the literature.

The mass balance study indicated how biological processes (i.e., phytoplankton uptake and CH_4 oxidation) in a eutrophic lake may substantially reduce CO_2 and CH_4 emissions. It was calculated that for the primary study lake, Okaro, ~31% of the carbon deposition to the sediment was released back to the atmosphere via diffusive flux each year. In addition, although eutrophic lakes may take up a considerable amount of CO_2 for primary productivity, a large amount of CO_2, as well as CH_4, is released to the atmosphere as a pulsed emission during the onset of lake overturn in winter. Thus, over an annual cycle, eutrophic lakes may still be regarded as a net carbon (CO_2 and CH_4 combined) source to the atmosphere.

In addition to diffusive emissions, gas bubbles have been identified as a major pathway of CH_4 release from the sediment to the atmosphere (Bastviken 2009). Ebullition fluxes to the atmosphere can account for >80% of the total CH_4 atmospheric flux from lakes (DelSontro *et al*., 2010; Martinez and Anderson 2013). Therefore, this study underscores that eutrophic lakes make an important contribution to global greenhouse gas fluxes and that our estimates of fluxes to the atmosphere may be conservative as a result of accounting only diffusion and not ebullition.

5.3. CO_2 and CH_4 emissions from a eutrophic monomictic lake under changing climate and nutrient regimes

The dynamics of CO_2 and CH_4 in a eutrophic monomictic lake were simulated in this study using a one-dimensional (1D) hydrodynamic-ecological model (GLM-AED2). This process based model integrates physical, geochemical and ecological dynamics to capture the complex interactions amongst different climate and nutrient regimes. Scenarios reflecting possible future changes (i.e. increasing air temperature by 2.5 °C, halving or increasing by one half internal and external nutrient loads) were applied to a four year calibrated model representing the present or

‘baseline’ condition. Model simulations showed that a warmer climate produced a longer duration of thermal stratification and a shallower surface mixed layer. Such conditions allow greater accumulation of nutrients (PO_4 and NH_4 in particular) and greenhouse gases (CO_2 and CH_4) in the hypolimnion. As lake productivity increased, the warmer climate promoted more primary production and CO_2 uptake from the atmosphere. In contrast, CH_4 was emitted as a diffusive flux to the atmosphere, in greater quantities during lake overturn, as a result of more accumulation in the hypolimnion. While an increasing nutrient load in the presence of a warming climate does not substantially affect CO_2 and CH_4 fluxes, a declining nutrient load reduces the total carbon emissions (CO_2 and CH_4 combined) from the lake. The total carbon emissions (as kg CO_2-eq m^{-2} y^{-1}) from the study lake, Okaro, were simulated to increase by 27% relative to present conditions in a warming climate, however, this increase could only be reduced to 19% if nutrient loading was reduced by one half. This study highlights that eutrophic lakes may contribute strongly to global warming by greenhouse gas emissions and that a warming climate may enhance the magnitude of these emissions.

5.4. CO_2 emissions and carbon deposition to the sediment of lakes of varying trophic state

This study synthesized CO_2 emissions and sediment carbon deposition in lakes of varying trophic states and mixing regimes to give a broad overview of the fate of carbon. It was shown that lakes may shift from being CO_2 sources to the atmosphere to being sinks due to seasonal changes in phytoplankton productivity and lake mixing dynamics. Nutrient concentrations (total phosphorus and total nitrogen) and chlorophyll *a* concentrations were negatively correlated with atmospheric CO_2 flux in lakes but with mostly low correlation coefficient values. Reductions in chlorophyll *a* and nutrient concentrations in lakes undergoing restoration were not necessarily matched to increasing CO_2 emissions within the period (ca. one decade) considered in this study.

In addition to nutrient and chlorophyll *a*, geothermal activity may also influence CO_2 concentrations in some of the study lakes, which are located in an active volcanic zone (Mazot *et al.*, 2014). Bicarbonate is the predominant salt in these lakes (McColl 1972; Timperley and Vigor-Brown 1986), however, a decrease in pH due to the influence of geothermal inputs will strongly modulate the carbonate equilibrium towards high CO_2 concentrations (Stumm and Morgan 1996).

Productive lakes, indicated by elevated levels of chlorophyll *a* concentration, were calculated to deposit more carbon in the bottom sediments than less productive lakes. This indicates that phytoplankton productivity is the dominant process contributing to carbon deposition in the sediment. However, the burial efficiency in productive lakes is low, meaning that only a relatively small proportion of the deposited carbon is permanently buried. Remineralization of the deposited carbon may produce dissolved organic and inorganic carbon as well as CO_2 and CH_4, and return these compounds back to the water column (Klump *et al.,* 2009). Therefore, except for lakes with strong geothermal influence (Rotomahana, Rotoiti, Rotorua, Tarawera: Timperley and Vigor-Brown 1986), mineralization of OC in the sediment of the study lakes is likely to influence CO_2 emissions as sediment carbon remineralization rates are of the same magnitude as atmospheric CO_2 emissions. Knowing that productive lakes remineralize more carbon in the sediment than less productive lakes, and that remineralization can be associated with CO_2 as well as CH_4 emissions, this study underlines that eutrophication may promote increased rates of greenhouse gas emissions and, therefore, global warming.

5.5. Concluding remarks and management implications

Moss *et al*. (2011) noted that climate change enhances eutrophication, and that eutrophication may concurrently promote climate change. Supporting this statement, the results presented in this thesis demonstrate that eutrophic lakes, as well as eutrophication generally, may contribute global warming through increased emissions of greenhouse gases.

Furthermore, climate warming is likely to enhance greenhouse emissions from lakes. Knowing that inland waters are dominated by small water bodies with surface areas of <1 km^2 (Downing *et al.,* 2006) and are prone to eutrophication and high areal rates of organic carbon burial (Downing *et al.,* 2008), it is important that inland waters should be included in global carbon accounting inventories. Lake restoration should also be considered as part of a mitigation strategy to combat global warming. Nutrients, from both external and internal sources could reduce water column autotrophic production and organic carbon deposition to lake sediments. Reducing the volume and duration of anoxic bottom waters may prevent CH_4 accumulation given that CH_4 is 34 times more potent than CO_2 in global warming (Myhre *et al*., 2013). Techniques such as hypolimnetic oxygenation (Debroux *et al.,* 2012) are highly suitable to reduce CH_4 emissions and reduce the potency of greenhouse gas emissions by oxidizing CH_4 to CO_2.

5.6. Future outlook

This PhD study demonstrated that better assessments of carbon emissions from lakes are required to make reliable contributions to global carbon budget calculations. Simulations of physical and biological interactions showed that CO_2 and CH_4 concentrations could be reproduced satisfactorily, but considerations of emissions in this study were limited to diffusive fluxes and not total emissions which include gas ebullition fluxes. To better estimate total emissions from lakes, direct measurement should be carried out. Advanced methods such as the eddy-covariance technique (Schubert *et al.,* 2012; Jonsson *et al.,* 2008) would enable accurate measurements and modelling of released gas from the surface of the lake, both via diffusion and ebullition, and to fill a gap in estimates of CO_2 fluxes (due to autotrophic and heterotrophic activity; Cole *et al.*, 2000) and episodic CH_4 releases due to ebullition (DelSontro *et al.*, 2015).

Insights into the future role of lakes in greenhouse gas emissions could also be made with model simulations that couple the hydrodynamic model

(GLM-AED^2) to a regional scale climate model (RCM, see Ackerley *et al*., 2012) as well as a catchment model (e.g. SWAT) (Hipsey *et al.,* 2015). The use of an interoperable model framework for hydrological, climate and lake models would help to address some of data deficiencies associated providing comprehensive hydrological and meteorological data to run hydrodynamic-ecological models such as GLM-AED^2.

5.7. References

Ackerley D, Dean S, Sood A, Mullan AB (2012) Regional climate modelling in New Zealand : Comparison to gridded and satellite observations . *Weather and Climate*, **32**, 3–22.

Bastviken D (2009) Methane. In: *Encyclopedia of Inland Waters* (ed Likens GE), pp. 783–805. Academic Press, Oxford.

Cole JJ, Pace ML, Carpenter SR, Kitchell JF (2000) Persistence of net heterotrophy in lakes during nutrient addition and food web manipulations. *Limnology and Oceanography*, **45**, 1718–1730.

Debroux J-F, Beutel MW, Thompson CM, Mulligan S (2012) Design and testing of a novel hypolimnetic oxygenation system to improve water quality in Lake Bard, California. *Lake and Reservoir Management*, **28**, 245–254.

DelSontro T, McGinnis DF, Sobek S, Ostrovsky I, Wehrli B (2010) Extreme methane emissions from a swiss hydropower reservoir: contribution from bubbling sediments. *Environmental Science & Technology*, **44**, 2419–2425.

DelSontro T, McGinnis DF, Wehrli B, Ostrovsky I (2015) Size does matter: importance of large bubbles and small-scale hot spots for methane transport. *Environmental science & technology*, **49**, 1268–76.

Downing JA, Prairie YT, Cole JJ et al. (2006) The global abundance and size distribution of lakes, ponds, and impoundments. *Limnology and Oceanography*, **51**, 2388–2397.

Downing JA, Cole JJ, Middelburg JJ et al. (2008) Sediment organic carbon burial in agriculturally eutrophic impoundments over the last century. *Global Biogeochemical Cycles*, **22**, 1–10.

Hipsey MR, Hamilton DP, Hanson PC et al. (2015) Predicting the resilience and recovery of aquatic systems : a framework for model evolution within environmental observatories. *Water Resources Research,* **51**, 7023–7043.

Jonsson A, Åberg J, Lindroth A, Jansson M (2008) Gas transfer rate and CO2 flux between an unproductive lake and the atmosphere in northern Sweden. *Journal of Geophysical Research: Biogeosciences*, **113**, 1–13.

Mazot A, Schwandner FM, Christenson B *et al.* (2014) CO_2 discharge from the bottom of volcanic Lake Rotomahana, New Zealand. *Geochemistry, Geophysics, Geosystems*, **15**, 577–588.

McColl RHS (1972) Chemistry and trophic status of seven New Zealand lakes. *New Zealand Journal of Marine and Freshwater Research*, **6**, 399–447.

Moss B, Kosten S, Meerhof M et al. (2011) Allied attack: climate change and eutrophication. *Inland Waters*, **1**, 101–105.

Myhre G, Shindell D, Bréon F-M et al. (2013) 2013: Anthropogenic and Natural Radiative Forcing. In: *Climate Change 2013: The Physical Science Basis. Contribution of Working Group I to the Fifth Assessment Report of the Intergovernmental Panel on Climate Change* (ed Stocker T.F., Qin D., Plattner G.-K., Tignor M., Allen S.K., Boschung J., Nauels A. , Xia Y. BV and MPM), pp. 659–740. Cambridge University Press, Cambridge, United Kingdom and New York, NY, USA.

Schubert CJ, Diem T, Eugster W (2012) Methane emissions from a small wind shielded lake determined by eddy covariance, flux chambers, anchored funnels, and boundary model calculations: A comparison. *Environmental Science and Technology*, **46**, 4515–4522.

Stumm W, Morgan JJ. 1996. *Aquatic chemistry: Chemical equilibria and rates in natural waters*. Hoboken, New Jersey: Wiley.

Timperley MH, Vigor-Brown RJ (1986) Water chemistry of lakes in the Taupo Volcanic Zone, New Zealand. *New Zealand Journal of Marine and Freshwater Research*, **20**, 173–183.

Appendix I Consequences of gas flux model choice on the interpretation of metabolic balance across 15 lakes

Hilary A. Dugan[1,2*,3*#], R. Iestyn Woolway[4,5*], Ari B. Santoso[6], Jessica R. Corman[7,2*], Aline Jaimes[8,9*], Emily R. Nodine[10,11*], Vijay P. Patil[12] , Jacob A. Zwart[13], Jennifer A. Brentrup[14], Amy L. Hetherington[15], Samantha K. Oliver[2], Jordan S. Read[16], Kirsten M. Winters[17], Paul C. Hanson[2], Emily K. Read[3,16*], Luke A. Winslow[2,16*], Kathleen C. Weathers[3]

[1]University of Illinois at Chicago, Chicago, Illinois
[2]University of Wisconsin-Madison, Madison, Wisconsin
[3]Cary Institute of Ecosystem Studies, Millbrook, New York
[4]Centre for Ecology & Hydrology, Lancaster, United Kingdom
[5]University of Reading, Reading, United Kingdom
[6]University of Waikato, Hamilton, New Zealand
[7]Arizona State University, Tempe, Arizona
[8]University of Texas El Paso, El Paso, Texas
[9]University of Delaware, Newark, Delaware
[10]Florida International University, Miami, Florida
[11]University of Vermont, Burlington, Vermont
[12]University of Alaska-Fairbanks, Fairbanks, Alaska
[13]University of Notre Dame, Notre Dame, Indiana
[14]Miami University, Oxford, Ohio
[15]Cornell University, Ithaca, New York
[16]U.S. Geological Survey Center for Integrated Data Analytics, Middleton, Wisconsin
[17]Oregon State University, Corvallis, Oregon
[#]Corresponding author: hilarydugan@gmail.com
*Current institution

Abstract

Ecosystem metabolism and the contribution of carbon dioxide from lakes to the atmosphere can be estimated from free-water gas measurements through the use of mass balance models, which rely on a gas transfer coefficient (*k*) to model gas exchange with the atmosphere. Theoretical and empirically based models of *k* range in complexity from wind driven power functions to complex surface renewal models. However, model choice is rarely considered in most studies of lake metabolism. This study used high-frequency data from 15 lakes provided by the Global Lake Ecological Observatory Network (GLEON) to study how model choice of *k* influenced estimates of lake metabolism and gas exchange with the atmosphere. Six models of *k* were tested on lakes chosen to span broad gradients in area and trophic states. A metabolism model was then fit to all six outputs of *k* data. We found that hourly values for *k* were substantially different between models, and at an annual scale, resulted in significantly different estimates of lake metabolism and gas exchange with the atmosphere.

Key words:

gas exchange, GLEON, lakes, lake models, metabolism, sensor network

Introduction

Atmospheric gas exchange in lakes is routinely used to evaluate the role of lakes in global carbon cycling (Cole et al. 2007, Tranvik et al. 2009, Raymond et al. 2013). The exchange of soluble gases, including oxygen and carbon dioxide (CO_2), across the air-water interface is influenced by physical processes, such as wind stress, convection, and currents, and is described by the gas transfer coefficient (*k*) (Zappa et al. 2007). Variability in *k* can span several orders of magnitude (Wanninkhof 1992), and is primarily driven by diel and seasonal variations in mass and energy fluxes at the lake surface. Methods to determine *k* include gas tracers (Cole and Caraco 1998), floating chambers (Cole et al. 2010, Vachon et al. 2010), and eddy covariance techniques (Jonsson et al. 2008, MacIntyre et al. 2010a, Heiskanen et al. 2014). If observational data are unobtainable, *k* must be estimated using models.

With an estimate of *k*, an atmospheric flux (F) can be calculated based on dissolved oxygen (DO) concentrations and surface-mixed layer depth in a lake. This flux is often incorporated into metabolism models, which assume that changes in DO can be used as a surrogate for CO_2 based on the stoichiometric relationship between the two gases as part of gross primary production (GPP) and aerobic ecosystem respiration (R) (Odum 1956, Hanson et al. 2008).

$$dO_2/dt = GPP - R + F + e \quad (1)$$

Lake metabolism is considered the net balance between GPP and R, which is equivalent to net ecosystem production (NEP) (Pace and Lovett 2013). As given in eq. 1, NEP must be balanced by F and changes in the standing stock of DO (dO_2/dt). Note that an additional term (*e*), which accounts for the errors introduced by the inflow and outflow of oxygen, is ignored. This is an assumption applied in cases where those terms are a small part of the budget (Staehr et al. 2010).

Most approaches to estimating NEP from free-water measurements of dissolved gas assume a model for gas exchange and treat metabolism as

a free parameter to be estimated (Hanson et al. 2008). Under these assumptions, any uncertainty not accounted for in *k* will compound error in NEP estimates. One of the most widely cited models of *k* is an empirically derived power function based solely on wind speed, which was developed from data collected on small lakes (Cole and Caraco 1998). Subsequently, Crusius and Wanninkhof (2003) derived a similar empirical model optimized for low wind speeds. More recently, surface renewal models have been used to incorporate the role of convective mixing on gas exchange (MacIntyre et al. 2010a, Read et al. 2012, Tedford et al. 2014). Every model has a different set of assumptions and varies in the complexity of terms and data requirements, and many models based on empirical data were developed for specific limnological and meteorological conditions. Only recently have studies begun to incorporate multiple *k* models (Staehr et al. 2010, Heiskanen et al. 2014, Bartosiewicz et al. 2015).

As the suite of available *k* models, as well as model complexity, grows, there is a need to analyze how *k* model choice ultimately influences NEP and gas exchange estimates (Figure 1). Here we focus on three central questions: How do k values estimated from a variety of gas flux models vary, and how does this variance influence inferred NEP values? Is model choice a larger contributor to error in NEP estimates than the uncertainty in parameterizing GPP and R? Under what limnological or meteorological conditions is gas flux model choice important? We capitalize on the availability of a high-frequency, multi-lake data set associated with the Global Lake Ecological Observatory Network (GLEON, www.gleon.org) to examine the sensitivity of lake metabolism estimates to six published models of *k* across a gradient of lakes. We compare how *k* values differ across lakes with a range of physical and trophic states, and what lake characteristics may influence the sensitivity of NEP and gas exchange estimates to changes in *k*. This comparison identifies the circumstances in which model choice is important, those in which it is not, and in what types of lakes further research is needed to establish model efficacy.

Methods

Study sites – Fifteen temperate lakes that range in surface area from 0.005 to 79 km^2 and in maximum depths from 2.5 to 36 m, and span a range of trophic status, from oligotrophic to eutrophic (Table 1), were selected based on the availability of high temporal frequency measurements (15 to 60 minute sampling interval) required for estimating ecosystem metabolism (Odum 1956, Cole et al. 2000, Van de Bogert et al. 2007). Measurements included DO, water temperature and surface meteorology (air temperature, wind speed, relative humidity, and photosynthetically active radiation [PAR]). All data were collected between 2007 and 2010, and data for each lake include between 133 and 338 days of observation. The data set was collected through GLEON and has been used previously in large scale limnological analyses (Solomon et al. 2013, Rose et al. 2014). Additional information about the lakes can be found in Solomon et al. (2013).

Metabolism model – For the purpose of this investigation we used the discrete form of eq. 1 similar to Solomon et al. (2013):

$$DO_{t+1} = DO_t + (ı \times I_t) - ρ + F_t + γ_t, \quad (2)$$

where DO_{t+1} is the concentration of DO at time t + 1, ı is the primary productivity per unit of PAR, I_t is the available PAR at time t, ρ is the whole-ecosystem respiration, and F_t is the flux of O_2 between the lake and the atmosphere at time t. We calculated model process error at time t as $γ_t$. A Nelder-Mead optimization algorithm was used to find the values of ı and ρ that minimized the negative log-likelihood of the errors, $γ_t$, for a given day. GPP at the daily scale was calculated from ı and the sum of PAR over the day ($GPP = ı \times \sum I_t$). This linear relationship was chosen because more complex non-linear equations do not generally improve metabolism estimates, especially in temperate lakes (Hanson et al. 2008). Both GPP and ρ have units of mg $O_2\, L^{-1}\, d^{-1}$, and are presented as g $O_2\, m^{-2}\, d^{-1}$ when multiplied by the depth of the mixed layer (z_{mix}).

Gas exchange, F_t (mg O_2 $L^{-1}d^{-1}$), was calculated as:

$$F_t = -kO_{2t} \times (DO_t - DO_{sat}) / z_{mix,t} \quad (3)$$

where DO_{sat} is the saturation concentration of O_2 (mg L^{-1}) at the current water temperature and atmospheric pressure (Benson and Krause 1984), and $z_{mix,t}$ (m) is calculated as the shallowest depth at which the rate of water density change exceeded 0.075 kg m^{-3} m^{-1} (Solomon et al. 2013). The term (DO_t − DO_{sat}) is the deviation from saturation (DO_{diff}), where negative values indicate under-saturation of dissolved oxygen in the surface waters of lakes. The gas exchange coefficient for oxygen (kO_2, cm h^{-1}) was calculated as

$$kO_2 = k \times (ScO_2 / 600)^{-n} \quad (4)$$

where k (cm h^{-1}) is the gas transfer coefficient, ScO_2 is the Schmidt number for O_2 calculated based on given temperature and water density (Wanninkhof 1992), and n is a dimensionless coefficient to represent the surface conditions. We followed Crusius and Wanninkhof (2003) for parameterized n values of 0.5 for wind speeds over 3 m s^{-1} and 0.67 otherwise.

Gas transfer coefficient (k) - We calculated k from six published gas flux models to estimate gas exchange across all lakes (Table 2). For five of the published models (abbreviated to CC98, CW03, VP13, T14, H14), we adhered to the published methods and parameters in our analysis (Cole and Caraco 1998, Crusius and Wanninkhof 2003, Vachon and Prairie 2013, Heiskanen et al. 2014, Tedford et al. 2014). Because CW03 does not describe any single model, rather four different models based on the same data set, we chose the exponential form, as it been used elsewhere in the literature (Staehr et al. 2012, Trolle et al. 2012). For the sixth model, we augmented the model used in Read et al. (2012) with the addition of a breaking wave component (Soloviev et al. 2007), and will refer to it as R12S. All models used in this study are included in the LakeMetabolizer R package (Winslow et al. 2014).

CC98 and CW03 are univariate models based solely on wind speed, and VP13 is a bivariate model based on wind speed and lake area. Both CW03 and VP13 were developed in low-wind environments, where wind speeds did not exceed 6 m s^{-1} (Table 2). R12S, T14, and H14 are surface renewal models that take into account processes that generate turbulence near the air-water interface, which is quantified as the dissipation rate of turbulent kinetic energy. In T14, the mixed layer depth was set constant at 0.15 m (Bartosiewicz et al. 2015). To calculate convection, the surface energy budget was computed according to Verburg and Antenucci (2010) and buoyancy flux following Kim (1976). For all models, wind speed was normalized to a reference height of 10 m and is presented as u10 (Schertzer et al. 2003). In certain cases, we extrapolate *k* models beyond the wind speeds they were developed under; however, only 2 % of hourly mean wind speeds exceeded 9 m s^{-1}.

Uncertainty Analysis – We were interested in understanding whether the gas flux model choice affected metabolism and gas exchange rates more or less than the uncertainty in parameterizing GPP and R (ı and ρ in Eq. 2) given a specific gas flux model. Within-model uncertainty, based on the parameter uncertainty of ı and ρ, was determined using a bootstrapping routine comparable to Solomon et al. (2013). To produce a distribution of metabolism estimates for each gas flux model, we determined the residual error between the optimized metabolism model and observed DO for each gas flux model. We then created pseudo-observations by selecting a random residual and constructing a timeseries of errors with a random normal distribution with the same autocorrelation and standard deviation, and adding them to the original DO model predictions. The metabolism model was fit to the 1000 pseudo-observations to provide 1000 estimates of NEP for each day and an estimate of ı and ρ parameter uncertainty. The bootstrapped estimates were then averaged for the entire season to give 1000 mean annual NEP estimates for each lake. Values were considered significantly different between *k* models when 95 % confidence intervals did not overlap. This bootstrapping routine provides a robust measure of within-model uncertainty. Mann-Whitney U-tests were run to test any

significant differences between distributions. All modeling and analyses were performed in the R statistical package (R Core Team 2014; Version 3.0.3).

Representative Lakes: For illustrative purposes, we highlight data and results from three example lakes chosen from the data set to represent a range in lake size and metabolism rates: Trout Bog, Acton, and Trout Lake.

- Trout Bog is a small (0.011 km^2) dystrophic lake in Northern Wisconsin, with a maximum depth of 7.9 m. Wind was measured at a height of 2 m, dissolved oxygen was measured at 0.25 m depth, and water temperatures were measured at 0, 0.5, 1, 1.5, 2, 2.5, 3, 4, and 5 m depths.

- Acton is a shallow, medium sized (2.530 km^2) eutrophic lake in southwestern Ohio, with a maximum depth of 8 m. Wind was measured at a height of 4.9 m, dissolved oxygen was measured at 1.5 m depth, and water temperatures were measured at 1 3, and 5 m depths.

- Trout Lake is a large (16.080 km^2) oligotrophic lake in Northern Wisconsin, with a maximum depth of 36 m. Wind was measured at a height of 2 m, dissolved oxygen was measured at 0.5 m depth, and water temperatures were measured from 0-19 m at 1 m increments.

Results

In all six models of gas flux, *k* values generally increased with wind speed, but showed markedly different variation and patterns among models (Figure 2). For a given wind speed, CC98 and CW03, univariate functions based on wind speed, returned a single *k* value whereas all other models covered a range of *k*. When wind was negligible, CC98, CW03, and VP13 predicted *k* minima of 2.1, 0.2, and 2.7 cm h^{-1}, respectively. At wind speeds of 5 m s^{-1}, *k* ranged from 3.9 to 11.9 cm h^{-1} across models, with

the greatest variation observed in H14. At wind speeds > 7 m s^{-1}, *k* values were upwards of 20 cm h^{-1}, and deviated substantially among models. Overall, T14 returned the highest *k* values at wind speeds < 7 m s^{-1}, and CC98 returned the lowest *k* values at wind speeds > 4 m s^{-1}. CW03 covered the largest range due to the extrapolation of the model to wind speeds > 6 m s^{-1}.

At diel scales, the dominant drivers of *k* changed across lakes and with alternative models; as illustrated in the three example lakes over a three-day period in July (Figure 3). Trout Bog is a small lake characterized by low wind speeds. Over the period of 3-6 July, daily wind speeds increased (Figure 3a). The influence of wind speed results in increasing daytime *k* values over this period upwards of 6 cm h^{-1}. At night, only the surface renewal models predicted increases in *k*, while CC98, CW03, and VP13 all reach a minima at night (Figure 3d). Acton is larger than Trout Bog, but similar dynamics are seen in the *k* estimates. In both lakes, H14 returns the highest *k* values at night, while CW03 returns the lowest values overall (Figure 3d, 3e). The third lake is Trout Lake, which is illustrative of a large water body. During early July hourly wind speeds exceeded 10 m s^{-1}, and *k* ranged from 12 to 30 cm h^{-1}. CW03 returned *k* values > 30 cm h^{-1}, but this model is extrapolated at wind speeds greater than 6 m s^{-1}. In Trout Lake, all gas flux models predicted a similar pattern of *k* (Figure 3c, 3f).

The density distribution of *k* differed in the three lakes (Figure 4). CC98 and CW03 were skewed right in all lakes, with dominant peaks near 0 and 2 cm h^{-1} for CW03 and CC98, respectively. The surface renewal models were more normally distributed. Often, the peak frequency of R12S was lower than VP13, which was lower than T14 and H14 (Figure 4).

Across the 15 lakes, there was marked variation in median wind speed, DO_{diff}, and modeled *k* values (Figure 5a, b, and c). Wind speeds and variability in wind speeds generally increased with lake size, with the exception of Annie, Acton, and Sunapee, which had lower median wind speeds than lakes of comparable size. Conversely, the range in DO_{diff} appeared unrelated to lake size. The smallest lakes (North Sparkling Bog,

Crystal Bog, Trout Bog, and Yuan Yang) were all under-saturated, while the larger lakes showed no pattern in oxygen concentration. Of the larger lakes, the range in DO_{diff} concentrations was greatest in Castle, Acton, and Mendota and smallest in Annie, Sparkling, Trout, and Sunapee.

Overall, the gas flux models generally predicted higher *k* with larger lake area, which is concomitant with an increase in wind speed (Figure 5a, and c); although this correlation is biased by single point measurements from the center of the lakes (see Schilder et al. 2013a, Vachon and Prairie 2013). CW03 and CC98 generally had the lowest range of *k*, while the highest *k* values were from H14 in the small lakes, and VP13 and H14 in the large lakes. In larger lakes, the intra-model variability was more similar across models, and estimates showed more overlap than in small lakes.

When comparing *k* models in our optimized metabolism model, there was no uniform pattern in best fit. Therefore, we cannot conclude that any one *k* model functions better across lakes. Estimated atmospheric gas exchange was highly correlated with modeled NEP, with $r^2 = 0.86$ across all models and all lakes. In the three example lakes, *k* models show broadly similar patterns in NEP through time (Figure 6). In Trout Bog, waters became highly under saturated in late October, and NEP estimates between models diverged beyond -10 g O_2 m^{-2} d^{-1} (Figure 6a). Acton, a large eutrophic lake, had positive NEP for most of the record, unless surface waters became under saturated in DO (Figure 6b, e, h). Trout Lake had near saturation of DO throughout the summer, resulting in NEP close to zero and considerable model overlap (Figure 6c, f, i).

In all 15 lakes, mean annual NEP was significantly different between models (Mann-Whitney U-tests, $p < 0.01$, n=1000). However, in lakes where the oxygen concentrations were near equilibrium, NEP estimates between models were similar (Figure 7). This includes Vestedsø, Gribsø, Sparkling, Hampensø, Trout, and Rotorua. The four smallest lakes, and Castle, Acton, Sunapee, and Mendota, had a large separation in mean NEP estimates based on model choice. The four smallest lakes tended to be under-saturated in DO and net heterotrophic (negative NEP), whereas

the larger lakes were mostly net autotrophic (positive NEP). In 8 of the lakes, H14 predicted the greatest absolute NEP values, whether for lakes with negative or positive NEP. In three of the largest lakes (Acton, Sunapee, and Mendota), the use of VP13 led to the highest estimated NEP. Gribsø was the only lake where model choice determined whether the estimated mean annual NEP was positive or negative. At this site, surface waters progressed from super-saturation of DO in April to under-saturation by mid summer, back to super-saturation in October.

Discussion

Our analysis demonstrates that gas flux model selection leads to a range in *k* values for all lakes due to the driving processes incorporated in each model. For instance, in low-wind environments, such as the bog lakes, gas exchange can be driven largely by diel heating and cooling (Read et al. 2012, Heiskanen et al. 2014, Podgrajsek et al. 2015). R12S, T14, and H14, which incorporate a convective forcing component, are potentially able to reproduce the diel variability in *k* caused by buoyant mixing (Figure 3). The wind-based models have no temporal variability in low wind environments. In the four smallest lakes, CW03 predicted the lowest *k* values (Figure 3, 5). As CW03 was calibrated for a lake similar in size to Gribsø, it may better represent medium sized lakes, where wind speeds are infrequently near 0 m s^{-1} and rarely greater than 7 m s^{-1}. Indeed, CW03 estimates become closer to other model outputs in the larger lakes (Figure 5).

In larger lakes, the convective aspect of the surface renewal models was less evident due to the dominance of wind-induced mixing, and these lakes exhibited a weaker diel pattern for all models (Figure 3f). In the large lakes within our data set (>16 km^2), the high variability in *k* (Figure 5) is a product of how each model treats exchange at medium to high wind speeds. For the six largest lakes, CC98 generally produces the lowest values of *k*, while CW03 covers the largest range. VP13 and H14 generally covered the same range of *k* values, while T14 was always

slightly lower. R12S covered a range that encompassed H14 and T14 (Figure 5). In the original R12 model (as presented in Read et al. 2012), *k* values became constant at high wind speeds. In our R12S model, this is compensated by the addition of a breaking wave component (Soloviev et al. 2007). In general, the large range in *k* estimates at wind speeds > 10 m s^{-1} stems from the infrequency of high mean daily wind speeds, and therefore empirical gas flux data (Figure 2). In our data set, 85 % of daily mean wind speeds were below 5 m s^{-1} (Figure 8).

From our dataset of 15 lakes, we show that gas flux model choice has a substantial effect on NEP estimates in most systems. In the small lakes, persistent under saturation results in a narrow range in intra-model NEP estimates, but median NEP estimates vary from 0 to -2 g O_2 m^{-2} d^{-1} (Figure 7). In Mendota and Acton, two large, eutrophic lakes, DO_{diff} is more variable throughout year, and as a result, the error in annual NEP estimates due to ı and ρ parameter uncertainty is ~ 1 g O_2 m^{-2} d^{-1}, which is much higher than seen in smaller lakes (Figure 5). This seasonality is a critical factor in scaling-up daily estimates to annual averages, and should be carefully considered when interpreting annual averages. In most lakes, the three surface renewal models studied here predict larger absolute NEP than wind-based models. The exception is VP13, which compares well to H14 and R12S in most of the 15 study lakes.

Our results highlight the uncertainty in both model choice and ı and ρ parameter uncertainty, but do not validate any specific model. Three important conclusions to be drawn from our results are:

1) There is more uncertainty in model choice than in the parameterization of the metabolism model.
2) NEP and DO saturation are inherently correlated as defined in Eq. 3. Therefore, as surface water DO concentrations deviate from saturation, the larger the absolute range in NEP estimates will become based on any difference in *k* values. If DO_{diff} is known, this relationship could be considered prior to running a metabolism model. This can also be incorporated lake-wide to

judge spatial heterogeneity (Vachon and Prairie 2013, Schilder et al. 2013b).

3) When dissolved oxygen concentrations fluctuate between under- and over-saturation throughout the year, model choice can govern whether the calculated mean NEP is positive or negative, as seen in Gribsø.

Furthermore, *k* values output from VP13 closely match those from both R12S and H14. As VP13 only requires the input of wind speed and lake area, it is easily applicable in circumstances where high-frequency meteorological and water temperature data are not available.

The eddy covariance studies cited here have argued that CC98 significantly underestimates gas flux (MacIntyre et al. 2010a, Heiskanen et al. 2014), and that *k* models that incorporate a buoyancy flux term better represent realistic gas flux (MacIntyre et al. 2010b, Tedford et al. 2014). Uncertainties in NEP have consequences for the interpretation of carbon budgets in lakes, and choice of *k* model may impact those interpretations. It may be that the traditional wind-based models have substantially underestimated the role of lakes as carbon sources and sinks. For example, CC98 has been used for large-scale lake carbon budget studies (Cardille et al. 2007, McDonald et al. 2013) and for simulating carbon balance across a broad range of load scenarios in lakes (Hanson et al. 2004). If the same studies had employed an alternative model such as H14, NEP estimates would have been roughly double the estimates produced using CC98 for many lakes (Figure 7). In lakes where NEP is negative, such an increase would require a doubling of the external organic carbon load to support NEP or greatly reducing the internal production of organic carbon. In lakes where NEP is positive, the converse would be true. Either scenario would force us to rethink how we parameterize models of primary production in lakes. Similarly, in an analysis of global carbon dioxide emission from lakes, Raymond et al. (2013) estimated a global average gas transfer velocity by taking the average of CC98 and a highly simplified version of the R12 model. In our

dataset, this would return a *k* value at the lower end of the range presented by all six gas flux models, regardless of lake size. Considering this, lakes worldwide may emit more than the estimated 0.3 Pg C yr^{-1} (Raymond et al. 2013).

We found that hourly values for *k* were substantially different between models, and at an annual scale, resulted in significantly different estimates of lake metabolism and gas exchange with the atmosphere. Ensemble modeling of gas exchange may provide a means of generalizing *k* in situations where the model is not calibrated to the lake. Lakes are major processing and storage sites for organic carbon (Tranvik et al. 2009, Raymond et al. 2013), thus constraining uncertainties in NEP and determining whether lakes are net auto or heterotrophic, and quantifying the resulting implications regarding organic carbon loads to lakes is a high priority for future research.

Acknowledgments:

This is a product of the Global Lake Ecological Observatory Network (GLEON) Fellowship Program, as conceived by KCW, PCH, and EKR (http://fellowship.gleon.org). We do not make a distinction among the contributions of the first eight authors in conceiving, designing, and carrying out the analysis and synthesis for this paper. All authors contributed to writing and editing of the manuscript. We thank Dr. Jonathon Cole for helpful feedback that improved this paper. Funding for this research was provided by U.S. National Science Foundation Macrosystem Biology grant #1137353, and #1137327. Any use of trade, firm, or product names is for descriptive purposes only and does not imply endorsement by the US Government. We acknowledge data providers of the Solomon et al. (2013) data set associated with GLEON (www.gleon.org). Data providers: Mike Vanni, Miami University (Acton Lake); Hilary Swain, Archbold Biological Station (Lake Annie); Peter Staehr, Aarhus University (Castle, St. Gribsø, Hampensø, Vedstedsø); North Temperate Lakes (NTL) Long Term Ecological Research (LTER) site and the NTL Microbial Observatory (Crystal Bog, Mendota, North Sparkling Bog, Sparkling, Trout, and Trout Bog); David Hamilton, University of Waikato, New Zealand (Rotorua); Charles Chiu, Academia Sinica, Taiwan (Yuan Yang).

References:

Bartosiewicz M, Laurion I, MacIntyre S. 2015. Greenhouse gas emission and storage in a small shallow lake. Hydrobiologia 757: 101–115.

Benson BB, Krause D. 1984. The concentration and isotopic fractionation of oxygen dissolved in freshwater and seawater in equilibrium with the atmosphere. Limnol. Oceanogr. 29: 620–632.

Van de Bogert MC, Carpenter SR, Cole JJ, Pace ML. 2007. Assessing pelagic and benthic metabolism using free water measurements. Limnol. Oceanogr. Methods 5: 145–155.

Cardille J, Carpenter S, Coe M, Foley JA, Hanson PC, Turner MG, Vano JA. 2007. Carbon and water cycling in lake rich landscapes: Landscape connections, lake hydrology, and biogeochemistry. J. Geophys. Res. **112**.

Carlson RE. 1977. A trophic state index for lakes. Limnol. Oceanogr. 22: 361–369.

Cole JJ, Bade DL, Bastviken D, Pace ML, Van de Bogert MC. 2010. Multiple approaches to estimating air-water gas exchange in small lakes. Limnol. Oceanogr. Methods 8: 285–293.

Cole JJ, Caraco NF. 1998. Atmospheric exchange of carbon dioxide in a low-wind oligotrophic lake measured by the addition of SF6. Limnol. Oceanogr. 43: 647–656.

Cole JJ, Pace ML, Carpenter SR, Kitchell JF. 2000. Persistence of net heterotrophy in lakes during nutrient addition and food web manipulations. Limnol. Oceanogr. 45: 1718–1730.

Cole JJ, Prairie Y, Caraco N. 2007. Plumbing the global carbon cycle: integrating inland waters into the terrestrial carbon budget. Ecosystems 10: 171–184.

Crusius J, Wanninkhof R. 2003. Gas transfer velocities measured at low wind speed over a lake. Limnol. Oceanogr. 48: 1010–1017.

Hanson PC, Carpenter SR, Kimura N, Wu C, Cornelius SP, Kratz TK. 2008. Evaluation of metabolism models for free-water dissolved oxygen methods in lakes. Limnol. Oceanogr. Methods 6: 454–465.

Hanson PC, Pollard AI, Bade DL, Predick K, Carpenter SR, Foley JA. 2004. A model of carbon evasion and sedimentation in temperate lakes. Glob. Chang. Biol. 10: 1285–1298.

Heiskanen JJ, Mammarella I, Haapanala S, Pumpanen J, Vesala T, MacIntyre S, Ojala A. 2014. Effects of cooling and internal wave motions on gas transfer coefficients in a boreal lake. Tellus B 66: 22827.

Jonsson A, Åberg J, Lindroth A, Jansson M. 2008. Gas transfer rate and CO_2 flux between an unproductive lake and the atmosphere in northern Sweden. J. Geophys. Res. 113: G04006.

Kim J. 1976. A generalized bulk model of the oceanic mixed layer. J. Phys. Oceanogr. 6: 686–695.

MacIntyre S, Jonsson A, Jansson M, Aberg J, Turney DE, Miller SD. 2010a. Buoyancy flux, turbulence, and the gas transfer coefficient in a stratified lake. Geophys. Res. Lett. 37: L24604.

MacIntyre S, Jonsson A, Jansson M, Aberg J, Turney DE, Miller SD, Eugster W, Kling GW. 2010b. The Critical Importance of Buoyancy Flux for Gas Flux Across the Air-water Interface M. Donelan, W. Drennan, E. Saltzman, and R. Wanninkhof [eds.]. Gas Transf. Water Surfaces **37**, doi:10.1029/2010GL044164

McDonald CP, Stets EG, Striegl RG, Butman D. 2013. Inorganic carbon loading as a primary driver of dissolved carbon dioxide concentrations

in the lakes and reservoirs of the contiguous United States. Global Biogeochem. Cycles 27: 285–295.

Odum H. 1956. Primary production in flowing waters. Limnol. Oceanogr. 1: 102–117.

Pace ML, Lovett G. 2013. Primary production: the foundation of ecosystems, p. 312. *In* K. Weathers, D. Strayer, and G. Likens [eds.], Fundamentals of Ecosystem Science. Academic Press.

Podgrajsek E, Sahlée E, Rutgersson A. 2015. Diel cycle of lake-air CO_2 flux from a shallow lake and the impact of waterside convection on the transfer velocity. J. Geophys. Res. Biogeosciences n/a–n/a.

R Core Team. 2014. R: A language and environment for statistical computing. R Foundation for Statistical Computing, Vienna, Austria. http://cran.r-project.org

Raymond PA, Hartmann J, Lauerwald R, Sobek S, McDonald C, Hoover M, Butman D, Striegl R, Mayorga E, Humborg C, et al. 2013. Global carbon dioxide emissions from inland waters. Nature 503: 355–9.

Read JS, Hamilton DP, Desai AR, Rose KC, MacIntyre S, Lenters JD, Smyth RL, Hanson PC, Cole JJ, Staehr PA, et al. 2012. Lake-size dependency of wind shear and convection as controls on gas exchange. Geophys. Res. Lett. 39: L09405.

Rose KC, Winslow LA, Read JS, Read EK, Solomon CT, Adrian R, Hanson PC. 2014. Improving the precision of lake ecosystem metabolism estimates by identifying predictors of model uncertainty. Limnol. Oceanogr. Methods 12: 303–312.

Schertzer WM, Rouse WR, Blanken PD, Walker AE. 2003. Over-lake meteorology and estimated bulk heat exchange of Great Slave Lake in 1998 and 1999. J. Hydrometeorol. 4: 649–659.

Schilder J, Bastviken D, van Hardenbroek M, Kankaala P, Rinta P, Stötter T, Heiri O. 2013a. Spatial heterogeneity and lake morphology affect diffusive greenhouse gas emission estimates of lakes. Geophys. Res. Lett. 40: 5752–5756.

Schilder J, Bastviken D, van Hardenbroek M, Kankaala P, Rinta P, Stötter T, Heiri O. 2013b. Spatial heterogeneity and lake morphology affect diffusive greenhouse gas emission estimates of lakes. Geophys. Res. Lett. 40: 5752–5756.

Solomon C, Bruesewitz D, Richardson DC, Rose KC, Van de Bogert MC, Hanson PC, Kratz TK, Larget B, Adrian R, Babin BL, et al. 2013. Ecosystem respiration: drivers of daily variability and background respiration in lakes around the globe. Limnol. Oceanogr. 58: 849–866.

Soloviev A, Donelan M, Graber H, Haus B, Schlüssel P. 2007. An approach to estimation of near-surface turbulence and CO_2 transfer velocity from remote sensing data. J. Mar. Syst. 66: 182–194.

Staehr PA, Bade D, Koch GR, Williamson C, Hanson P, Cole JJ, Kratz T. 2010. Lake metabolism and the diel oxygen technique : State of the science. Limnol. Oceanogr. Methods 8: 628–644.

Staehr PA, Testa JM, Kemp WM, Cole JJ, Sand-Jensen K, Smith S V. 2012. The metabolism of aquatic ecosystems: history, applications, and future challenges. Aquat. Sci. 74: 15–29.

Tedford EW, MacIntyre S, Miller SD, Czikowsky MJ. 2014. Similarity scaling of turbulence in a temperate lake during fall cooling. J. Geophys. Res. Ocean. 119: 4689–4713.

Tranvik L, Downing J, Cotner J, Loiselle SA, Striegl RG, Ballatore TJ, Dillon P, Finlay K, Fortino K, Knoll LB, et al. 2009. Lakes and reservoirs as regulators of carbon cycling and climate. Limnol. Oceanogr. 54: 2298–2314.

Trolle D, Staehr PA, Davidson TA, Bjerring R, Lauridsen TL, Søndergaard M, Jeppesen E. 2012. Seasonal dynamics of CO_2 flux across the surface of shallow temperate lakes. Ecosystems 15: 336–347.

Vachon D, Prairie Y, Cole JJ. 2010. The relationship between near-surface turbulence and gas transfer velocity in freshwater systems and its implications for floating chamber measurements of gas. Limnol. Oceanogr. 55: 1723–1732.

Vachon D, Prairie YT. 2013. The ecosystem size and shape dependence of gas transfer velocity versus wind speed relationships in lakes. Can. J. Fish. Aquat. Sci. 70: 1757–1764.

Verburg P, Antenucci JP. 2010. Persistent unstable atmospheric boundary layer enhances sensible and latent heat loss in a tropical great lake: Lake Tanganyika. J. Geophys. Res. 115: D11109.

Wanninkhof R. 1992. Relationship between wind speed and gas exchange. J. Geophys. Res. 97: 7373–7382.

Winslow LA, Zwart J, Batt R, Corman J, Dugan HA, Hanson P, Holtgrieve G, Jaimes A, Read J, Woolway R. 2014. LakeMetabolizer: Tools for the analysis of ecosystem metabolism. R Packag. version 1.1

Zappa CJ, McGillis WR, Raymond PA, Edson JB, Hintsa EJ, Zemmelink HJ, Dacey JWH, Ho DT. 2007. Environmental turbulent mixing controls on air-water gas exchange in marine and aquatic systems. Geophys. Res. Lett. 34: L10601.

Table 1. Physical properties of the 15 GLEON lakes included in this study. Trophic status is defined using water quality data (Carlson 1977) provided in Solomon et al. (2013) and Staehr et al. (2010). Wind height is the height at which the original wind data was recorded prior to u10 adjustment.

Lake	Lat.	Long.	Max. Depth (m)	Mean Depth (m)	Area (km^2)	Trophic status	Wind Height (m)	Date Range		Total Days
Acton	39.575	-84.744	8	4	2.530	eutrophic	4.9	Apr-10	Sep-10	133
Annie	27.207	-81.351	20.7	9	0.365	mesotrophic	10	Mar-08	Feb-09	305
Castle	55.934	12.303	9	-	0.223	hyper-eutrophic	1.3	Apr-06	Nov-06	226
Crystal Bog	46.008	-89.606	2.5	2	0.005	dystrophic	2	May-08	Nov-08	149
St. Gribsø	55.983	12.303	12	5	0.100	eutrophic	1.3	Apr-06	Nov-06	227
Hampensø	56.020	9.333	14	4	0.760	mesotrophic	1.3	Apr-07	Oct-07	166
Mendota	43.099	-89.652	25.3	13	39.377	eutrophic	2	Apr-09	Nov-09	213
N. Sparkling Bog	46.005	-89.705	4.3	-	0.005	dystrophic	2	Apr-09	Dec-09	228
Rotorua	-38.066	176.266	21	11	78.780	mesotrophic	1.5	Jul-07	Jul-08	338
Sparkling	46.008	-89.701	20	11	0.640	oligophic	2	May-09	Nov-09	200
Sunapee	43.383	-72.033	32	10	16.670	oligophic	2	May-08	Oct-08	148
Trout	46.029	-89.665	36	15	16.080	oligophic	2	May-08	Nov-08	155
Trout Bog	46.041	-89.686	7.9	6	0.011	dystrophic	2	May-08	Nov-08	155
Vedstedsø	55.167	9.333	12	5	0.090	mesotrophic	1.3	May-08	Dec-08	202
Yuan Yang	24.583	121.402	4.5	1.7	0.036	mesotrophic	2	Jan-09	Jan-10	316

Table 2. The locations and methods used in developing each of the six published gas flux models. A list of data required to implement each model as well as any model constraints are provided.

Model	Study area and methods	Results and model requirements	Reference(s)
CC98	An SF_6 tracer experiment on Mirror Lake, NH (area 0.15 km^2) was compared with whole-system estimates from nine lakes.	Power function based on wind speed: $k600 = 0.215 \times u10^{1.7} + 2.07$ □ Developed for wind speeds < 9 m s^{-1}	Cole and Caraco (1998)
CW03	An SF_6 tracer experiment on Lake 302N (0.128 km^2) in the Experimental Lakes Area, Ontario.	Bilinear, linear and power functions based on wind speed. Power function used in this study: $k600 = 0.228 \times u10^{2.2} + 0.168$ □ Developed for wind speeds < 6 m s^{-1}	Crusius and Wanninkhof (2003)
R12S	High-frequency measurements of water temperature and meteorological variables from 40 temperate lakes (0.0006-640 km^2).	k600 is calculated using a surface renewal model. The Read et al. (2012) model, which calculates the dissipation rate of turbulent kinetic energy as the sum of a wind shear and convection component, is augmented with a breaking wave component as in Soloviev et al. (2007). Minimum inputs: u10, air temperature, relative humidity, short-wave radiation or PAR, lake area, light attenuation coefficient of PAR, depth-resolved water temperature measurements.	Read et al. (2012) Soloviev et al. (2007)
VP13	64 floating chamber measurements from a large reservoir (602 km^2) and eight smaller temperate lakes (0.19-4.0 km^2) in Quebec.	Linear model based on wind speed and lake area (LA) was the best predictor of k600. $k600 = 2.51 + (1.48 \times u10) + (0.39 \times u10 \times \log_{10}LA)$ □ Developed for wind speeds < 6 m s^{-1}	Vachon and Prairie (2013)
T14	High-frequency water temperature and eddy covariance measurements on a temperate lake in New York, USA (4 km^2).	k600 is calculated using a surface renewal model, where the dissipation rate of turbulent kinetic energy is calculated separately for periods of heating and cooling. Minimum inputs: same as R12S, mixed layer depth (fixed at 0.15 m).	Tedford et al (2014)

Table 2. Continued

Model	Study area and methods	Results and model requirements	Reference(s)
H14	High-frequency water temperature, dissolved CO_2, and eddy covariance measurements on Lake Kuivajärvi, Finland (0.63 km^2)	k600 is calculated using a boundary layer model that includes wind shear and cooling components. Minimum inputs: same as R12S, mixed layer depth (fixed at 0.15 m).	Heiskanen et al (2014)

Figure Headings

Figure 1. Hypothetical uncertainty in net ecosystem production (NEP) estimates given a range of gas flux models. As a given lake attribute changes, each gas flux model may predict varying levels of NEP. Lake attribute could represent lake area, trophic status, or other lake characteristic.

Figure 2. Gas transfer coefficient (*k*) derived from six different models with respect to wind speeds (u10) less than 9 m s^{-1}. Data points represent hourly values for 15 GLEON lakes from a global data set.

Figure 3. a, b, c) Hourly wind speed (u10) for a three day period in early July at Trout Bog, Acton and Trout Lake. d, e, f) Hourly *k* estimates from six gas flux models over the same three day period. Note the difference in the scale of the y-axis for all variables across the three lakes.

Figure 4. Density distribution for the entire hourly record of *k* in Trout Bog (WI), Acton (OH) and Trout Lake (WI), for each of the six models.

Figure 5. Box plots of data from the full time series of a) wind speed (u10), b) DO_{diff} and c) *k* at all 15 lakes ordered by lake area. The box edges and middle line represent the 25^{th}, 50^{th} (median), and 75^{th} quartiles of the data set.

Figure 6. a, b, c) Entire record of mean daily NEP estimates at Trout Bog, Acton and Trout Lake for the six models. Shaded areas around mean lines represent the 5th and 95th percentile of mean NEP estimates from the bootstrapping routine, and are used to illustrate the uncertainty around ı and ρ parameter choice in the metabolism model. d, e, f) Mean daily NEP estimates from 1 July to 8 July for the three lakes. g, h, i) Hourly observed dissolved oxygen concentrations (black) and concentration at saturation (gray) from 1 July to 8 July. Note the difference in the scale of the y-axis for all variables across the three lakes.

Figure 7. Box plots of mean NEP estimates generated from the bootstrapping routine (n=1000) for the full time series and for the six models. The plots were separated to expand the y-axis range. Lakes are ordered in ascending area, with a) eleven smallest lakes, and b) four largest lakes. The exception is the order of Trout and Acton, which have been switched for legibility. Each box represents the uncertainty the ı and ρ parameter estimates in the metabolism model. The box edges are the 25^{th} and 75^{th} quartiles, and the whiskers extend the full range of the data.

Figure 8. Frequency distribution of mean daily wind speeds (u10) stacked across the 15 lakes.

Figure 1

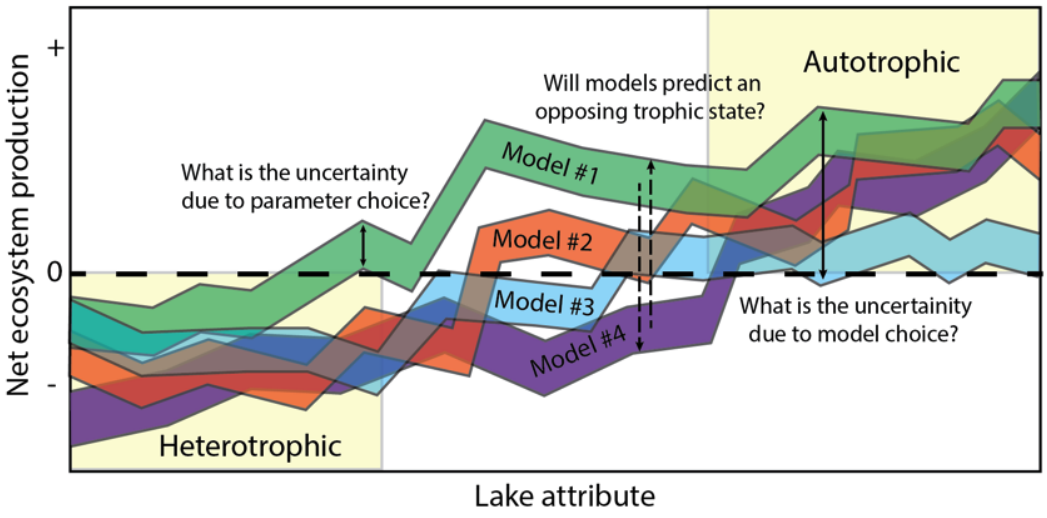
Net ecosystem production
+
0
-
Autotrophic
Heterotrophic
Will models predict an opposing trophic state?
What is the uncertainty due to parameter choice?
What is the uncertainity due to model choice?
Model #1
Model #2
Model #3
Model #4
Lake attribute

Figure 2

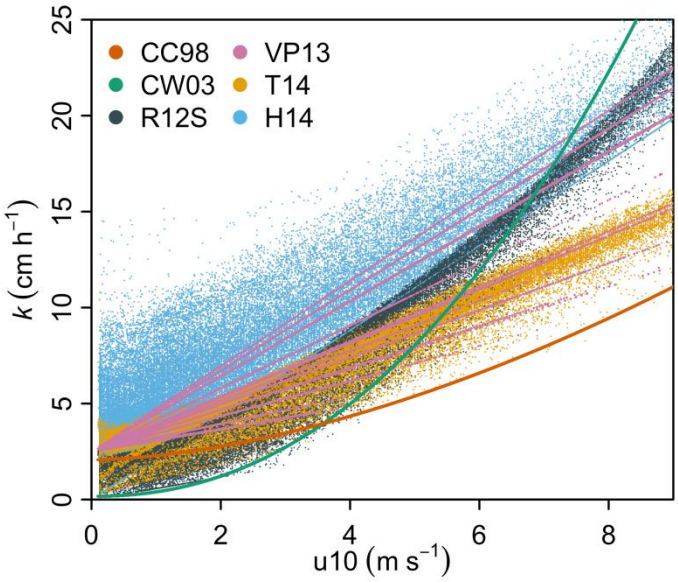

Figure 3

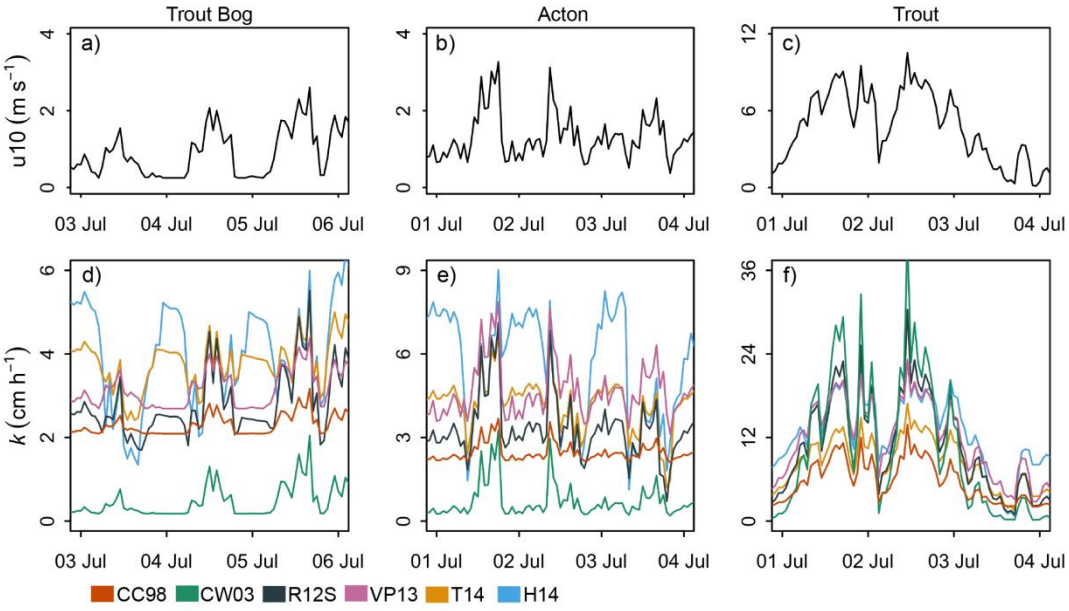
Trout Bog
Acton
Trout
a)
b)
c)
d)
e)
f)
u10 (m s^{-1})
k (cm h^{-1})
03 Jul
04 Jul
05 Jul
06 Jul
01 Jul
02 Jul
03 Jul
04 Jul
CC98
CW03
R12S
VP13
T14
H14

Figure 4

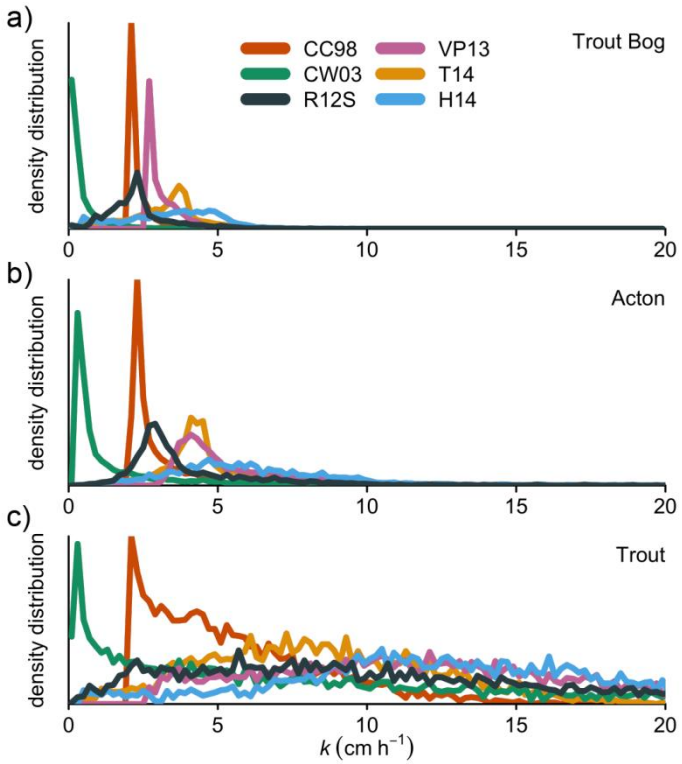
a)
b)
c)
density distribution
CC98
CW03
R12S
VP13
T14
H14
Trout Bog
Acton
Trout
0
5
10
15
20
k (cm h−1)

Figure 5

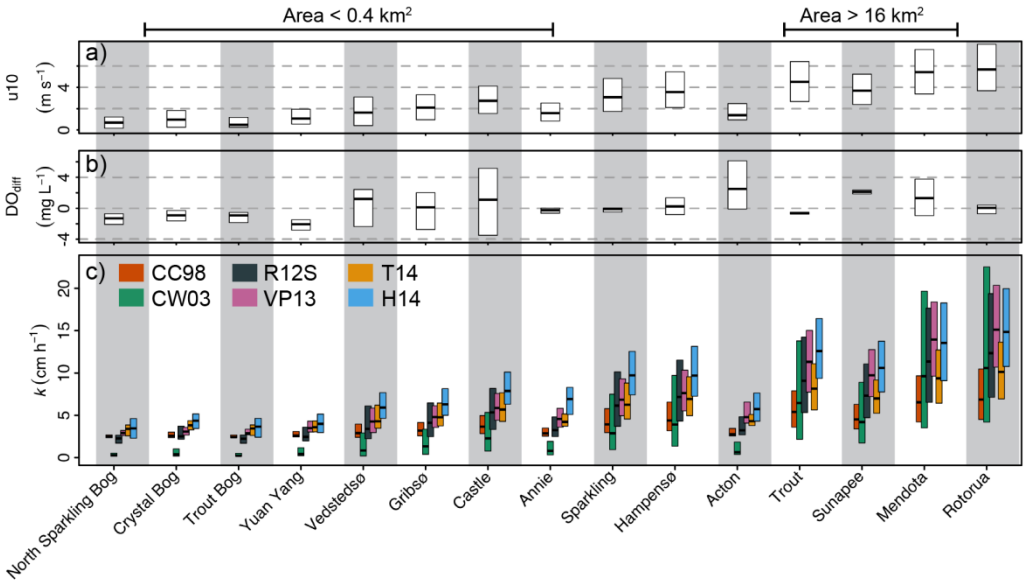
Area < 0.4 km²
Area > 16 km²
a)
u10
(m s⁻¹)
b)
DO_diff
(mg L⁻¹)
c)
k (cm h⁻¹)
CC98
CW03
R12S
VP13
T14
H14
North Sparkling Bog
Crystal Bog
Trout Bog
Yuan Yang
Vedstedsø
Gribsø
Castle
Annie
Sparkling
Hampensø
Acton
Trout
Sunapee
Mendota
Rotorua

Figure 6

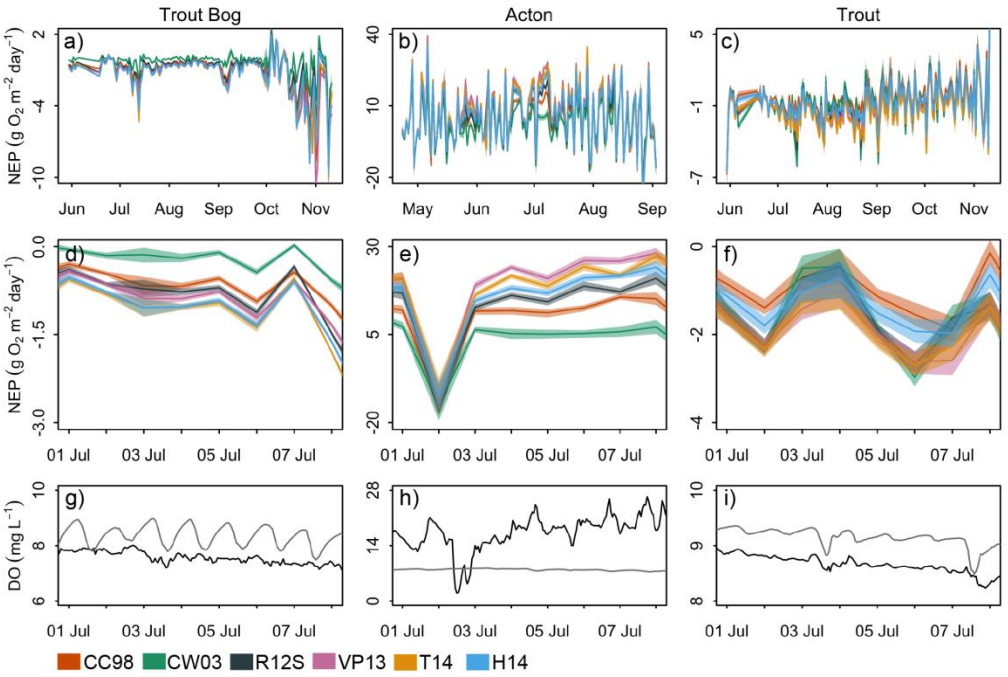
Trout Bog
Acton
Trout
a)
b)
c)
d)
e)
f)
g)
h)
i)
NEP (g O2 m-2 day-1)
DO (mg L-1)
Jun Jul Aug Sep Oct Nov
May Jun Jul Aug Sep
01 Jul 03 Jul 05 Jul 07 Jul
CC98 CW03 R12S VP13 T14 H14

Figure 7

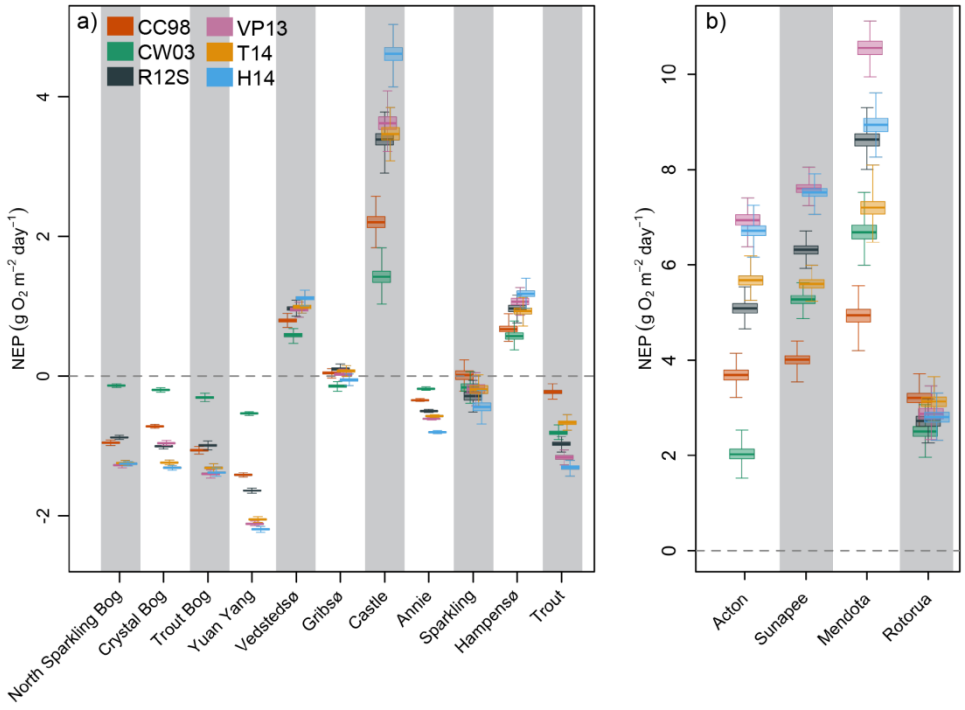
a)
CC98
CW03
R12S
VP13
T14
H14
NEP (g O2 m-2 day-1)
-2
0
2
4
North Sparkling Bog
Crystal Bog
Trout Bog
Yuan Yang
Vedstedsø
Gribsø
Castle
Annie
Sparkling
Hampensø
Trout
b)
NEP (g O2 m-2 day-1)
0
2
4
6
8
10
Acton
Sunapee
Mendota
Rotorua

Figure 8

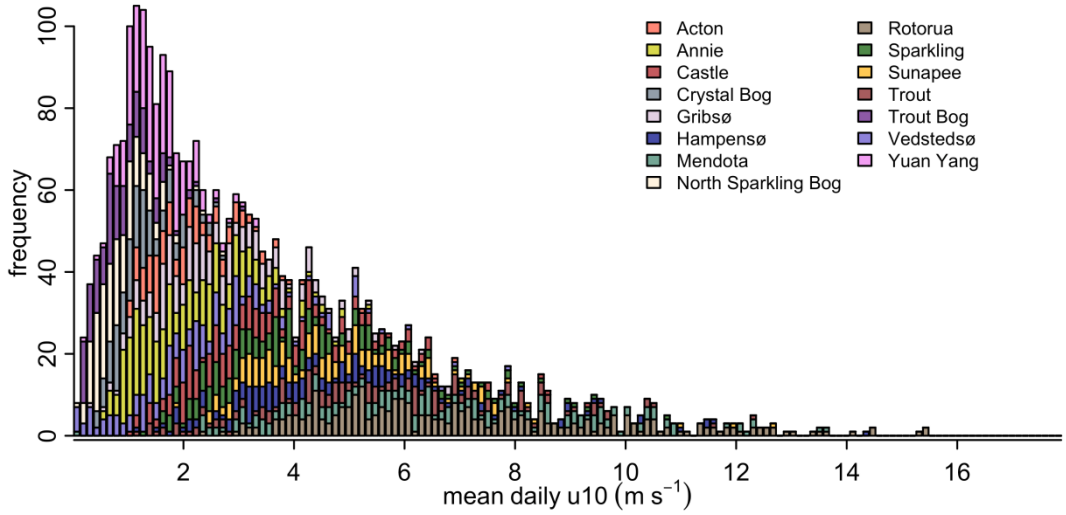
Acton
Annie
Castle
Crystal Bog
Gribsø
Hampensø
Mendota
North Sparkling Bog
Rotorua
Sparkling
Sunapee
Trout
Trout Bog
Vedstedsø
Yuan Yang
frequency
0
20
40
60
80
100
2
4
6
8
10
12
14
16
mean daily u10 (m s^{-1})